Slip-Turning Motion of the Musculoskeletal Robot on Toe Joints Using DSP-SLIP Model

Kawinna Nipatphonsakun

SEPTEMBER 2024

Slip-Turning Motion of the Musculoskeletal Robot on Toe Joints Using DSP-SLIP Model

A dissertation submitted to
THE GRADUATE SCHOOL OF ENGINEERING SCIENCE
OSAKA UNIVERSITY
in partial fulfillment of the requirements for the degree of
DOCTOR OF PHILOSOPHY IN ENGINEERING

BY
Kawinna Nipatphonsakun
SEPTEMBER 2024

Abstract

This thesis explores critical advancements in bipedal and humanoid robotics, focusing on improving slip-turning maneuvers through the integration of musculoskeletal structures, toe joints, and intrinsic muscles. By incorporating biomechanical features inspired by the human musculoskeletal system, the research demonstrates significant enhancements in the motion flexibility, stability, and postural control of robots, allowing them to execute more fluid and precise movements.

The focus of this study is the understanding of the biomechanics of human feet, particularly the role of toe joints and plantar intrinsic muscles in efficient locomotion. By integrating these elements, robotic designs achieve substantial improvements in stability and maneuverability, especially during slip-turning motions. The compliant structures within the musculoskeletal robots facilitate energy storage and release, enhancing their adaptability across various environments.

The thesis introduces the DSP-SLIP model, which combines a slider-like mechanism with a double-support parallel spring-loaded inverted pendulum model to address stability issues during slip-turning. This model uses foot support polygons and plantar intrinsic muscles for enhanced toe stabilization. Despite its advantages, the reliance on feedforward control systems without precise feedback mechanisms and the instability caused by pneumatic actuators pose significant obstacles.

Experimental investigations validate the hypothesis that incorporating toe joints enhances the flexibility and stability of robotic motion. Results indicate a reduction in frictional torque and an improvement in rotational angles, demonstrating the effectiveness of toe joints and intrinsic muscle control in achieving adaptive and more stable slip-turns by the ability to maintain longer foot contact duration. The study also delves into friction control methods through weight-shifting dynamics, providing insights into optimizing robotic movements to prevent slipping and maintain balance.

However, the research identifies several challenges. The absence of an upper body in the robot design results in a posterior inclination of the center of mass, complicating postural stability during rapid motions. Additionally, the use of pneumatic artificial muscles (PAMs) introduces issues such as lower accuracy in joint control and unstable velocities due to the compressibility of air. These challenges necessitate the exploration of alternative actuation methods and advanced control systems in future work.

Future research should aim to integrate slip-turning motion into walking robots, enhancing dynamic stability and locomotion capabilities. Incorporating additional sensors and feedback mechanisms will be crucial for improving the precision and adaptability of robotic movements. Addressing these challenges is essential for developing more adaptable, efficient, and human-like robotic systems, with significant implications for robotics, automation, and assistive technologies, potentially enabling robots to navigate challenging environments with greater agility and stability.

Table of Contents

Chapter 1: Introduction **1**

Chapter 2: Slip-turning of the musculoskeletal robot on toe joints **9**

2.1 Introduction . . . 10
2.2 Design of musculoskeletal robot with toe joints . . . 11
2.2.1 Hardware design . . . 11
2.2.2 Pneumatic actuators and controller . . . 13
2.3 Slip-turning motion . . . 15
2.3.1 Slip-turning strategy . . . 15
2.3.2 Muscle activation pattern . . . 15
2.4 Experiments . . . 17
2.4.1 Experimental setup . . . 18
2.4.2 Different conditions of toe joints . . . 18
2.5 Results . . . 20
2.5.1 Slip-turning in foot with and without the toe joint . . . 20
2.5.2 Foot stiffness and toe over-dorsiflexion . . . 21
2.5.3 Propulsion and postural stability . . . 22
2.6 Discussion . . . 24
2.7 Conclusion . . . 25

Chapter 3: Intrinsic Toe Joint Stabilization with DSP-SLIP Model **27**

3.1 Introduction . . . 28
3.2 Foot-Slip Turning with DSP-SLIP Model . . . 29
3.2.1 Foot-Slip Turning Motion and Slider-Like Mechanism . . . 29
3.2.2 Body Rotation with the DSP-SLIP Model and Compliant Leg Structure . . . 31
3.3 Development of the Musculoskeletal Robotics Foot with Plantar Intrinsic Muscle . . . 33
3.3.1 Robotics Foot with Plantar Intrinsic Muscle . . . 33
3.3.2 Importance of Toe Joint Stabilization in Stability Margin . . . 34
3.4 Foot-Slip Turning Experiments and Results . . . 36
3.4.1 Experimental Setup . . . 36

3.4.2 Experimental Results 40
3.5 Disscussion 45
3.6 Conclusion 46

Chapter 4: Friction Control Using Dual-Mass DSP-SLIP Model **49**
4.1 Introduction 50
4.2 Slip-turning motion of the bipedal robot with a musculoskeletal structure 51
4.2.1 Structure of the musculoskeletal robot 51
4.2.2 Slip turning motion 51
4.2.3 DSP-SLIP model with dual-mass system 52
4.3 Friction control method with dual-mass system simulating weight transfer 53
4.3.1 Weight transfer in bipedal locomotion 53
4.3.2 Friction control in slip-turning motion 53
4.4 Experiments 54
4.4.1 Experimental Setup 54
4.4.2 Comparative conditions 55
4.4.3 Results 56
4.4.4 Discussions 57
4.5 Conclusion 59

Chapter 5: Conclusion **63**

Acknowledgements **69**

Bibliography **71**

Publication List **87**

Chapter 1

Introduction

Bipedal robots [1, 2, 3, 4], specifically humanoid robots [5, 6], have been continuously studied in recent decades. Significant advancements in the research and development of those robots driven by artificial intelligence, materials science, and robotics engineering breakthroughs have been seen in various places. Researchers have focused on enhancing these robots' stability, agility, and autonomy, enabling them to navigate complex terrains and perform intricate tasks with human-like dexterity. Innovations such as advanced sensor systems, machine learning algorithms, and lightweight yet strong materials have been pivotal objectives. Notable projects include Boston Dynamics' Atlas, which showcases impressive parkour capabilities, and Honda's ASIMO, which demonstrates fluid human-robot interactions. These advancements propel bipedal and humanoid robots from research labs into real-world applications, ranging from disaster response and healthcare to customer service and domestic assistance, promising to revolutionize various sectors by augmenting human capabilities and improving efficiency.

Bipedal locomotion represents a pinnacle of evolution in human movement, inspiring significant advancements in robotics. Traditional motor-driven robots have long been the cornerstone of industrial and service applications, characterized by precision control through rigid structures. For example, Honda's ASIMO has been in the development stage since 1998 [1, 2]. These robots typically employ Zero Moment Point (ZMP) control [7, 8, 9, 10] and postural control method [11, 12, 13, 14] for stability, ensuring that the center of gravity remains within the support base. The models that are usually used to control motion in the bipedal system are the linear inverted pendulum model (LIMP) [15, 16, 17] and the spring-loaded inverted pendulum model (SLIP) [18, 19, 20, 21, 22, 23, 24] for an even more dynamic spring-mass system [25]. The models come with various applications, such as 3D models [26], with additional damping [27], with a swing leg [28] or trunk [29], or dual model [30, 31, 32, 33], to improve its stability [34, 35, 36, 37] or adaptability [38]. Humanoid robots, designed to replicate human appearance and movement, have extended these capabilities, incorporating full-body control [39] to manage complex tasks. However, despite their advanced control

systems requiring feedback control [40, 41], these robots often lack the flexibility and adaptability inherent in biological organisms.

To close the structural gap between humans and robots, incorporating biomechanical features such as a musculoskeletal structure [42, 43, 44, 45, 46] and enhanced flexibility is crucial. With those features, humans can efficiently perform bipedal locomotion daily, such as walking or running [47, 48, 49]. The musculoskeletal structure mimicking the intricate network of muscles, tendons, and bones in the human body allows robots to achieve a higher degree of motion fluidity and adaptability while maintaining their balance and postural control [50, 51]. Flexible joints and compliant mechanisms further enhance their ability to perform delicate and complex movements, closely emulating the natural biomechanics of the human body [52]. This approach improves the robots' functional capabilities and their interaction with human environments, making them more adept at tasks requiring precision and adaptability.

Musculoskeletal robots aim to replicate the human body's complexity by incorporating flexible and adaptive structures [53, 54, 55, 56, 57, 58, 59] that mimic the upper limb [60], lower limb [61, 62], gluteus [63], and ankle-foot complexes [64]. These robots utilize compressible structures that absorb and release energy, similar to human muscles and tendons, providing enhanced movement fluidity. The musculoskeletal robots are made by integrating artificial muscles [65, 66, 67, 68, 69, 70, 71] made from developed techniques like pneumatic artificial muscle or multifilament muscle. Those robots are able to replicate the dynamic range and force generation similar to those of human muscles. However, controlling such complex systems presents significant challenges. Coordinating multiple degrees of freedom and integrating compliant materials often result in limited movement ranges and difficulty in achieving precise control. Addressing these challenges is crucial for advancing the capabilities of musculoskeletal robots, enabling them to perform more sophisticated tasks and navigate complex terrains with human-like dexterity.

Numerous research studies have shown that musculoskeletal robots are capable of walking, running, and even jumping. In comparison, the study on the turning motion of these robots is lacking. Turning maneuvers often require more degrees of freedom to execute a single task compared to other kinds of motion [72, 73, 74], while it moves in a multi-directional plane, not restrained to a vertical plane. In robotics and biomechanics, two primary types of turning maneuvers are the step-turn and the spin-turn [75], each with distinct characteristics and applications. A step-turn involves a gradual change in direction, where the robot or individual takes a series of steps, shifting weight and adjusting the body orientation incrementally [76, 77, 78]. This method is typically more stable and precisely controlled, making it suitable for navigating complex and spacious environments or when balance is critical. On the other hand, a spin-turn, or a slip-turn, involves a rapid pivot around a fixed point, usually on one foot, by utilizing the foot slippage [79, 80], allowing for a swift change in direction with minimal steps [81, 82, 83, 84, 85]. Slip-turns are advantageous for quick reorientation, such as in dynamic sports or evasive maneuvers, but they require precise control to maintain balance

and avoid tipping. Both turning techniques are crucial in enhancing the agility and maneuverability of bipedal robots, enabling them to adapt to diverse situations with human-like efficiency. As for the musculoskeletal robots, which usually have a simple structure to avoid difficulty in control method, making them have a limited range of movements, the usage of the slip-turn could be a solution for the issue.

Meanwhile, the slip-turning motion of those robots was made on their toe, so the toe joint's role needed to be studied to understand its functional features properly. The toe joints are said to help in minimizing frictional power during the slip-turning motion [83]. While most of the research on toe joints focuses on improved flexibility [86, 87, 88, 89, 90, 91], many research studies on robotic toe joints focus on enhancing locomotion [92, 93], stability, and adaptability in various terrains, mimicking human-like capabilities. These studies explore both passive and active toe mechanisms to optimize such movements. With their inherent compliance and energy absorption [94, 95, 96], passive toe joints contribute to smoother and more stable motion [97, 98, 99]. In contrast, active foot allow dynamic adjustments of foot stiffness, improving the robot's grip, push-off, and optimal adaptability on various surfaces [100]. The effect of toe length and the structural design of the joints are thoroughly investigated to achieve optimal performance [101]. By understanding and harnessing the biomechanics of human toes, researchers aim to develop robotic systems capable of executing precise and efficient slip-turns, thereby significantly enhancing their operational versatility and effectiveness in diverse environments.

Studying the biomechanical features of the foot and their biological functions is essential for advancing human-like robotic feet and mimicking its features [102]. The human foot is a complex structure that efficiently supports weight, enables balance, stability [103], and facilitates movement through intricate interactions between bones, muscles, tendons, and ligaments. Understanding these interactions provides critical insights into how to design a foot that more accurately mimics natural movement, improving the motion. Additionally, replicating the foot's capabilities can significantly enhance the agility, stability, and versatility of robotic systems. By examining the biological functions of the foot, researchers can develop more sophisticated robotic feet that perform better in real-world environments, navigating uneven terrain and executing complex maneuvers with greater precision. For example, the windlass mechanism [104, 105, 106, 107, 108] is one of the biomechanical processes in the foot that enhances its arch stability and contributes to efficient locomotion. When the toes dorsiflex (lift upwards), the plantar fascia, a thick band of connective tissue running along the sole, tightens and pulls the heel bone closer to the forefoot. This action raises the medial longitudinal arch of the foot [109, 110], making it more rigid and capable of withstanding the stresses of walking and running [111, 112, 113]. The foot arch, particularly the medial arch, acts as a shock absorber and provides leverage, distributing the body's weight across the foot and enabling efficient movement [114, 115]. This interplay between the windlass mechanism and the foot arch is crucial for maintaining balance, absorbing impact, and propelling the body forward.

In the past, some researchers have studied the foot arch in robotic foot [116], and the windlass mechanism in the jumping bipedal robot [117], with many more studies on the bio-inspired robotic foot [118, 119, 120, 121, 122, 123, 124, 125].

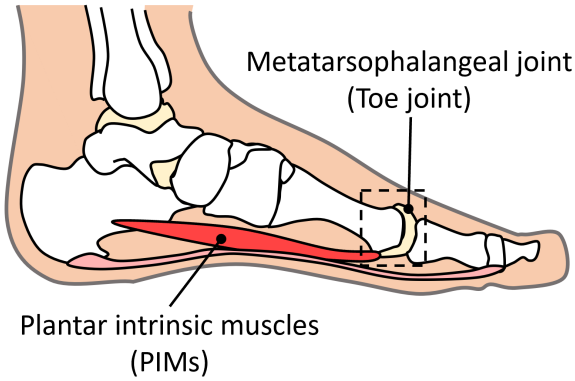

Figure 1.1: Position of the toe joint and plantar intrinsic muscle of the foot

In the foot's structure, the toe joint and plantar intrinsic muscles are critical components of foot biomechanics (see Fig. 1.1), contributing to stability, balance, and movement. The toe joints, or metatarsophalangeal joints, allow for flexion, extension, and slight lateral movements of the toes, improving their flexibility and adaptability [126, 127, 128, 129, 130]. These joints, working along with The plantar intrinsic muscles located within the sole of the foot [131, 132], play a pivotal role in weight distribution [133, 134, 135, 136] and propulsion [137] during walking and running [138, 139]. These muscles stabilize the arches of the foot, support toe movements, stabilize foot posture [140], and enhance the foot's ability to adapt to varying surfaces. Together, the toe joints and plantar intrinsic muscles ensure efficient energy transfer, shock absorption, and fine motor control, enabling smooth and agile locomotion [141]. Some research mentioned that toe weakness affects the postural stability of humans [142, 143]; therefore, improving the foot muscle strength should be able to improve the overall stability of the foot [144].

The purpose of this thesis is to realize the slip-turning motion of the musculoskeletal robot with a simple structure by utilizing its compliant and adaptive structure and improving its optimal performance and postural stability. To prove the contributions of attaching toe joints to the robot can improve its motion flexibility despite a limited range of movements, and using its plantar intrinsic muscle can passively enhance the foot's stability by distributing the ground reaction force along the toe extension [145], improving its postural control. Additionally, the compliant structure [146, 147, 148] of the robot was studied to understand the relationship between the motion and the musculoskeletal structure, which made the motion possible with its energy-storing capability [149, 150, 151]. Furthermore, the investigation of frictional force was studied in order to apply a friction control method by simulating weight changes [152, 153, 154] on one foot of the slip-turning motion

in the future. Various methodologies and a series of experiments were concluded in three chapters, resulting in two journal publications and one conference paper.

In Chapter 2, we conducted an experimental investigation of the slip-turning of musculoskeletal robots on toe joints. This chapter explores an innovative approach to enhancing the mobility and stability of musculoskeletal robots through the implementation of slip-turning on toe joints. This study resulted in one publication, which investigates the mechanics and benefits of incorporating passive toe joints in the turning motion of the musculoskeletal robot. The primary objective is to improve the robot's turning capabilities, expanding its range of motion and adaptability in complex tasks.

Starting from the introduction of the chapter, musculoskeletal robots are designed to mimic the anatomical and functional aspects of biological beings, aiming to achieve more natural and human-like movements. Despite these advanced designs, these robots often face challenges due to their limited range of motion and degrees of freedom (DoFs). This limitation is particularly evident in complex tasks such as turning, which require precise control and extensive movement coordination. The traditional approaches to turning, such as step turning and spin turning, often involve substantial effort and multiple steps, which can be inefficient and cumbersome. Slip-turning, a turning mechanic that reduces physical constraints and energy expenditure, presents a potential solution to these challenges. Previous studies have indicated that slip-turning can be more energy-efficient than traditional turning methods. By utilizing toe joints, musculoskeletal robots can achieve higher mobility, allowing for quick and effective turning with minimal friction-induced power loss. The study investigates two main hypotheses:

1. Implementing slip-turning on toe joints will enhance the rotational angle of the robot, improving its turning efficiency and range of motion.

2. Applying the stiffness of the plantar intrinsic muscles (PIM) to the foot can help enhance the motion or its postural stability and the robot's overall balance.

The methodology used in this chapter involved a series of experiments designed to evaluate the impact of toe joints and PIM on the slip-turning motion. The experiments were structured to compare different foot conditions:

- Fixed Toe: Emulating a rigid foot without toe joints.

- Unrestricted Toe: Allowing free movement of the toes without stiffness control.

- Passive Toe: Utilizing a fixed-length PIM to provide constant stiffness.

- Active Toe: Actively controlling the PIM to adjust stiffness dynamically during motion.

The experiments measured various performance indicators, including frictional torque, rotational angle, and ground reaction forces, to assess the effectiveness of each foot condition in enhancing the robot's turning capabilities and stability.

The experimental results demonstrated that using toe joints significantly reduced frictional torque and improved the robot's rotational angle, thus enhancing its mobility. Additionally, the activation of the PIM was found to be beneficial in preventing over-dorsiflexion of the toes, which contributed to better postural stability. These findings suggest that integrating toe joints and actively controlling PIM stiffness can provide a versatile solution for achieving agile and efficient movements in musculoskeletal robots.

This research contributes to the field of robotics by introducing a novel approach to improving the locomotion of musculoskeletal robots through the use of toe joints and PIM control. The enhanced slip-turning capabilities can lead to more adaptable and efficient robots capable of performing complex tasks in various real-world scenarios. Future research could focus on further optimizing the design and control of toe joints, exploring their applications in more complex locomotion tasks, and investigating potential medical applications such as gait training and rehabilitation.

The chapter is organized as follows: Section 2 details the structural design and control system of the musculoskeletal robot. Section 3 explains the slip-turning strategies and muscle activation patterns. Section 4 describes the experimental setup and methodology. Section 5 presents the experimental results and analysis, followed by a discussion in Section 6. Finally, Section 7 concludes the chapter by highlighting the contributions and suggesting directions for future research.

In Chapter 3, the chapter explores the innovative concept of intrinsic toe joint stabilization in foot-slip turning motion for musculoskeletal robots, presenting findings from a study conducted and published as a journal paper. This research addresses the challenges associated with achieving turning motions in bipedal locomotion using musculoskeletal robots, which typically rely on complex control systems. By comparing traditional motor-driven robots with musculoskeletal ones, the chapter underscores the latter's advantages, including passively enhanced motion and stability facilitated by feedforward systems and simplified structures.

Various turning strategies, including slip-turning, are discussed, with studies demonstrating reduced energy consumption and improved stability. To simplify the execution of slip-turning motions, the chapter introduces the DSP-SLIP model, which combines a slider-like mechanism with the double-support parallel spring-loaded inverted pendulum model. This model aims to address challenges in stability during slip-turning, proposing enhancements using foot support polygons and plantar intrinsic muscles (PIM) for toe stabilization.

The chapter delves into the foot-slip turning mechanism with the DSP-SLIP model, outlining the three stages of the turning motion: standing, turning, and bouncing/landing. It emphasizes the compliance of the robot's leg structure, which allows for minor errors in foot positioning, compensating for precision limitations. The DSP-SLIP model simplifies the robot's turning motion by

incorporating compliant leg structures, which deform and adapt to the environment while maintaining foot contact with the ground. The structure rendered the slip-turning motion possible with a simple feedforward control as it utilized its spring-like properties to resist the motion and passively maintain the hip level on both sides to be closely equal.

Furthermore, the chapter discusses the development of a musculoskeletal robotics foot equipped with a PIM to enhance postural stability during slip-turning motion. The PIM, implemented using pneumatic artificial muscles (PAMs), stabilizes the toe joint, aiding in anterior-posterior stabilization. This development underscores the importance of toe joint stabilization in improving stability margin, particularly in bipedal robotics with musculoskeletal structures.

Experimental results from slip-turning experiments with the musculoskeletal robot "PneuTurn-T" validate the significance of compliance structures and passive intrinsic mechanisms in improving stability. The experiments analyze leg compliance during various muscle-supplying durations and assess the effectiveness of PIMs in stabilizing the robot's posture during the landing phase. Results demonstrate the potential of compliant structures and passive mechanisms to enhance stability and performance in musculoskeletal robots.

In conclusion, the chapter introduces a novel approach to foot-slip turning motion for musculoskeletal robots, highlighting the benefits of the DSP-SLIP model and intrinsic toe joint stabilization. These findings contribute to robotics by offering a simple yet effective strategy that reduces the complexity of control systems and structural design. Future research aims to integrate slip-turning motion into walking robots, further enhancing dynamic stability and locomotion capabilities.

The chapter is organized as follows: Section 2 describes the slip-turning motion of the robot using the DSP-SLIP model and its compliant structure. Section 3 explains the development of the robotics foot with PIM and its role in toe joint stabilization. Section 4 details the experimental setup, experimental results, and analysis. Followed by a discussion of the research challenges in Section 5. Finally, Section 6 concludes the chapter by highlighting the contributions and suggesting directions for future research.

Chapter 4 introduces a novel approach to friction control in the slip-turning motion of musculoskeletal robots. The study focuses on simulating weight-shifting dynamics akin to bipedal locomotion using the Double-Support Parallel Spring-Loaded Inverted Pendulum (DSP-SLIP) model, integrated with a dual-mass system and compliant structure.

The chapter aims to combine our novel DSP-SLIP model with simulated weight transfer between both feet to manipulate foot friction and control rotational angle. Bipedal locomotion in robots aims to replicate human dynamic movement capabilities. The introduction discusses various models developed for this purpose, including the LIMP, SLIP, and 3D-SLIP models, culminating in the DSP-SLIP model, which integrates a dual-mass system for effective weight transfer between legs, enhancing stability and adaptability. Weight transfer between feet is fundamental in bipedal locomotion, influencing balance and stability. The chapter hypothesizes that mimicking this weight

transfer can adjust frictional forces to prevent slipping during turns. It explores how weight transfer and friction control are crucial for slip-turning motions in bipedal robots.

The chapter further discusses the structure of the musculoskeletal robot used in the study, detailing its degrees of freedom, pneumatic artificial muscles, and control mechanisms. Slip-turning motion, a maneuver for enhancing robot agility, is explained along with the DSP-SLIP model's integration with a compliant structure and dual-mass system.

Friction control methods using the dual-mass system to simulate weight transfer are elaborated, focusing on weight transfer mechanisms in bipedal locomotion and their implications for friction control during slip-turning motions. Equations describing frictional forces and rotational angles are provided, emphasizing the role of compliant structures in enhancing friction control.

The chapter outlines experimental setups and conditions, including varying attached weights and modifying turning patterns, to investigate weight transfer dynamics and friction control in slip-turning motions. Results from force plate data processing and discussions on frictional torque and rotational angles are presented, highlighting the influence of weight distribution and swing duration on slip prevention and stability.

Lastly, the chapter concludes with future work considerations, emphasizing the practical implications of the study's findings for designing and controlling bipedal robots in challenging environments.

The chapter is organized as follows: Section 2 describes the slip-turning motion of the robot using the DSP-SLIP model and its dual-mass model. Section 3 explains the friction control method in the slip-turning motion based on the body weight transfer. Section 4 details the experimental setup, comparative conditions, experimental results, and analysis, followed by a discussion of the research challenges. Finally, Section 5 concludes the chapter by highlighting the contributions and suggesting directions for future research.

In conclusion, this thesis investigates the enhancement of bipedal and humanoid robots, particularly focusing on slip-turning maneuvers using musculoskeletal structures with toe joints and intrinsic muscles. By integrating biomechanical features inspired by human anatomy, such as toe joints and compliant structures, the research demonstrates significant improvements in robotic motion flexibility, stability, and postural control. Experimental results validate that toe joints enhance motion efficiency and stability by reducing frictional torque and improving rotational angles. The study also highlights challenges, including postural stability issues due to the lack of an upper body and the instability of pneumatic artificial muscles. Future research should aim to optimize these features, explore more complex locomotion tasks, and investigate medical applications. By addressing these challenges, the field of robotics can develop more adaptable, efficient, and human-like robotic systems, with potential applications in various environments and assistive technologies.

Chapter 2

Slip-turning of the musculoskeletal robot on toe joints

This chapter based in following publication:

K. Nipatphonsakun, T. Kawasetsu, and K. Hosoda, "The experimental investigation of foot slip-turning motion of the musculoskeletal robot on toe joints", Frontiers in Robotics and AI, 10:1187297, 2023.

Abstract

Owing to their complex structural design and control system, musculoskeletal robots struggle to execute complicated tasks such as turning with their limited range of motion. This study investigates the utilization of passive toe joints in the foot slip-turning motion of a musculoskeletal robot to turn on its toes with minimum movements to reach the desired angle while increasing the turning angle and its range of mobility. The different conditions of plantar intrinsic muscles (PIM) were also studied in the experiment to investigate the effect of actively controlling the stiffness of toe joints. The results show that the usage of toe joints reduced frictional torque and improved rotational angle. Meanwhile, the results of the toe-lifting angle show that the usage of PIM could contribute to preventing over-dorsiflexion of toes and possibly improving postural stability. Lastly, the results of ground reaction force show that the foot with different stiffness can affect the curve pattern. These findings contribute to the implementations of biological features and utilize them in bipedal robots to simplify their motions, and improve adaptability, regardless of their complex structure.

2.1 Introduction

Musculoskeletal robots are designed to imitate the structure and movement of actual beings [53, 54, 56, 61] to utilize their biological features and realize more natural motion or human-like motion in humanoid robots [58, 59, 62]. However, one of the main challenges facing these robots is their limited range of motion due to the lack of degrees of freedom (DoFs) [57], caused by minimizing the robot design to reduce complications of the controller, which can affect their ability to perform both static and dynamic tasks that require complex controls and coordination of muscles. Turning motion is one of those complicated motions that require substantial effort and multiple steps to execute. Furthermore, turning motion is a maneuver that often requires precise control and a wide range of movements, which are the limitations of musculoskeletal robots. To overcome these limitations and improve the functionality of bipedal robots, researchers are focusing on developing new techniques and methods for enhancing their ability to perform motion, such as slip-turning motion.

Slip-turning is a turning mechanic that is said to overcome the physical limitations of robots [85]. Previous studies have shown that slip-turning is more energy-efficient than traditional step turning methods [81]. Together with the utilization of toe joints, the robots could reach higher mobility, allowing for effective and quick slip-turning using the toes as contact points [84]. These studies have demonstrated that utilizing these toe joints enables the robots to perform slip-turning motions by minimizing friction-induced power generation and maintaining foot contact on a small support area for a short duration [83]. Meanwhile, the plantar intrinsic muscle (PIM), which connects to the toes underneath the foot, plays a role in stiffening the toe joints, preventing them from over-dorsiflex or floating toes, possibly leading to improved postural stability and balance during an unstable state [133, 134, 143]. Additionally, the stiffness of the PIM contributes to the ability to perform quick motions [141] and enhance the push-off force [132, 137].

In this paper, we propose an experimental investigation of the foot slip-turning motion of the musculoskeletal robot equipped with toe joints and PIM. the objective is to improve the musculoskeletal robot's slip-turning capabilities. According to our hypothesis, implementing slip-turning on toe joints in a musculoskeletal robot is expected to yield increased body rotational angle, regardless of whether there are joints in the yaw axis or the vertical axis of the human. Additionally, we propose that the activation of the PIM during motion can affect foot stiffness, which can influence the robot's postural stability and capability to perform quick movements.

A series of experiments were conducted to assess the effectiveness of toe joints in enabling foot slip-turning. The first experiment aimed to compare slip-turning performance between a foot equipped with toe joints and a foot without toe joints. The second experiment focused on demonstrating the role of the PIM in preventing over-dorsiflexion of the toes, thus improving the robot's postural stability. In the final experiment, the active utilization of the PIM was investigated to determine its impact on motion propulsion.

The findings of this study could contribute to the advancement of musculoskeletal robot locomotion by introducing a novel approach using the foot structure to improve slip-turning capabilities. The flexibility of the joints combined with the active control of the PIM could provide a versatile solution for achieving agile and efficient movements, enhancing the robot's adaptability in various real-world scenarios. Future research can focus on further optimizing the design and control of the toe joints, exploring their potential applications in more complex locomotion tasks, and investigating the integration of similar mechanisms in other robotic systems or implementations for medical purposes such as gait training or rehabilitation.

The remainder of this paper is organized as follows: Section 2 provides the structural design of the musculoskeletal robot as in hardware design, pneumatic actuators, and its control system, including the range of motion of the constructed robot. Section 3 explains the slip-turning strategies and the generation of the muscle activation pattern to be used in the experiments. Section 4 describes the experimental setup and methodology of using various foot conditions for evaluating the slip-turning performance. Section 5 presents the results and analysis of the experiments, followed by a discussion of the findings in Section 6. Finally, Section 7 concludes the paper,highlighting the contributions of this research and outlining future directions for investigation.

2.2 Design of musculoskeletal robot with toe joints

2.2.1 Hardware design

For imitation of the movements of biological beings, applying the musculoskeletal structure to a robot is a viable approach to mimic the biomechanical characteristics of living systems. This approach allows robots to replicate the biological features that motor-driven robots cannot achieve with their mechanical design alone. On the other hand, the entire musculoskeletal structure could be challenging to implement in a robot due to its complexity and sophistication. To address this problem, a simplified version of the design is adopted, focusing on the key components necessary for realizing the desired robot motion to alleviate the complexities associated with control architecture.

The number of muscles required for the robot's turning motion was chosen based on the biomechanical studies on human turning gait [75] and muscle synergy studies related to human turning mechanics [155, 156]. From these studies, we identified six key muscles that exhibited significant activations during the observation: erector spinae, gluteus medius, vastus lateralis, biceps femoris, soleus, and tibialis anterior. Since the gluteus medius has a complex fanshaped structure and serves as both the flexor and extensor of the hip, we decided to include an additional muscle, the iliopsoas, to specifically act as the flexor muscle of the hip in our robot. As our robot focuses on the lower half of the body, the erector spinae muscle was excluded. In addition to these muscles, our research also explores the utilization of the foot structure, including toe joints and the PIM, as both features were added to the design of our robot. The placement of joints was carefully done along the pitch

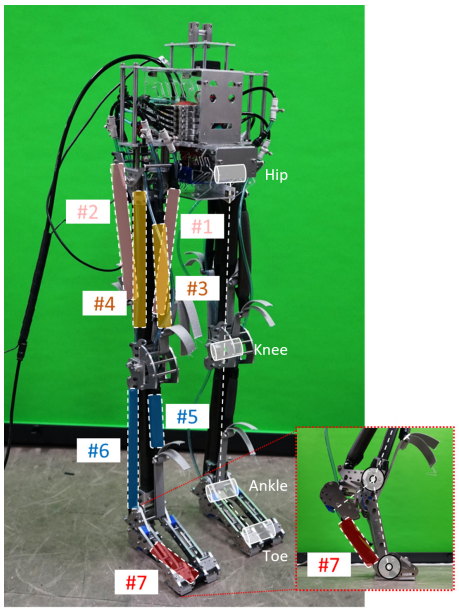

Degree of Freedoms: 8
Pitch joints at hip, knee, ankle, toe joint in both legs

Number of PAMs: 14
Number of valves: 12

No. (#R,L)	Muscle Name
#1,8	Iliopsoas(IL)
#2,9	Gluteus maximus (GM)
#3,10	Vastus lateralis (VL)
#4,11	Biceps femoris (BF)
#5,12	Tibialis anterior (TA)
#6,13	Soleus (SO)
#7,14	Plantar intrinsic muscles (PIM)

Figure 2.1: Structural design of the musculoskeletal robot "PneuTurn-T". The musculoskeletal robot has a total of eight DoFs, four joints in each leg at the hips, knees, ankles, and toes. Each leg has seven PAMs to actuate and restrict the motion of joints, controlled by 12 valves.

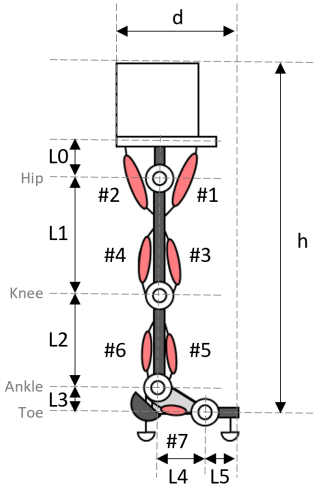

Total weight: 6.4 kilograms

Value	Length (millimeters)
Width (w)	300
Height (h)	1000
Depth (d)	300
L0	50
L1	350
L2	300
L3	80
L4	140
L5	40

Figure 2.2: Size and dimension of the bipedal robot.

axis (or the lateral axis of the human body) to ensure a sufficient range of motions for recreating the swing motion of both legs in the front and back direction, which is considered enough to realize slip-turning in this study

As a result, the structure of the bipedal robot consists of four joints and seven muscles in each leg, eight DoFs in total. Figure 2.2 illustrates the leg configuration, which includes a hip joint, a knee joint, an ankle joint, and a toe joint, all placed in the pitch axis. These joints are connected to specific muscles: the gluteus maximus (GM) and iliopsoas (IL) actuate the hip joint, the biceps femoris (BF) and vastus lateralis (VL) actuate the knee joint, the soleus (SO) and tibialis anterior (TA) actuate the ankle joint, and finally, the plantar intrinsic muscle (PIM) actuates the toe joint.

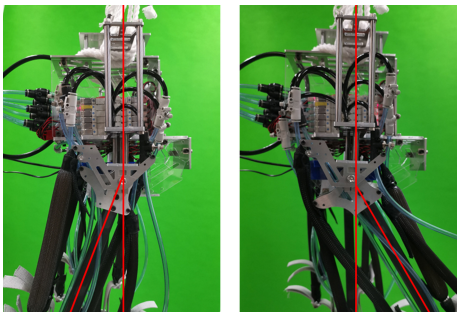

Figure 2.3: Hip joints range from -20°to 30°.

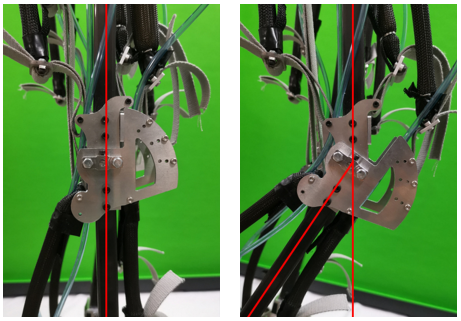

Figure 2.4: Knee joints range from -45°to 0°.

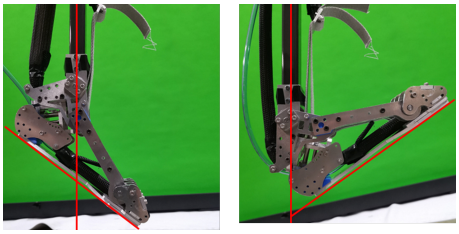

Figure 2.5: Ankle joints range from -30°to 45°.

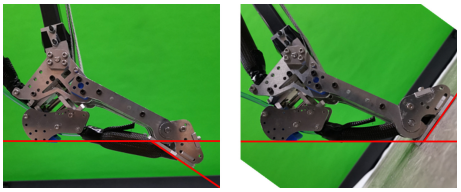

Figure 2.6: Toe joints range from -35°to 60°.

The bipedal musculoskeletal robot named "PneuTurn-T" (see Figure 2.1) was developed for experimental purposes in this study. The robot has a dimension of 300 mm × 1,000 mm × 300 mm (W × H × D), with a weight of 6.4 kg. During the experiments, the robot was connected to an external power supply and air supply to operate.

2.2.2 Pneumatic actuators and controller

The musculoskeletal robot is driven by pneumatic actuators called pneumatic artificial muscles (PAMs) or the McKibben's artificial muscles. The PAMs are capable of acting as muscles of the biological being by contracting and stretching themselves, pulling tendons, and driving the joints. Pneumatic actuators offer some advantages over hydraulic or electric actuators, other than their elasticity. They provide a simple and cost-effective solution with a high power-to-weight ratio, making them suitable for building lightweighted robots. The PAMs offer quick and responsive

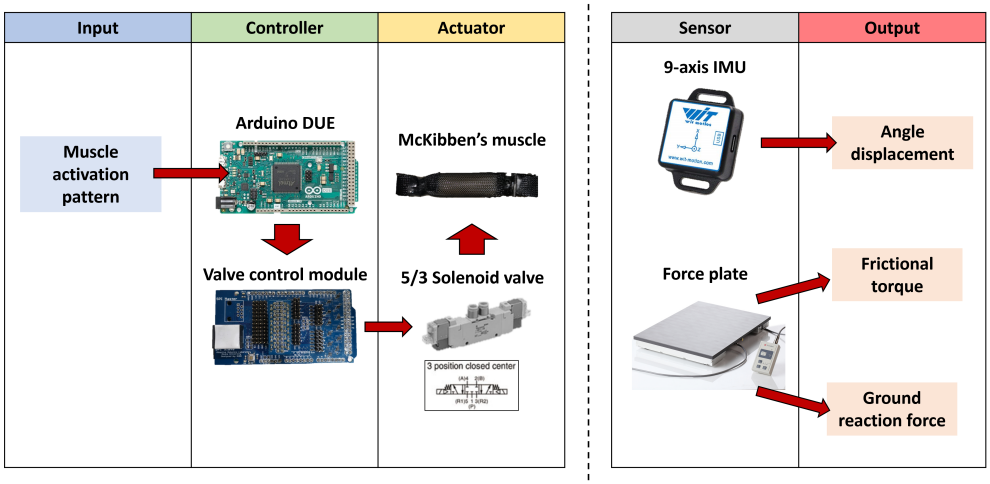

Figure 2.7: The control system of the musculoskeletal robot and data acquisition method.

operation, allowing for rapid changes in direction with a wide range of motions, and can be easily replaced to change the parameter. Our McKibben's muscles are made of an 8-mm-diameter rubber tube with 1 mm thickness, with both ends plugged using pneumatic fittings; one closed-end and one open-end connected to an air tube and covered with polyester braided sleeves. The length of each PAM and its contraction ratio is calculated before the fabrication of the PAMs and then measured and tested before being implemented in the robot to accomplish the desired range of motion, referring to the average human range of motion (see Figure 2.3 to 2.6).

The control system of the robot is depicted in Figure 2.7. To control the PAMs, a microcontroller (Arduino Due) connected to our laboratory valve control module was employed. The solenoid valves (VQZ1321-6L1-C6) used for controlling the muscles are of the five-port, three-position type, capable of supplying, exhausting, and closing the air opening. The musculoskeletal robot consists of 12 valves corresponding to 12 schematically connected muscles, as shown on the left side of Figure 2.2, as one solenoid valve is capable of controlling a single muscle activation pattern. The supplying air pressure used in this study is 0.6 MPa.

The slip-turning motion of the robot is achieved by providing a muscle activation pattern to the controller. The muscle activation pattern was created to actuate all 14 PAMs simultaneously in the correct sequence to realize the motion.

2.3 Slip-turning motion

2.3.1 Slip-turning strategy

The slip-turn was previously demonstrated by some motordriven robots: WABIAN-2 [81], HRP-4C [83], and others [85]. Contrary to these robots, the slip-turning of our musculoskeletal robot refers to human biomechanics, where the slip-turning often occurs shortly for a small duration during walking. Among the aforementioned research, one research distinguishes the turning mechanics of humans into two types [75]: step turn and spin turn. The spin turn strategy of these studies was used as the base model of our slip-turning motions for recreating the muscle activation pattern by studying the muscles' activation timing with the electromyography signal (EMG) during the spin turn.

2.3.2 Muscle activation pattern

The control method for the bipedal robot is a joint control method that directly controls the angle of each joint through the activation of PAMs. To realize the slip-turning motion, the muscle activation pattern was specifically generated to replicate the joint movements observed during human spin turns. Each muscle was activated for a comparable duration and speed as indicated by the reference EMG pattern and joint angle measurements. The EMG pattern was used for generating the activation timing, as the signal provided explicit indications of muscle activation without any delay caused by signal transmission. In contrast to an electroencephalogram (EEG), the EMG pattern allowed for more accurate and immediate detection of muscle activation, making it a suitable choice for generating precise activation timings in the control process. By studying the EMG pattern, we can roughly estimate the activation time of the muscles. When the graph indicates muscle activation, the corresponding valve connected to the PAM represents that the muscle will undergo a change in its state. This change may involve supplying air, exhausting air, or closing the air supply, depending on the specific requirements of the muscle's activation. Previous studies have highlighted that determining the timing of muscle activation alone does not provide sufficient information [57]. Once the activation timing is established, additional adjustments need to be made through a process of trial and error to determine the appropriate valve states. This iterative approach allows for fine-tuning and optimization of the muscle activation patterns to achieve the desired performance and motion of the musculoskeletal robot.

The activation time of the PAMs is controlled through the microcontroller, changing the valve state while causing some delays between each phase. The angular speed of each joint is a fixed value, manually adjusted by using flow control valves (SMC AS2002F-06) connected to the supplying air tube. In comparison to their experiments [75], our robot turns while standing still, instead of turning while walking, partials of the pattern were modified to adjust to our experiment. The total duration of the slip-turning pattern is 800 milliseconds. The completed muscle activation pattern used in this

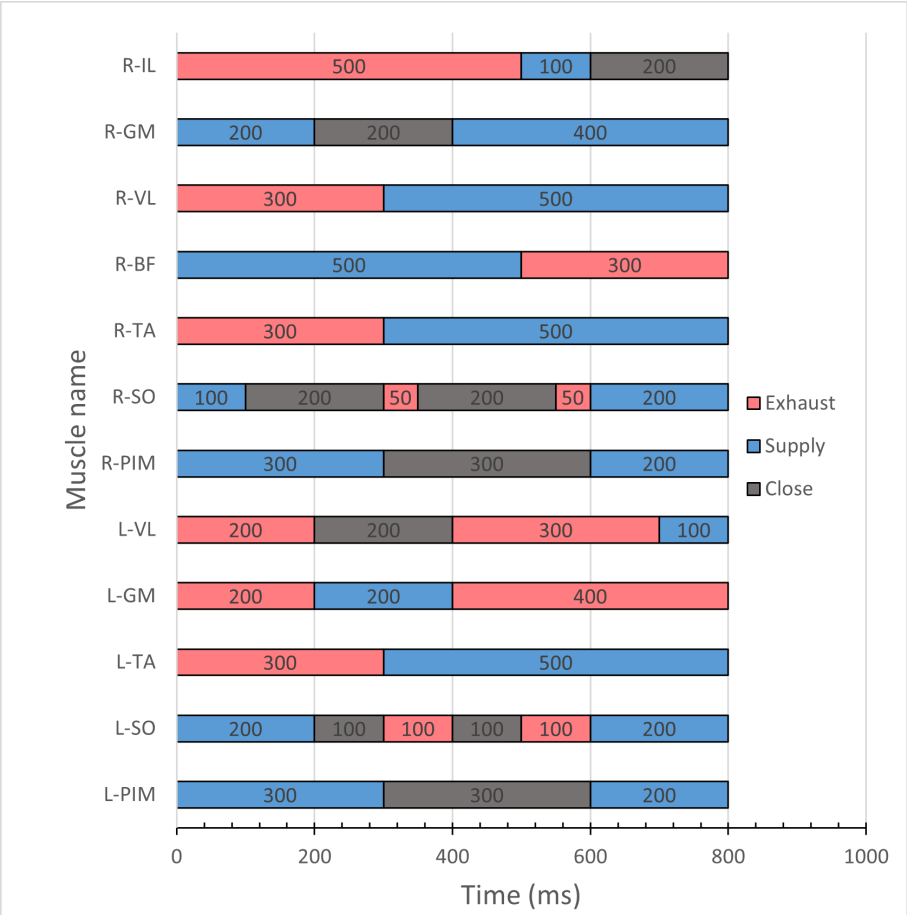

Figure 2.8: Muscle activation pattern for the slip-turning motion on the toe joint. Twelve valves was used for controlling all of fourteen PAMs. Muscle name with R-XXX are the activations of the right leg while L-XXX are the muscles on the left leg. The red portions indicate exhaustion of the PAMs, the blues indicate supplying air to the PAMs, and the gray portions indicate the valve's closing period.

study is shown in Figure 2.8. Figure 2.9A, B depict the motion from standing to slip-turning.

Figure 2.9B describes the direction of each joint corresponding to the muscle activation pattern, noting that all joints and muscles behave similarly, as shown in the spin turn study. Figure 2.9C presents the simulation of the motion by using the joint control method. In the simulation, the forward kinematics method was used to calculate the joint positions, starting from the left toe and progressing upward to the left hip, toward the right hip, and then downward to the right ankle. Additionally, inverse kinematics was utilized to determine the placement of the right foot, pivoting around the toe joint, which demonstrates the foot's adaptability and flexibility in response to different ground levels. The estimated COM trajectory is also shown in Figure 2.9C. The simulation

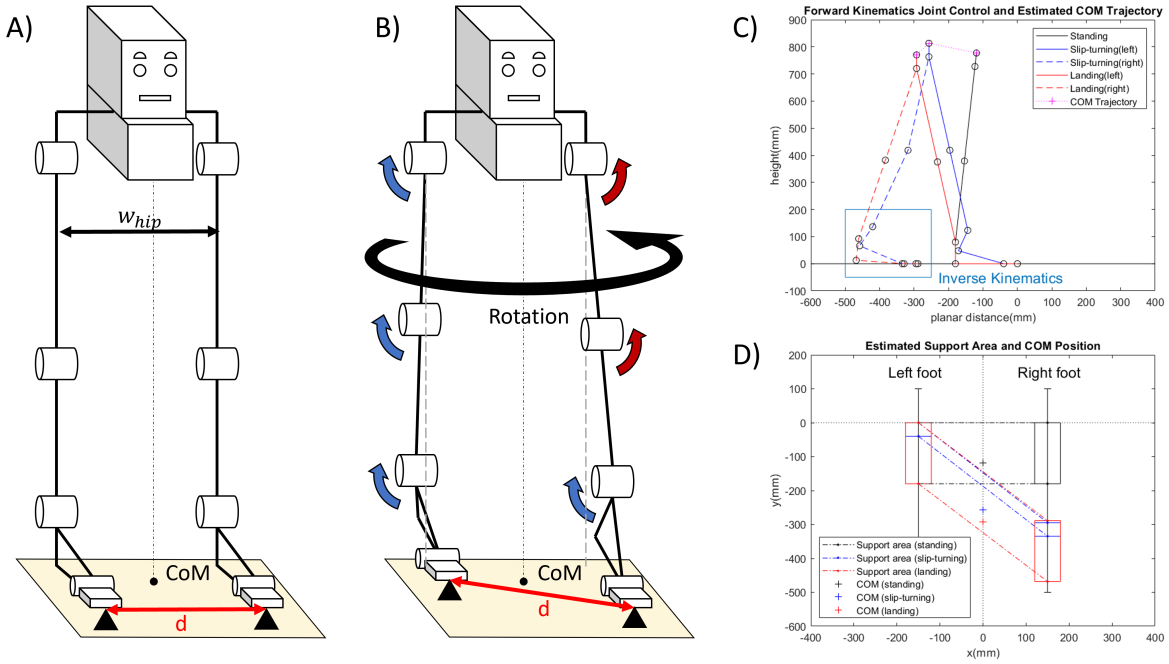

Figure 2.9: Slip-turning strategy based on the design from the human spin turn. While the width of the hip w_{hip} stays the same before (A) and after (B) the motion, there was a small increased in the toe distance d from foot displacement after the slip-turning. (C) Simulation of forward kinematics by joint control method to find the estimated COM trajectory and foot placement (D) Comparing the estimated support area to the COM position

was conducted with both hip joints set at the same height and without lateral swaying. The support polygon was calculated based on the foot position. Figure 2.9D illustrates the support polygon with the COM position, providing visual confirmation of the system to validate the equilibrium and stability of the system.

2.4 Experiments

The experiments were conducted to investigate the impact of utilizing toe joints and the PIM in the slip-turning motion. The realization of the slip-turning motion, implemented in our robot "PneuTurn-T" using the muscle activation pattern, is shown in Figure 2.10. This motion was utilized consistently across all experiments, with slight variations in PIM activation based on the specific foot condition under investigation, allowing for data collection and analysis (see Figure 2.12).

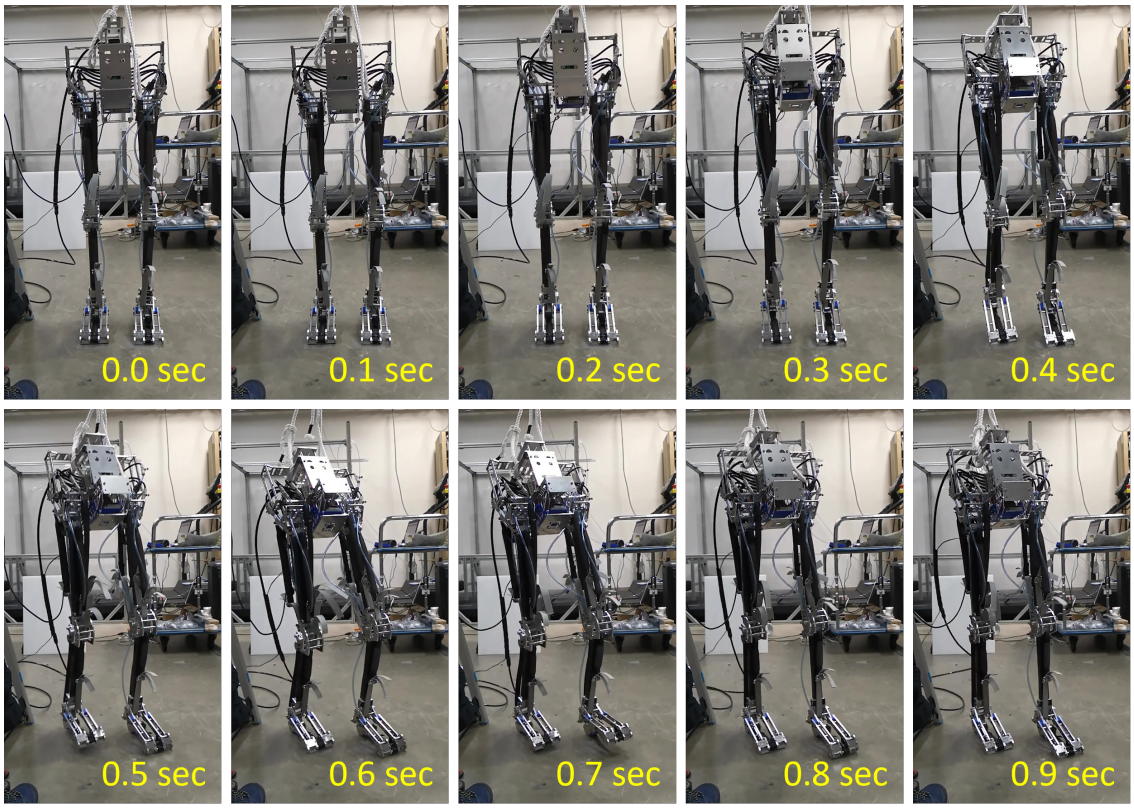

Figure 2.10: The realization of the slip-turning motion on toe joint of the musculoskeletal robot "PneuTurn-T"

2.4.1 Experimental setup

The experimental setup for data collection is illustrated in Figure 2.11. The robot was placed on a platform, with its left leg positioned on a force plate (TF-3040), for measuring the ground reaction force and frictional torque of the primary supporting foot. To monitor the robot's rotational angle, a 9-axis IMU (BWT901CL) was installed on its body, with a positive angle indicating counterclockwise rotation as the robot turns to the left. Additionally, an IMU was affixed to the toe joint to measure the toe-lifting angle.

2.4.2 Different conditions of toe joints

The objective of the experiments was to investigate the effects of slip-turning on different types of feet. Four distinct foot configurations were utilized in the experiments, each contributing to the study as shown in Figure 2.12. The first type is a fixed toe foot, which emulates the behavior of a rigid foot or a foot without a toe joint. The second type is an unrestricted toe foot without PIM

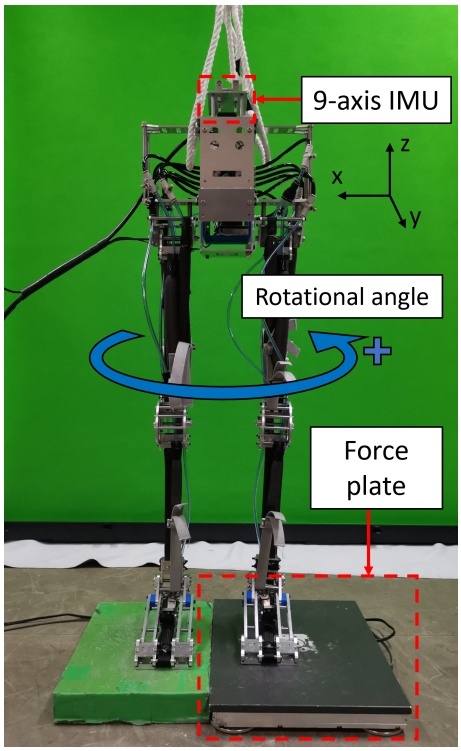

Figure 2.11: Experimental setup for collecting data with an IMU and a force plate under the left foot.

attachment, allowing the toe to move freely and lack stiffness. The third type is a passive toe foot with a movable toe connected to the PIM, where the length of the PIM is predetermined by the supplied volume with constant stiffness. The fourth type is an active toe foot, where the toe is actively actuated in response to the motion, generating slight movement in the toe joints.

The first experiment aimed to compare the turning behavior of a foot with a fixed toe to a foot with a passive toe, demonstrating the advantages of utilizing toe joints in slip-turning motion. In the second experiment, the toe-lifting angle was compared between a foot with an unrestricted toe and a foot with a passive toe, highlighting the role of foot stiffness provided by the PIM. Lastly, an experiment was conducted to compare the ground reaction forces among all foot types, investigating propulsion and postural stability during similar robot movements. The summary of all three experiments is shown in Figure 2.12B.

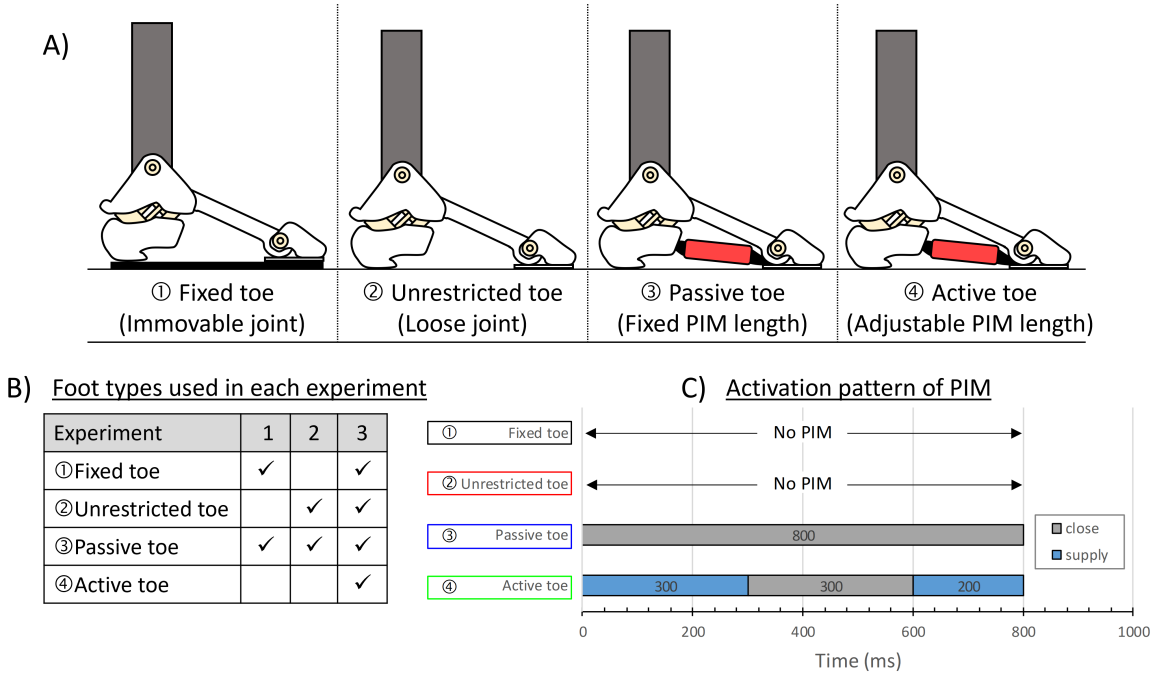

Experiment	1	2	3
①Fixed toe	✓		✓
②Unrestricted toe		✓	✓
③Passive toe	✓	✓	✓
④Active toe			✓

Figure 2.12: Different conditions of the toe were used in the experiments. (A) From the left: "Fixed toe" is a foot with a fixed toe joint acting as a rigid foot, "Unrestricted toe" is a foot with a loose toe joint without PIM, "Passive toe" is a foot with a fixed PIM length, and "Active toe" is a foot with an adjustable PIM length which is actuated at a certain moment. (B) The summary of foot conditions use for comparison in each experiment. (C) The activation pattern of PIM.

2.5 Results

2.5.1 Slip-turning in foot with and without the toe joint

In the first experiment, the contribution of using the toe joint in the slip-turning motion was examined by comparing the foot with a fixed toe to the foot with a passive toe. The results of frictional torque revealed a noticeable change in frictional torque at 0.2 s, as depicted in Figure 2.14. The foot with the toe joint exhibited a smaller frictional torque during the motion, likely attributed to the reduction in the foot contact area and its diagonal length [83], as illustrated in Figure 2.13.

The second results show the rotational angle of the robot's body measured by the 9-axis IMU installed on the robot's body during slip-turning motion, as shown in Figure 2.15. The results in Figure 2.16 demonstrate that the foot with a fixed toe achieved a rotational angle of approximately 50°, whereas the foot with a passive toe achieved a significantly improved rotational angle of up to 70°. This improvement suggests enhanced mobility, potentially resulting from the reduced frictional torque and increased flexibility of the foot with the passive toe joint [87, 91, 92].

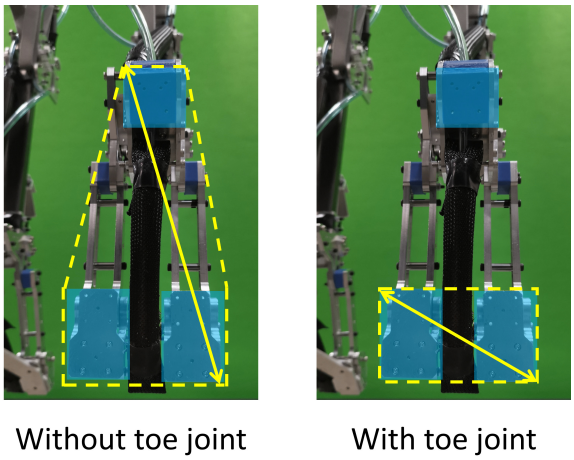

Figure 2.13: The diagonal length of the foot contact area was reduced by the utilization of the toe joint.

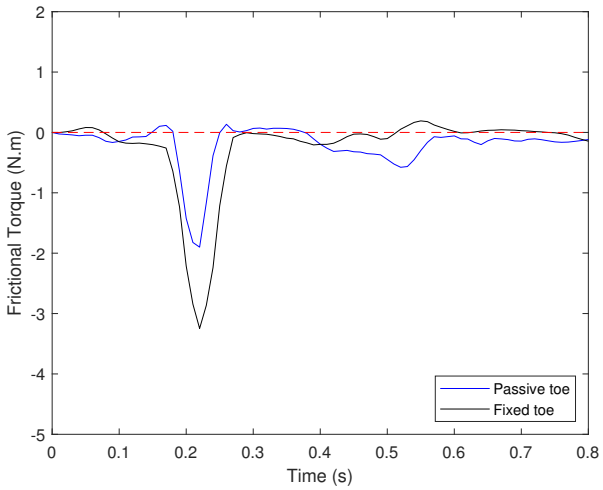

Figure 2.14: The results of frictional torque measured during the slip-turning motion. The frictional torque was reduced in the foot with toe joint ("Passive toe") compare to the foot without toe joint ("Fixed toe").

2.5.2 Foot stiffness and toe over-dorsiflexion

In the experiment comparing slip-turning on the foot with and without foot stiffness from the PIM, restraining the motion, the toe-lifting angle θ_L was measured to analyze the results. Figure 2.17 displays the toe-lifting angle, which was measured using an additional 9-axis IMU installed on the robot's toe. Figure 2.18 indicates that the foot with an unrestricted toe or the foot without the PIM

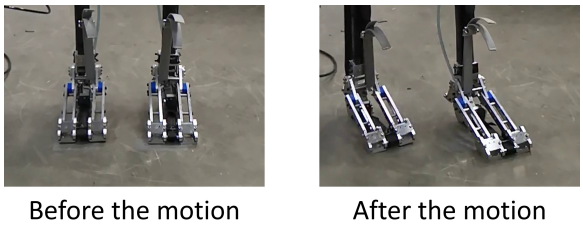

Figure 2.15: The direction of the foot was changed along with its body alignment after the slip-turning motion.

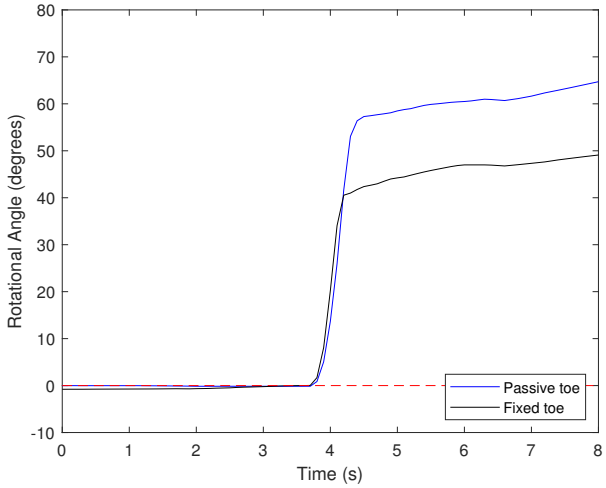

Figure 2.16: The results of rotational angle measured during the slip-turning motion. The foot with "Passive toe" yielded a larger rotational angle compared to the foot with "Fixed toe".

is more prone to experiencing toe over-dorsiflexion, while the stiffness provided by the PIM in the foot with a passive toe helps restrain and prevent over-dorsiflexion.

The occurrence of toe over-dorsiflexion can lead to a loss of postural balance in the robot due to reduced foot contact area in an unstable state, similar to individuals with floating toes [143].

2.5.3 Propulsion and postural stability

The final experiment aimed to compare the ground reaction force (GRF) among all types of feet to assess the impact of the changing foot stiffness on the motion. The GRF pattern provided insights into the contributions of foot stiffness (see Figure 2.19). The results indicated that at the beginning of the motion, specifically at 0.2 s, the foot with an active toe exhibited the strongest propulsion among the four types of feet, followed by the fixed toe, passive toe, and unrestricted toe, respectively.

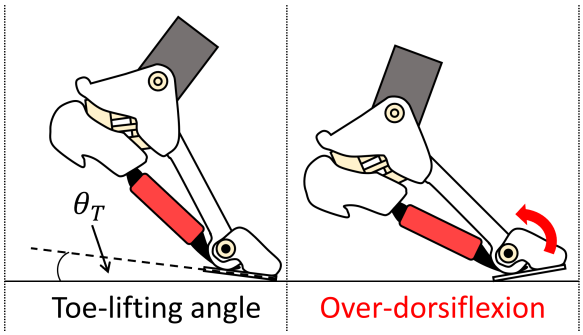

Figure 2.17: Toe-lifting angle and the over-dorsiflexion of the toe joint.

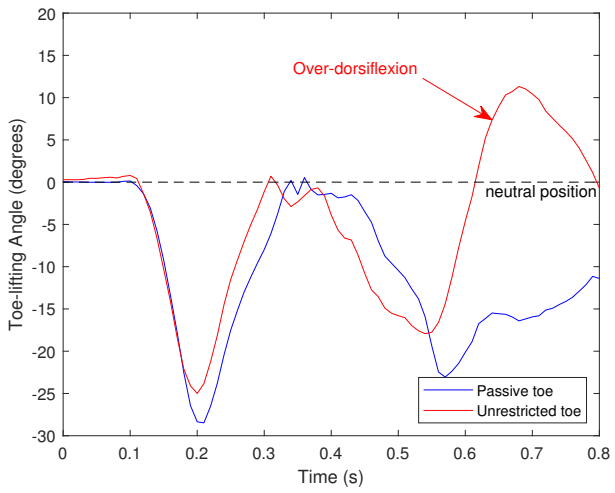

Figure 2.18: The results of toe-lifting angle measured during the slip-turning motion. The foot with a "Passive toe" prevent the toe joint from over-dorsiflexion compared to the foot with a "Unresrticted toe" without toe stiffness.

The strong propulsion might indicate the capability of enhancing the motion of the toe joint with the PIM (Hughes et al., 1990; Agarwal and Popovic, 2018), transmitting the force from the upper leg to the phalanges, increasing its push-off force.

On the other hand, following the initial propulsion at 0.2 s, a noticeable decrease in ground reaction force (GRF) was observed in all types of feet, suggesting a potential disruption or an enhancement in postural stability during the robot's motion. A higher GRF value indicated a greater weight transfer toward the left foot in the front, shifting the COM position closer to the anterior direction, which is favorable for maintaining the robot's posture at the end of the motion.

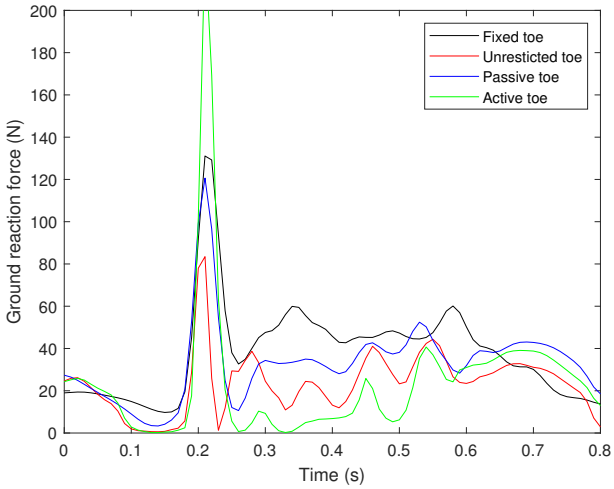

Figure 2.19: The results of ground reaction force.

2.6 Discussion

As our robot was designed with a human-like musculoskeletal structure, the position of the COM of the body was supposed to be placed in a similar manner. In humans, the support polygon aligns with the direction of the toes, pointing toward the anterior side of the body. During the neutral stance of a human, the COM tilts slightly forward in favor of balancing the whole-body stability, where the shifting of the COM is possible within the area of the support polygon. However, our robot, lacking an upper body, exhibits a posterior inclination of the COM, making it challenging to achieve a proper positioning of the COM for maintaining postural stability. Moreover, during rapid motions, although the foot structure aids in stabilizing the body, the absence of a balanced body weight amplifies the robot's backward tendency, further compromising postural stability. Nonetheless, this characteristic of the robot could be utilized to further investigate the body stability in the absence of upper extremities, offering potential applications in medical practices for patients with upper-limb paralysis.

Due to the compressibility of air, the robots driven by the PAMs provide lower accuracy of joint control and unstable velocity [68, 80, 69], which made them reluctant to achieve the task in the best manner constantly. Combined with the feedforward system of the robot, without any feedback control to improve the motion, and attempt to improve the motion solely by its structure and fine-tuning, making it even more difficult to remain in the right posture.

As previous studies have mentioned, the PIMs are more likely to contribute to foot stabilization than to balance control during postural challenges [134, 133], such as body swaying, and the role of the PIM in this study focuses on the stabilization of the foot instead of attempting to control

postural stability directly.

2.7 Conclusion

This paper demonstrated a turning motion of the musculoskeletal robot, which is usually unfavorable to execute due to its limited range of motion and complex controls. The bipedal robot could realize the slip-turning motion on toe joints about its yaw axis, while all eight joints of the robot were placed on the pitch axis. The foot with toe joints has enabled the heel-off motion of the musculoskeletal robot and could reduce the foot contact area during the turning motion compared to the rigid foot with a fixed toe, resulting in a reduction of frictional torque, minimizing its power, and an increase in the rotational angle. The second experiment proved that by using the PIM to restrain the toe joint, the robot could prevent the over-dorsiflexion of the toe, which can contribute to the improvement of static postural stability in the anterior–posterior direction. Meanwhile, the active toe could generate an even stronger propulsion, which can be useful in a quick motion. The unique structure of the human foot needs to be studied further to understand its contributions to the intrinsic tension force and the stability of the foot in a quick motion. Our findings contribute to the advancement of robotic systems that mimic biological structures and movements and widen the possibilities for future research in the field of robotics.

Future works include studies for optimizing control strategies for the PIM, exploring the adaptability of the foot, enhancing the motion, and integrating sensory feedback into the control system. These advancements will contribute to the development of more versatile and capable robots with improved locomotion abilities, enabling applications in various fields such as search and rescue, exploration, medical practice, and human-assistive robotics.

Chapter 3

Intrinsic Toe Joint Stabilization with DSP-SLIP Model

This chapter based in following publication:

K. Nipatphonsakun, T. Kawasetsu, and K. Hosoda, "Intrinsic Toe Joint Stabilization in Foot-Slip Turning Motion of Musculoskeletal Robot with DSP-SLIP Model", Advanced Robotics, pages 1-13, 2024.

Abstract

This paper introduces the foot-slip turning motion by combining a slider-like mechanism with the double-support parallel spring-loaded inverted pendulum model, in which the musculoskeletal robot uses the model to simplify the slip-turning motion with its compliant structure and utilizes the foot muscle to improve its postural stability. The slip-turning motion, characterized by slight movements for swift turning via foot slippage, is advantageous for musculoskeletal robots due to their limited range of movement. The challenge lies in the reduced support area during the motion, which impacts stability. In our previous study, the robot "PneuTurn-T" successfully executed said motion, whereas the details of the turning mechanism were lacking. This study investigated the utilization of leg compliance in the motion and its static postural stability in the landing stance. Experimental results exhibited a leg compression rate derived from the collected data in the early phase of the motion and validated intrinsic toe joint stabilization with foot muscle for passive postural control. The ground reaction force proves the capability to maintain the posture for 130% longer in the foot with plantar intrinsic muscle. Despite structural challenges, this approach shows promise for musculoskeletal robots, highlighting their ability to handle a turning task with simple control.

3.1 Introduction

Turning motions in bipedal locomotion pose a considerable challenge to musculoskeletal robots due to the demand for complex, precise control and the extensive range of motion. Traditionally, motor-driven robots often need multiple steps and precise coordination to execute the task [17, 76]. Compared to the musculoskeletal robots [55, 56], which mainly depend on the feedforward system and often simplify their structure to reduce the load of complexity control [53], make the task even more challenging due to the lack of precise control and their limited range of movement. Many of the advantages of musculoskeletal robots and their bio-inspired features have been studied in the past, such as enhancing the motion [107, 117, 137], maintaining the foot shape [116]. The compliance of the musculoskeletal structure is also researched in the motion [146], or using the compliance to improve the stability of the motion structure[148]. While we need the advantages of the musculoskeletal structure, we also need them to overcome their structural and architectural challenges to realize a complex motion. To find the solution to these problems, a strategy to execute the task while minimizing the control effort or the required range of motion is needed.

The slip-turn motion of bipedal robots has been extensively studied for improved maneuverability and stability. WABIAN-2 compared "slip-turn," the turning strategy that utilizes foot slippage, and "step-turn," a strategy that primarily relies on precise footstep planning, finding that the foot-slip turning strategy reduced the energy consumption [81]. Yeon et al. proposed a slip-turning on a single support, a quick slip-turn on one leg, enhancing a fast-turning performance and stability [85]. Miura et al. studied the slip-turn of the robot with the precise control approach, in which they can predict the amount of slippage from the calculation of friction, foot shape, and planned trajectories [84]. The robot HRP-4C demonstrated a slip-turn on its toes utilizing a rotation model [83]. However, those robots are controlled by the traditional method, which relies heavily on precise control, one of the weaknesses in the musculoskeletal robot system. In our previous research, our musculoskeletal robot "PneuTurn-T" realized the slip-turning motion [157], while the robot has much fewer degrees of freedom (DoFs) and is controlled exclusively with a feedforward control system. The combination of slip-turning and a toe joint mechanism allows the musculoskeletal robot to execute turns with minimal movements. Nevertheless, the explicit description of the turning strategy causing the body to rotate has yet to be revealed in our previous study.

To unravel the perplexing mechanism behind the motion, this paper proposed a "Double-Support Parallel Spring-Loaded Inverted Pendulum (DSP-SLIP)" model based on the traditional SLIP model [28, 48] to simplify the bipedal robot model in executing the foot-slip turning motion with the slider-like mechanism. However, the struggle that the robot finds in the slip-turning motion is that during the motion, the support area of the robot tends to be small, which might cause its center of mass (CoM) to fall out of its support polygon, causing the robot to be less stable without proper postural adjustment. A method to improve the stability of motion is also presented in this paper, which includes the composition of foot support polygon and toe muscle strength. First, to improve the

stability margin, we can improve the support polygon of the robot. Kimura et al. [145] use a passive wheel and a stability margin maximization method to approach this technique. However, in the musculoskeletal robot, such a method cannot be applied to its structure, which brings us to the combination of the second solution: the application of the plantar intrinsic muscle (PIM). As considerable research has studied the functions of foot muscles in humans, one of the PIM features, is that it may serve as a local stabilizer for the foot [131, 134], especially when there are large fluctuations in the center of pressure (CoP) [133], and it has some contribution to overall static [140, 143] or dynamic stability [135, 144, 158]. We hypothesize that in the musculoskeletal robot, the PIM will act as the stabilizer of the toe joint, thus stabilizing the foot posture and improving the overall postural stability of the musculoskeletal robot.

In this study, our objective is to investigate slip-turning motion by proving the importance of the compliance structure in realizing motion with our novel DSP-SLIP model and utilizing its passive structure to improve its postural stability. Two experiments were conducted: the first investigated leg compliance with the musculoskeletal structure, and the second investigated intrinsic toe stabilization with PIM. After the experiments, the data was collected, processed, and analyzed. The insights gained from this study provided the potential possibility of a strategy to achieve a complex task with a feedforward control system with the stabilization from its structure, reducing the complexity in its control system.

3.2 Foot-Slip Turning with DSP-SLIP Model

3.2.1 Foot-Slip Turning Motion and Slider-Like Mechanism

In our previous research, we successfully implemented the slip-turning motion in the musculoskeletal robot "PneuTurn-T" [157] by developing a muscle activation pattern inspired by the spin turn observed in humans during walking [75], utilizing muscle synergies as a reference. The robot has only eight joints, four on each leg, and all joints are placed in the pitch direction (see Figure 3.1a). However, in this study, neither the turning mechanism nor the static model of the robot was explicitly defined, thus raising the perplexity of how the robot, with such a simple structure and without any joint placed in the yaw direction, can cause such a motion.

In this research, we envision the foot-slip turning mechanism of our robot as a combination of the slider-like mechanism illustrated in Figure 3.1 and the compliant leg structure. The foot-slip turning motion is separated into three stages, from standing posture progressing to turning and ending with bouncing and landing. First, from the standing stance, the robot is standing on its feet, which are in complete contact with the ground (Figure 3.1a). The motion generated with the forward kinematics starting from its left leg travels up to its hip; the right leg maintains a matching hip level while achieving its desired position of the right foot with its adaptive structure. Next, in the turning phase (Figure 3.1b), when the foot position changes a little, the body begins to rotate

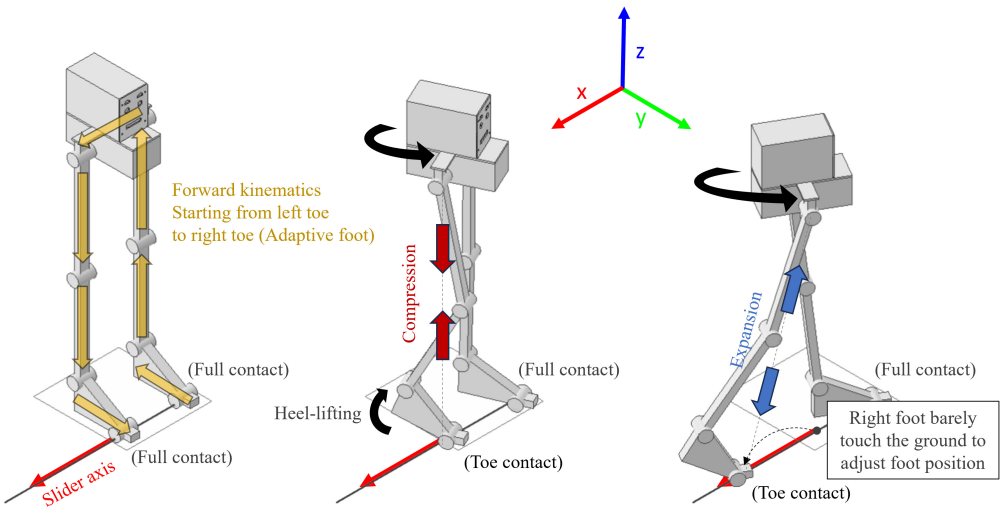

Figure 3.1: Three stages of the foot-slip turning motion. The motion progresses from (a) standing to (b) turning to (c) bouncing and landing. (b) and (c) show leg compliance, which allows a little error in both the hip level and the position of the right foot while storing up the displacement as the energy in its right leg is compressed. This compliant structure is crucial as it renders the motion possible for the musculoskeletal robot to compensate for its lack of precision.

accordingly. During this stage, the leg of the robot becomes compliant. Note that heel-lifting is necessary as the robot tries adjusting its foot position, causing it to lose a small area of its support margin. Finally, when a certain amount of force is reached, the compressed stage of the right leg will be released, causing a rapid expansion of the leg and bouncing its leg backward before landing in a new position (Figure 3.1c).

Figure 3.2 explains the slider-like mechanism. The sliding occurs in the robot's adaptive right foot. As the hip level is maintained by its compliance structure, and the robot only has joints placed in the pitch direction, the angle between the pelvis link and both legs stay perpendicular to each other. Assuming there was no foot slippage along the y-axis, the body rotational angle θ_{rot} changes in response to an increase in the foot distance d, made possible by the variable length L_v. The correlation between the foot distance d and the body rotational angle θ_{rot} is represented by Equation 1.

$$d = L_p \cos\theta_{rot} + L_v \sin\theta_{rot} \tag{3.1}$$

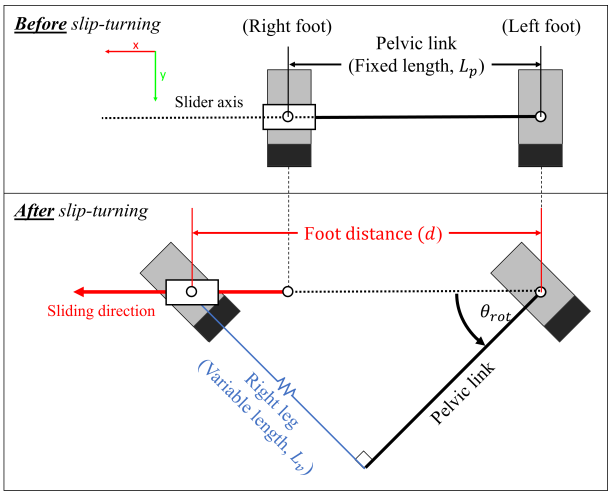

Figure 3.2: The slider-like turning mechanism of the robot, with the right foot moving along the sliding axis while the body revolves around the left foot. The light grey squares indicate the feet, the dark grey squares indicate the toes, and the red arrow shows the direction of the foot sliding. The pelvis link of the robot, represented by the black line, has a fixed pelvis length denoted as L_p. The right compliant leg, depicted by the blue line, has a variable length denoted as L_v.

3.2.2 Body Rotation with the DSP-SLIP Model and Compliant Leg Structure

This paper used the "Double support parallel leg spring-loaded inverted pendulum" model or the "DSP-SLIP" model to simplify the robot's turning motion, as shown in Figure 3.3a. The model sees the robot as two spring-loaded inverted pendulum (SLIP) models connected with a rigid pelvis link to maintain its hip level horizontally parallel to the ground. While the robot's left leg mainly acts as the reference hip level and the pivot point where the free moment is generated, the right leg generates most of the force and torque contributing to the motion while keeping its right foot's adaptability to adjust its foot to the ground surface. When the inverted pendulums create torque on both hips, the torques applied to the left and right hip opposing each other cause the pelvis to rotate the body around (See Figure 3.3a (right)).

As mentioned previously, the robot's compliant structure plays an essential role in the motion, as it allows a small structure deformation due to its passive joint deformation from using pneumatic actuators. The deformation allows a slight error in the joints and the position of the right foot, which can be utilized to compensate for the lack of precision in the PAMs-driven musculoskeletal robots. The compliant structure also helps the legs adapt to the environment passively, regardless of the posture, keeping the foot on the ground with its intrinsic muscle tension from the PAMs. With this structure, the robot will allow minimal structural deformation if the bending force does not exceed the resistance force (e.g., friction or ground reaction force (GRF)). While the foot position

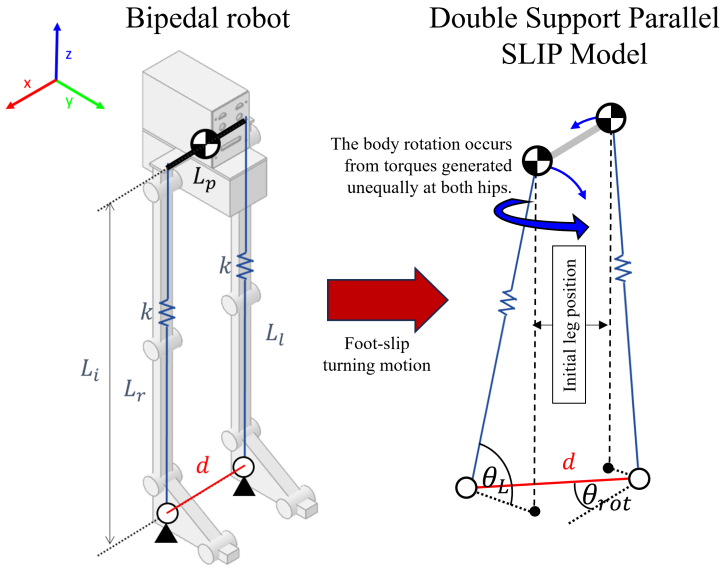

(a) Bipedal robot to DSP-SLIP model

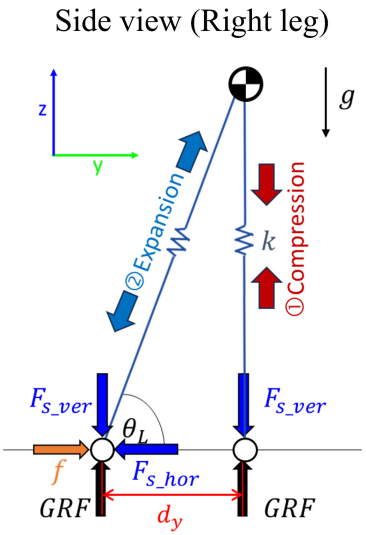

(b) Compression and expansion of the compliant leg (right leg)

Figure 3.3: (a) The DSP-SLIP model of the robot creates torques on both hips, which are connected to the pelvis link, rotating the body around its feet. (b) The compression and expansion of the compliant leg in the DSP-SLIP model. 1) In the compression state, as the leg moves backward, the foot remains in place when the maximum horizontal friction f has not yet been reached. 2) In the expansion state, the foot moves backward while adjusting the leg posture to the floor

remains in its initial position through frictional force with the floor, torque is generated on the robot's pelvis, inducing body rotation. Subsequently, when the maximum frictional force is reached, the foot smoothly adjusts to its proper position, where the leg has no internal compression (or at its resting leg length), maintaining the achieved turning angle from the torque.

According to Figure 3.3b, the spring-like compression force is separated into two directions along the vertical and horizontal axes. During the turning motion, the friction resists the slippage of feet, trying to make them stay in their initial position. As the leg progresses backward, the vertical force F_{s_ver} will gradually shift into horizontal force F_{s_hor}. The compression forces in each axis are described as

$$|F_{s\_ver}| = |F_s \sin\theta_L| = |GRF_{RightFoot}| \tag{3.2}$$

and

$$|F_{s\_hor}| = |F_s \cos\theta_L| < |f| = |\mu_s N| \tag{3.3}$$

Where F_{s_ver} represents the force along the vertical axis, F_{s_hor} represents the force along the horizontal axis, F_s characterizes the compression force within the compliant leg, θ_L denotes the angle between the floor and the leg, f represents the floor friction,μ_s describes the static friction coefficient and N indicates the weight of the robot putting on the leg.

3.3 Development of the Musculoskeletal Robotics Foot with Plantar Intrinsic Muscle

3.3.1 Robotics Foot with Plantar Intrinsic Muscle

Given the focus of this study on improving the postural stability of the slip-turning motion with toe joint stabilization, the robotic foot was implemented with a foot muscle to help stabilize the joint. The muscle helps stabilize the foot in the anterior-posterior direction. The pneumatic artificial muscle (PAM) was made to replicate the muscle features of PIM to actuate the joint. The muscle is made of an 8-mm diameter tube covered with polyester sleeves with a total length of 12 cm (measured from attached points). The muscle connects the foot from the heel to its toe, actuating the toe joint directly when supplied with air pressure. The toe joint has a movement range from -5° (downward, when actuated) to +60° (upward, unrestricted). The robotic foot was then integrated into the robot to assess its functionalities, as illustrated in Figure 3.4a.

As one of the functions of the PIM, the muscle can contract itself, stiffening the foot structure

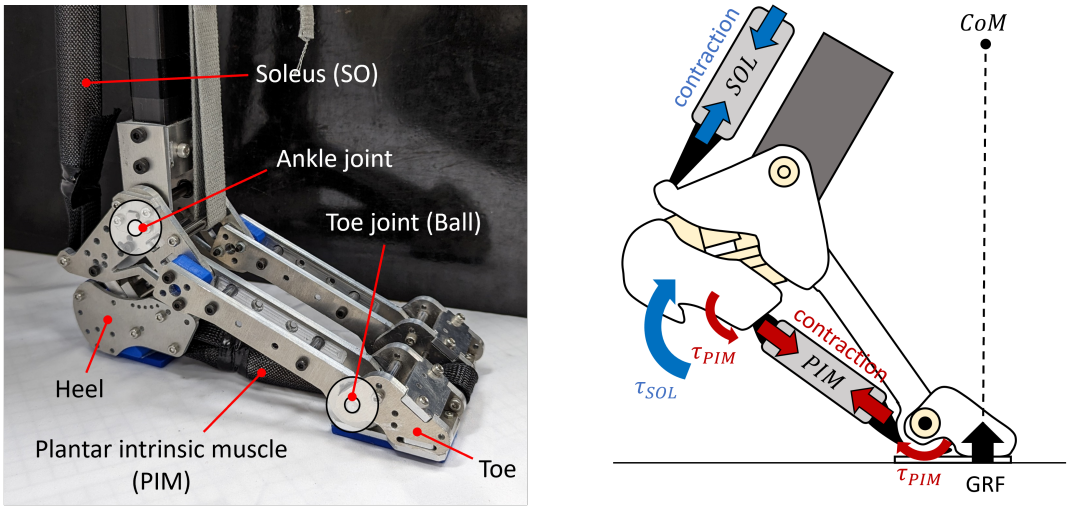

(a) (b)

Figure 3.4: (a) The structure of the robotics foot with toe joint and the PIM used in the experiments. (b) The contraction of PIM affects both the ankle joint and toe joint in heel-off posture. The torque generated from PIM τ_{PIM} acting on the ankle joint will resist the motion of the Soleus (SO) acting on the ankle, while the τ_{PIM} on the toe end will create a torque that keeps the whole toe on the ground.

to act as a foot stabilizer and preserving the foot's shape with the windlass mechanism. The PIM may minimize fluctuations during unstable states, such as heel-off or in a single support stance. During the single-leg stance, our body exhibits mediolateral (left-right) fluctuations. While the heel-off stances induce significant anterior-posterior (front-back) fluctuations due to the reduced foot contact area, comparable to standing without toe [134, 143]. Similarly, the PIM may help stabilize static posture during the turning phase of the slip-turning motion, where the support area was considerably reduced.

When the PIM is supplied, the muscle contracts and generates torques at both ends (see Figure 3.4b). At the ankle end, it creates a torque to resist a motion from the SO muscle. Meanwhile, torque at the toe end actuates the joint directly, making it possible to adjust the CoP or the position where the GRF is focusing on the toe.

3.3.2 Importance of Toe Joint Stabilization in Stability Margin

The stability of the posture is often related to its foot placement and body orientation, as it is crucial to control the robot precisely to place its CoM inside its stable boundary. For the musculoskeletal robot, which usually operates on the feedforward system, tasks that require high precision are difficult to achieve. Additionally, in bipedal robotics with musculoskeletal structure, apart from its advantages of lightweight hardware with strong force generation, they often come with jumpy and

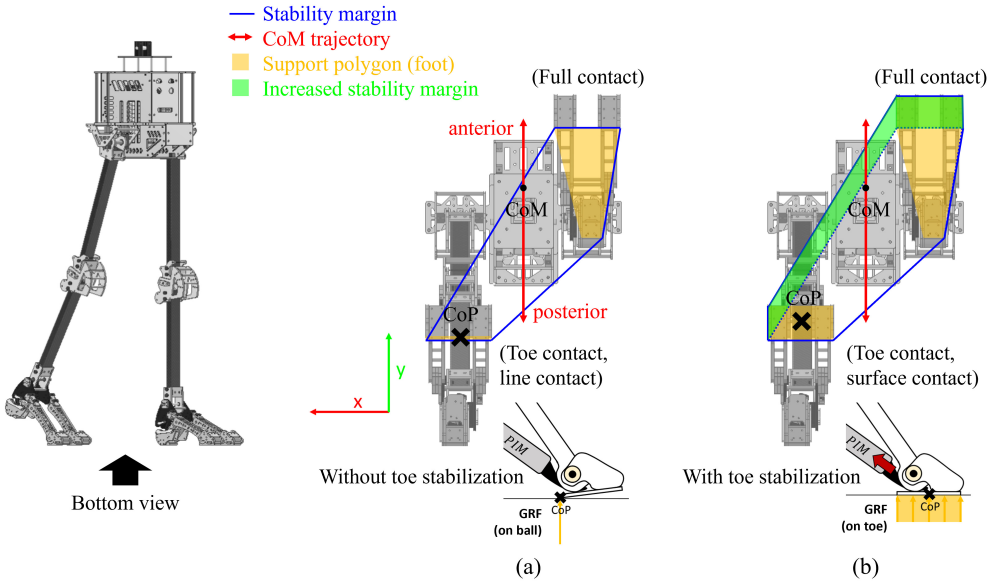

Figure 3.5: The stability margin of the robot during the turning motion in landing phase, observed from the bottom. (a) Without the toe stabilization, most of the robot weight will fall under the toe joint or ball directly without distributing the weight properly along the toe, making the anterior side unstable as it is close to its CoM. (b) With the toe stabilization with PIM, the toe will distribute the weight equally, passively extending the size of the support polygon covering up to the toe, effectively increasing its stability margin in the anterior direction.

unstable motion, especially in the foot-slip turning motion. While the motion efficiently reduces the robot's mechanical load to generate a turning motion with a few movements, it is a fast motion with a small support area [83] due to the incomplete foot contact area. The intrinsic stability of the motion needs to be improved to achieve a better stable motion.

As some research mentioned, the weak toe muscle induces falls in humans, indicating increasing instability [142]. Based on this theory, we adapt it to our robot system, which works biomechanically similarly to humans. In other words, the PIM acts as the toe joint stabilizer when supplied with air pressure, and without the air supply, the PIM will be too weak to help support the robot's weight (see Figure 3.5). In figure 3.5a, the robot stands on its legs without toe stabilization from PIM, causing the toe to be weak and unable to bear any of the robot's weight. As a result, most of the robot's weight falls directly on the ball of the foot. In figure 3.5b, where the toe stabilization was applied with the PIM, the robot can now adjust its CoP position and distribute its weight equally along its toe length, significantly improving its stability margin overall. The increased stability margin will be added in the direction of the toe or the anterior side of the robot, which can help improve the slip-turning motion as its ending posture shown in Figure 3.5a has the CoM placed very close to the margin on the anterior side of the robot which is very risky for the musculoskeletal

Table 3.1 The dimension of the robot

Parameter	Length (mm)
L_i	780
L_P	200
$L0$	50
$L1$	350
$L2$	300
$L3$	80
$L4$	140
$L5$	40

robot with strong and jumpy movements.

The improved margin on the anterior side Figure 3.5b could be beneficial if applied to the motion moving forward, such as walking, even if it is for static stabilization. As one research mentioned, improving the stability margin might help stabilize a dynamic motion as the improvement of static stabilization will help improve dynamic stability in the anterior-posterior direction [103].

3.4 Foot-Slip Turning Experiments and Results

3.4.1 Experimental Setup

The Musculoskeletal Robot "PneuTurn-T"

In the experiments, we used our musculoskeletal robot "PneuTurn-T"(Figure 3.6a), which successfully realized the foot-slip turning motion from our previous research [157]. However, the difference between this experiment and our previous one, which focused on realizing the motion, is that this research prioritizes studying its perplexing turning mechanism with compliance structure and using PIMs to improve the stability margin. The robot consists of eight DOFs, with four hinge joints revolving in pitch direction in each leg at the hips, knees, ankles, and toes. These joints are actuated by seven pairs of PAMs, as shown in Figure 3.6b. The PAMs are made with an 8-mm-diameter rubber tube with 1 mm thickness covered by polyester braided sleeves. The PAM actuators are supplied through an external air supply with an air pressure of 0.6 MPa. The robot has a total weight of 6.2 kg. Table 3.1 and Table 3.2, respectively, describe the dimension and the musculoskeletal structure. The robot controls with a feedforward control system by inputting the muscle activation pattern (see Figure 3.7b) to control the valves by programming through the microcontroller (Arduino MEGA 2560 Rev3) connected to our valve control board. The overall experimental setup is shown in Figure 3.7a.

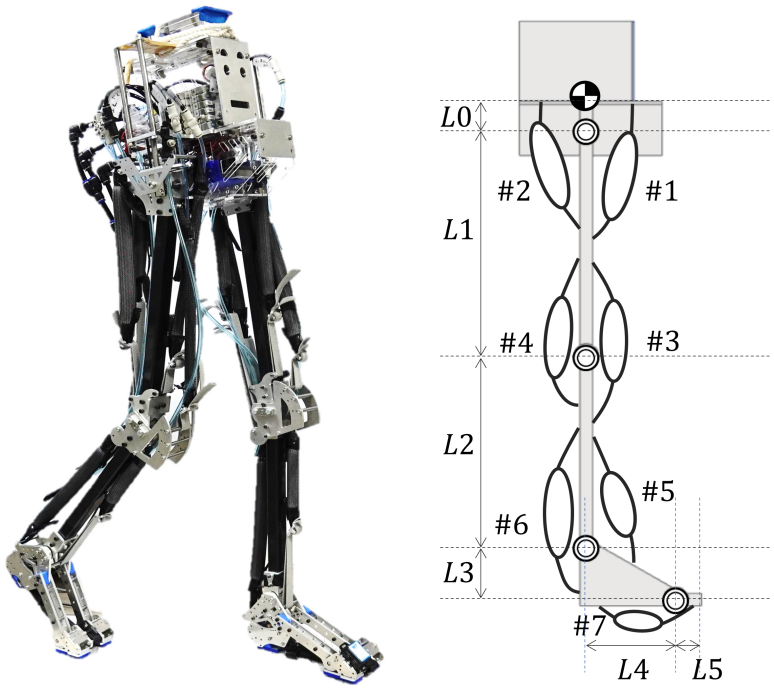

(a) (b)

Figure 3.6: The structural design of (a) The musculoskeletal robot "PneuTurn-T" used in the experiments. (b) The dimension between CoM and each joint is shown in Table 3.1. The figure also shows the muscles' placement, which the muscle name describes in Table 3.2 with the corresponding number.

Table 3.2 The muscle components of the robot

Muscle Number	Muscle Name
1	Iliopsoas (IL)
2	Gluteus maximus (GM)
3	Vastus lateralis (VL)
4	Biceps femoris (BF)
5	Tibialis anterior (TA)
6	Soleus (SO)
7	Plantar intrinsic muscle (PIM)

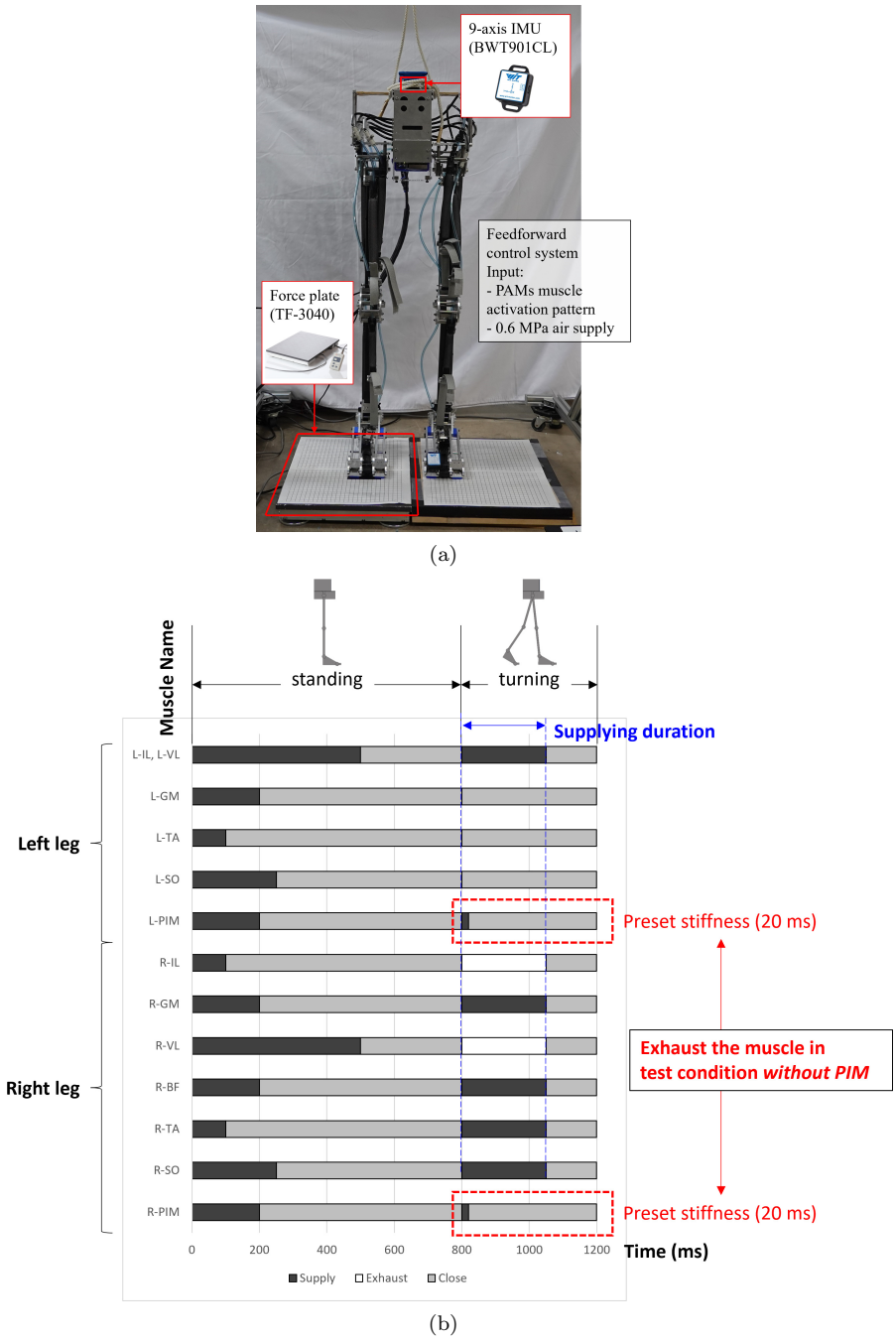

Figure 3.7: The study's experimental design employs the musculoskeletal robot "PneuTurn-T". (a) The experimental setup in its initial position: standing posture. (b) The muscle activation pattern controls each set of PAMs for generating foot-slip turning motion. The conditions of the first experiment are decided by changing the supplying duration of the turning motion (blue). The second experiment changes the parameter of PIM by supplying PIM with a preset stiffness or exhausting it (red).

Comparative Conditions

As our hypotheses suggest, we would like to prove two points in this paper. One is that the compliant structure of the musculoskeletal leg made the foot-slip turning with the DSP-SLIP model possible. The other is that the intrinsic muscle of the foot will passively stabilize the robot's posture in an unstable state.

In the first experiment, we test the compliance of the robot's leg by measuring the body rotational angle and the foot distance in different muscle supplying durations to find the compressed leg length compared to its resting leg length to see its function to store the energy in the spring-like structure when compressed, and release the energy and extend itself when the maximum resistance is reached and bouncing its leg backward a little before landing them at an uncompressed state. This experiment helps us understand the relationship between the feedforward input of leg angle through supplying duration and the outputs of foot distance and body rotational angle. We also interpreted its behavior and possible cause of errors from the results.

Secondly, we investigated the function of passive intrinsic toe stabilization with the activation of PIM in the musculoskeletal structure. The assessment was measured in an unstable state for the clarity of integrating the feature to the robot, such as the landing phase at the end of the turning motion, in which the posture is prone to instability with a smaller stability margin due to incomplete foot contact area on the right foot. Therefore, the experiments focus on the right foot, which is the adaptive foot with passive flexible adaptability with the toe joint stabilization with PIM. The experiment was done in two conditions: one with the preset activation of PIM and another without the PIM activation. The GRF data was collected to indicate the robot's stability after the landing by how long it can maintain its posture after an abrupt motion.

Data Acquisition Method

The data to be gathered for analysis included rotational angle, foot distance, and GRF. In the first experiment, the compression behavior of the leg can be observed and estimated using the data of body rotational angle and foot distance. A 9-axis IMU (BWT901CL, WitMotion) was used to measure the body orientation and rotational angle. The foot distance was measured directly from the center of each toe. The second experiment assessed the GRF of the right foot using a force plate (TF-3040, Tec Gihan). The raw GRF data with a sampling rate of 1 kHz then processed through a Python program that incorporates a first-order low-pass Butterworth filter with a cut-off frequency of 20 Hz.

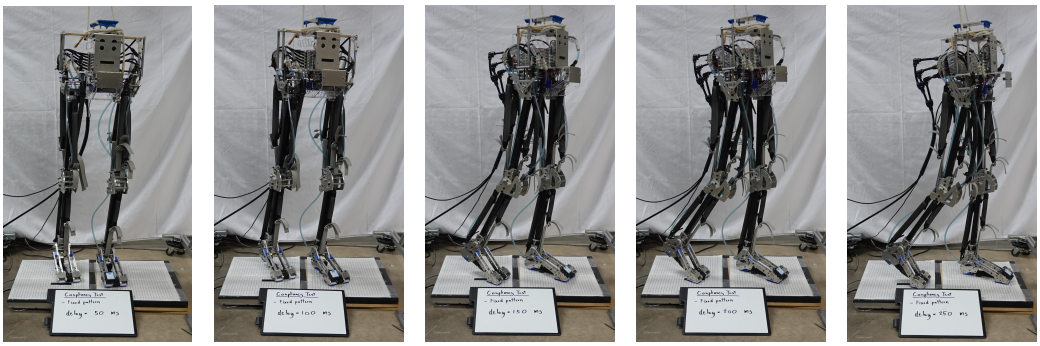

(a) 50 ms (b) 100 ms (c) 150 ms (d) 200 ms (e) 250 ms

Figure 3.8: The robot's posture at the end of the motion in its rest length is without leg compression during each supply duration. (a)-(e) The robot generated the motion from the same pattern with different muscle-supplying durations to actuate the joints in each condition. The delay in the figure indicates the timing delay of the muscle activation pattern, starting from supplying the muscle until closing the valve.

3.4.2 Experimental Results

The Compliance of the Leg

In the test of leg compliance, we tested the leg compression with different muscle-supplying durations using the same muscle activation pattern to study its relationship in the feedforward supplying system and the results of the body rational angle and the leg compression. The supplying duration varies from 50,100,150,200, and 250 ms (See Figure 3.8). Following the feedforward input in the repetitive test, the rotational angle and the foot distance results are shown in Figure 3.9 and Figure 3.10, respectively. Table 3.3 shows each condition's mean and s.d. of the rotational angle. Similarly, Table 3.4 describes the mean and s.d. of the measured foot distance. The largest gap in data can be seen in the 50-ms and 100-ms supplying duration, while not much of a gap is shown between the other conditions. The rotational angle increased from 15.0±6.4° in 50-ms supplying duration to 49.5±15.2° in 100-ms supplying duration. It can also be assumed from the data trend that the gap tends to be smaller the longer the leg is supplied. Next, in the results of foot distance, the trend shows an exponential increase as the supply duration becomes longer. From 50-ms to 150-ms supplying duration, the foot distance seems even smaller than its initial position, probably due to its structural deformation from the foot's inability to slide backward due to the resistance from the static friction. The structural deformation made the minimum foot distance shrink as far as from 200 mm to 185.14±6.91 mm in 50-ms supplying duration. From 150-ms to 250-ms supplying duration, the foot distance exponentially increased, possibly because it had stored enough compression force in its leg and generated enough force to overcome the friction.

After obtaining the necessary data (i.e., body rotational angle and foot distance), we proceeded to calculate the compressed lengths and compare them with the leg in their rest length to see the

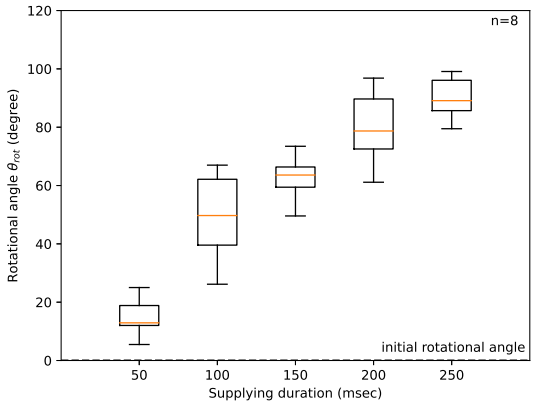

Figure 3.9: The results of the body rotational angle collected from the IMU in different pattern supplying durations. The orange line shows the median of the data. The box indicates data range from Q1 to Q3. The whisker describes the minimum and maximum data. The n represents the number of trials. The initial value at the standing posture is 0°.

Table 3.3 Mean and standard deviation of the rotational angle θ_{rot}

Supplying duration (ms)	50	100	150	200	250
Mean±S.D.	15.0 ± 6.4	49.5±15.2	62.6±7.9	80.3±13.1	92.0±11.4

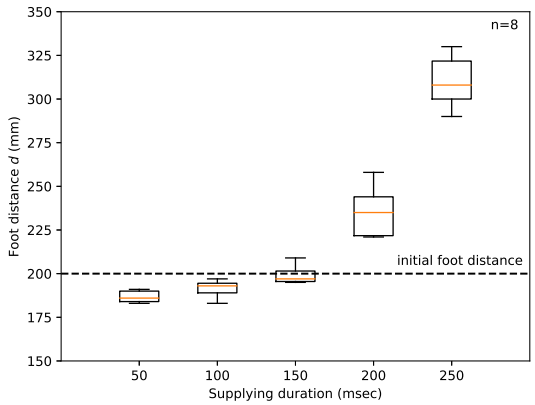

Figure 3.10: The results of the foot distance measured directly from toe-to-toe in different pattern supplying durations. The orange line shows the median of the data. The box indicates data range from Q1 to Q3. The whisker describes the minimum and maximum data. The n represents the number of trials. The initial value at the standing posture is 200 mm.

Table 3.4 Mean and standard deviation of the foot distance d

Supplying duration (ms)	50	100	150	200	250
Mean±S.D.	185.14 ± 6.91	191.43±4.79	199.29±5.50	235.25±13.33	310.38±12.74

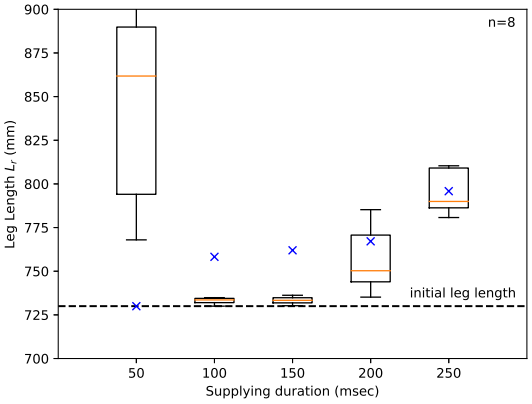

Figure 3.11: The leg length L_r is calculated by substituting the collected data in Equation 4. Compared to the uncompressed rest length denoted as a blue mark, leg compression mainly occurs in shorter supplying conditions or the early motion phase. The n represents the number of trials. The initial value at the standing posture is 730 mm.

Table 3.5 Mean and standard deviation of the calculated leg length L_r and the leg compression rate

Supplying duration (ms)	50	100	150	200	250
Mean±S.D.	905.51 ± 198.75	736.04±8.85	733.94±3.51	757.17±19.26	801.73±28.43
Compression rate	-0.2404	0.0293	0.0368	0.0130	-0.0074

compliance of the leg structure. The leg length can be calculated with the Equation 4, achieved through Equation 1.

$$L_r = \frac{d}{\sin\theta_{rot}} - L_p \cot\theta_{rot} \tag{3.4}$$

Substituting the parameters in Equation 4, we then acquired the calculated L_r compared to the uncompressed leg length in each supplying duration. The results depicted in Figure 3.11 indicate that the leg likely remained compliant from its initial state up to 150-ms supplying duration. Preferably, the results in 50-ms was neglected in the analysis with this method as the error of calculation due to a cotangent nature is exhibited. The L_r in the 100-ms and 150-ms supplying condition is comparable to its initial L_r at 730 mm, as the calculated L_r are 736.04±8.85 mm and 733.94±3.51 mm, respectively (see Table 3.5). Additionally, the compression rate is calculated by comparing the displacement of the length to the uncompressed length. The compression rate is more notable in the 100-ms and 150-ms supplying, whereas the compression rate is lower in the 200-ms supplying condition and almost nonexistent in the 250-ms condition, indicating that leg compression mainly occurs in the early phase of the motion.

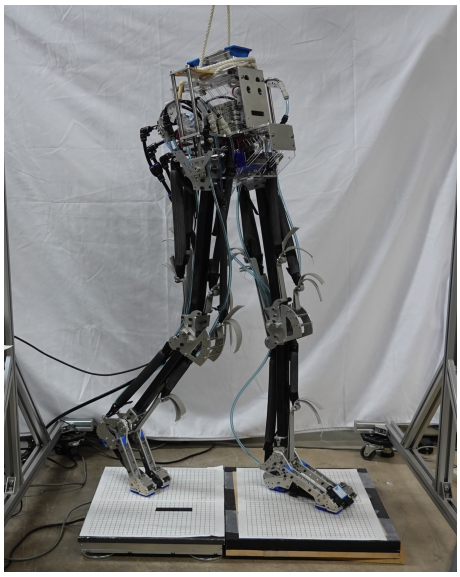

Figure 3.12: The static posture at the end of the turning motion in the landing phase is prone to instability due to its small area of support and awkward body orientation, which leans CoM to the anterior side. The GRF was measured on the right foot of the robot to investigate the intrinsic structure of the toe stabilizing feature.

As mentioned previously, compression rate might result from the compliant leg being pressed between its body and the floor in the compliant state, opposing motion while internally storing energy. Once the horizontal force equal to static friction is reached, as defined by Equation 3, the leg initiates the foot-slip turning motion, utilizing the stored energy to generate a significant body rotational angle and substantial foot displacement. Therefore, it is possible to assume that the compliant structure helps make the slip-turning motion from our DSP-SLIP model possible.

The Intrinsic Toe Stabilization

In the experiments, we let the robot fall back on its adaptive right leg in the back, in the same manner as the landing phase at the end of the slip-turning motion, as shown in Figure 3.12. As for the pattern, we chose the pattern with a supply duration of 250 ms, as it was shown to exhibit the lowest compression rate, lacking internal strength, while its stability margin is pulled backward with the right leg, away from the CoM in the anterior side, thus cause this condition more challenge. After the turning phase, the compliant leg has released itself from the compressed state into the expansion state and draws its leg backward, progressing to the bouncing phase; the leg is now in its resting state without any compression while retaining the same stiffness in its structure. The leg then goes into the landing phase, attempting to keep its foot on the ground and its posture upright. The PIM stiffness is fixed to a specific value by a preset supplying duration.

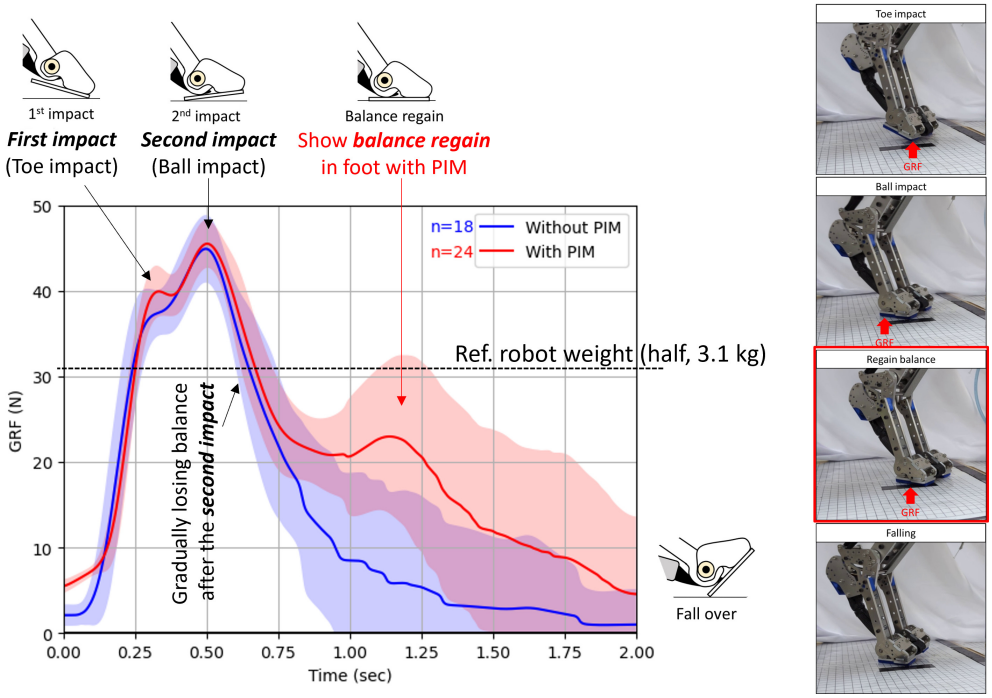

Figure 3.13: The results of the average GRF data were measured from the right foot during the landing phase of the motion. The blue line shows the robot's landing behavior in the foot without PIM. The red line describes the robot's behavior in the foot with a preset PIM stiffness. The shadow indicates the standard deviation of the data. Each peak of the curves defines the times the robot initiated hard contact with the ground. The area under the curve assumed the duration the robot tried to adjust its foot to the floor to maintain its posture before falling over. The n represents the number of trials. The reference robot weight put on the foot in the stable state is 3.1 kg.

The GRF curves in Figure 3.13 show that the foot structure with PIM as a toe stabilizer clearly has a larger area under the curve compared to the foot without PIM. The curves also show the foot's behavior during the robot's landing phase. Few peaks emerged in the curves to indicate each time the foot came into contact with the ground with visible amplitude. In the first impact, the robot's foot falls on the anterior side (front) of its toe, where the impact size of 36.58±3.67 N was measured in the foot without PIM and 39.89±3.05 N in the foot with PIM. The peak is more prominent in the foot with PIM, possibly due to the enhanced toe strength, compared to the weak toe of the foot without PIM, where the peak is hardly visible. Meanwhile, in the second impact, where the robot fell on the ball of the toe, no clear difference was seen in both cases. The second impact for the foot without PIM and the foot with PIM is 44.91±3.95 N and 45.51±2.82 N, respectively.

After the second impact, the robot gradually loses balance as its jumpy structure bounces its body forward. Consequently, the robot falls over due to instability, especially in the landing posture, where the CoM stays close to its stability margin on its anterior side. The GRF results showed that

the foot without PIM would start to fall over right after the second impact without any means or attempt to regain its stability. However, a clear difference can be seen in the foot with PIM starting from t = 0.75 sec, as the robot regains its balance and tries to put some body weight on the right foot. The closer weight putting the foot to the reference weight implies better postural balance as the weight is supposed to be equally distributed to both supporting legs in a balanced posture. Furthermore, the third peak can be seen in the foot with PIM at t = 1.15 sec; the impact is smaller compared to the other peaks with the size of 22.95±9.2 N, whereas at the same time frame, the robot was almost completely losing foot contact in the foot without PIM with the GRF size of 5.18±10.67 N.

In this research, we estimate the postural stability from the foot contact duration before gradually losing the balance and falling over. Due to the falling indicator not being clear, as the robot was hung to strong support with a security rope to prevent itself from falling damage, we chose to decide the stable duration from the time of the final foot impact in motion. The foot without PIM last keeps contact with the ground approximately at t = 0.5 sec in the second impact, while the foot with PIM maintains the curve until the third impact at t = 1.15 sec. Thus, the foot contact duration increased by 130%, indicating improvement in postural stability.

3.5 Disscussion

In our study, the musculoskeletal robot system was simplified to reduce complexity. The robot was based on the feedforward control system and lacked any feedback or precise control methods, which made it struggle to realize the motion with the conventional method like other robots (e.g., [83, 85]). This paper investigates the slip-turning motion with the DSP-SLIP model and its compatibility with the compliant structure of the musculoskeletal robot. The results provided us with insight into the vital role of compliant structure in motion, which makes motion possible because it tends to allow a little joint deformation due to the usage of pneumatic actuators. While utilizing this type of actuator, the motion of the joint and activation timing are to be studied based on that of humans. The muscle activation pattern of our robot is also based on research on human turning strategy [75]. Furthermore, the pneumatic-driven system is prone to instability due to its compressible actuators. The robot's capabilities will be limited without implementing more complex architecture.

Another challenge for musculoskeletal robots with adaptive compliant structures is that they lack precision from the stable, rigid joint control. This problem stems from using pneumatic actuators, which can raise numerous obstacles for the robot, starting from stability. With soft actuators, the robot will allow a small amount of deformation in each joint. The error of one joint might not affect the robot much, but combining the errors of every DoF of the robot becomes an adversity. For example, even the position of CoM is challenging to place directly in the desired position with

accumulated errors. Therefore, this research was designed to utilize its adaptive structure to compensate for the problem. The PIM is incorporated into the foot structure as some references study its relationship with postural stability [133, 134, 135, 142, 140, 143, 158]. The result has proven the effectiveness of using the PIM as a passive toe joint stabilizer with a preset stiffness and increased foot contact duration for approximately 130% longer in unstable posture compared to the foot with a weak toe. Although the robot can execute a problematic turning task with the help of its passive structure in this study, it still has many challenges.

On an important note, the disadvantage of using the calculation method from this research can be seen in the results in Figure 3.11. The data in the 50-ms supplying duration has a significant error of calculation due to the nature of the trigonometric functions' cotangent after the angle substitution in Equation 4; as the rotational angle comes close to zero, the value becomes closer to infinity, which causes the error.

While this study utilizes the yaw moment or the free moment generated on foot to turn the robot's body around, there are many research that study these moments [159, 160], and there are many attempts that have tried to eradicate of this moment by various methods. For example, Chen et al. use a bevel-gear-like structure to generate an internal moment to compensate for the external yaw moment [161], or there is some other research using the angular constrain method[162].

The next step in this work is to apply the slip-turning motion to the walking motion to recreate smooth locomotion for the bipedal robot. The turning pattern is initially based on the human turning while walking, which might even provide us with a better insight into the motion.

In our future work, it is possible to integrate the robot with additional sensors (e.g., joint angle sensor, IMU, force sensor) to provide feedback on its current orientation, apply the model to the system, and help the robot create more precise motion.

3.6 Conclusion

This paper introduces a foot-slip turning mechanism for a musculoskeletal robot with a novelty DSP-SLIP model with toe stabilizing to improve its postural stability. The robot utilizes its compliant structure to realize motion with the DSP-SLIP model and a feedforward control system while implementing the stabilization of the toe joint to achieve a turning motion with enhanced stability. The first experiment highlights the robot leg's compliance and ability to store compressed energy with the deformation of its pneumatic-compliant structure, described as compression rate, making our foot-slip turning strategy possible in this research. The second experiment demonstrates intrinsic toe stabilization, showcasing its passive role in stabilizing posture during an unstable state without any feedback or precise control methods, improving its foot contact duration by 130%. These findings contribute to the field of robotics by offering a simple strategy that demands less complexity to realize complex tasks with a feedforward control system and structural design. Our next plan is

to incorporate the slip-turning motion into the walking robot to realize the turning while walking, which poses a significant challenge in dynamic stability.

Chapter 4

Friction Control Using Dual-Mass DSP-SLIP Model

This chapter based in following publication:

K. Nipatphonsakun, and K. Hosoda, "Friction Control in Foot-Slip Turning of the Musculoskeletal Robot Using DSP-SLIP Model with Dual-Mass System", IEEE Robotics and Automation Letters (RA-L), 2024. (Submitted)

Abstract

This study investigated a novel approach to friction control in the slip-turning motion of a musculoskeletal robot by simulating the weight-shifting of bipedal locomotion using the Double-Support Parallel Spring-Loaded Inverted Pendulum model integrated with a dual-mass system and compliant structure. The model utilizes the robot's compliant structure to facilitate motion, while the dual-mass system simulates dynamic weight distribution across each foot. The hypothesis posited that mimicking the weight transfer between legs would adjust frictional forces to prevent slipping and maintain balance during turns. The study investigates two key experimental conditions: the impact of attaching different weights to analyze friction control and varying turning patterns to assess foot slippage and leg compliance. The first condition demonstrated that dynamic weight distribution is crucial for optimal frictional forces, stability, and slip prevention during complex maneuvers. The second condition highlighted the compliant structure's energy storage capability, emphasizing the delicate balance between the swing and stance phases for efficient locomotion. This research advances the development of more adaptable and efficient bipedal robotic systems with applications in robotics, automation, and assistive technologies.

4.1 Introduction

Musculoskeletal robots, designed to replicate human biological features [53, 55, 57], have advanced significantly while still facing challenges in executing complex motions. Slip-turning motions offer a practical approach to simplifying turning motion, allowing robots to navigate sharp turns [83, 84] and sudden direction changes more effectively [81], with fewer mechanical restrictions [85]. In contrast to traditional robots [77, 78], musculoskeletal robots have trouble with precise control, making it difficult to achieve such a task. To address the challenge, we introduce the Double-Support Parallel Spring-Loaded Inverted Pendulum (DSP-SLIP) model to slip-turning motion and utilize the compliant structure of the musculoskeletal robot to realize the motion.

Bipedal locomotion in robots aims to replicate humans' dynamic and adaptive movement capabilities, allowing robots to navigate complex environments with agility and stability. Several models have been developed to understand and simulate this type of movement. The LIMP model (Linear Inverted Pendulum Model) [15, 36] simplifies walking dynamics by approximating the body's movement as an inverted pendulum, aiding in basic stability and balance, while its application expands to even more complex motion [17, 35]. The SLIP model (Spring-Loaded Inverted Pendulum) [18, 20, 21, 28] introduces compliance through spring-like behavior, better mimicking the dynamic nature of human locomotion to improve the adaptivity [38] and stability [29] of the motion. The 3D-SLIP model [48] extends this concept into three dimensions, allowing for more realistic simulations of movement. The dual-SLIP considers the bipedal feature of the two supporting legs, creating a dynamic model similar to human [31, 32, 33]. Our approach, the DSP-SLIP model, integrates a dual-mass system into the SLIP model, enabling effective weight transfer at the hip level between two feet, allowing for more precise control of the robot's center of gravity and enhancing stability and adaptability during movement.

Human weight transfer between two feet is a fundamental aspect of bipedal locomotion, enabling a wide range of movements such as walking, running, and turning. This process involves shifting the body's center of gravity from one foot to the other, allowing for dynamic adjustments in balance and stability [152]. During weight transfer, the friction between the feet and the ground plays a crucial role in preventing slips and falls. This intricate interplay between weight transfer and friction allows humans to navigate varied and unpredictable terrains with agility and precision. In order to transfer the body weight between two supports, a flexible structure is necessary to replicate the dedicated motion. By utilizing the compliant structure [147, 148, 154], versatile motions could be achieved.

This study investigates the impact of weight transfer in the DSP-SLIP model to manipulate friction and examines the effects of changing the mass in the hip level during the slip-turning motion. Through a series of experiments, we aim to demonstrate how these adjustments can optimize friction control and enhance the flexibility of the motion. We hypothesize that altering the mass distribution and leveraging the compliant structure will give the musculoskeletal robot superior performance in slip-turning motions.

4.2 Slip-turning motion of the bipedal robot with a musculoskeletal structure

4.2.1 Structure of the musculoskeletal robot

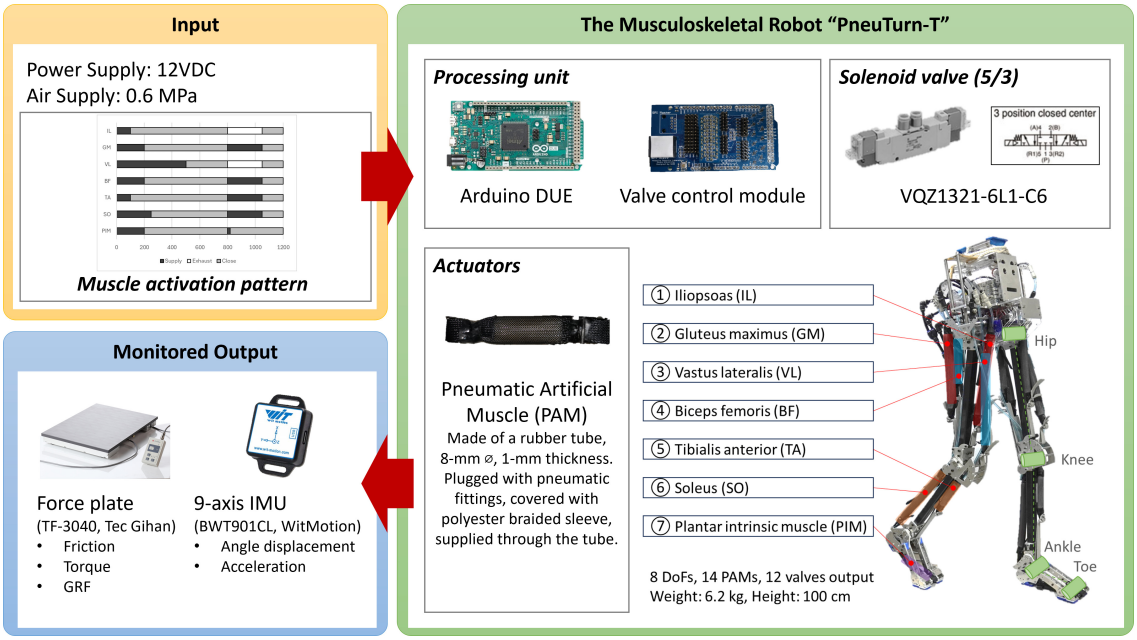

Figure 4.1: The operating system of the musculoskeletal robot "PneuTurn-T".

This study is based on the musculoskeletal robot used in our previous research, the bipedal robot "PneuTurn-T" [157]. The robot consists of eight Degrees of Freedom (DoFs) and fourteen Pneumatic Artificial Muscles (PAMs) controlled by twelve solenoid valves. Four revolving joints are placed in the pitch direction at the hip, knee, ankle, and toe of each leg. The motion is generated by inputting 12VDC power, 0.6 MPa air pressure, and the muscle activation pattern to the processing unit, Arduino DUE, driving the PAMs in sequence. The robot is then monitored through the external sensor to collect experiment data. The overall system of the robot is shown in Fig.1. Despite its simple structure and limited range of motions, the robot successfully realized a turning task in those studies.

4.2.2 Slip turning motion

Slip-turning motion is a maneuver used to enhance the agility and efficiency of bipedal robots. This motion involves a controlled slip of the foot during a turn, allowing the robot to change direction more smoothly and efficiently without requiring several extra steps, similar to a human's spin turn

[75]. The technique requires precise control of friction minimization to prevent excessive slipping and maintain balance. By adjusting the pressure and angle of the foot, the robot can utilize the slip-turning motion to navigate tight corners and make rapid directional changes. This approach reduces the complexity of the required movements and enhances the robot's ability to operate in dynamic and unpredictable environments.

4.2.3 DSP-SLIP model with dual-mass system

The DSP-SLIP (Double-Support Parallel Spring-Loaded Inverted Pendulum) model is based on our robot with a compliant musculoskeletal structure. This model incorporates a dual-mass system, where the robot's mass is divided into two main components: the left hip and the right hip (See Fig.2). The compliant structure within the model, which includes spring-like elements, mimics the elasticity and damping properties of human muscles and tendons, enabling leg compression and expansion during motion. The leg compliance can be described as,

$$F_S = k(L_v - L_i) \tag{1}$$

where F_S represents the intrinsic force of the compliant leg, k describes the leg stiffness, L_v shows the variable leg length, and L_i indicates the initial leg length without compression or expansion.

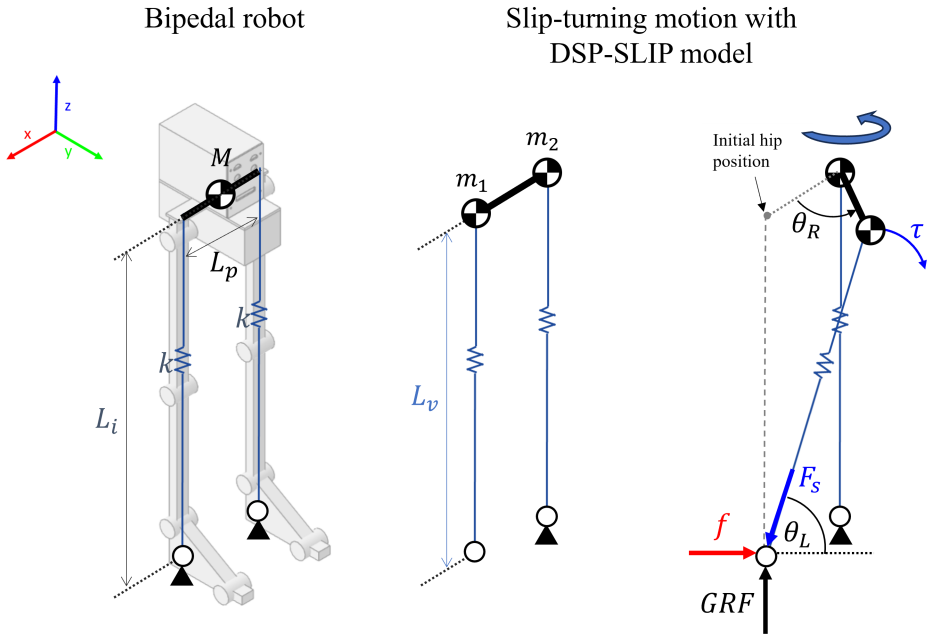

Figure 4.2: The bipedal robot transformed into a DSP-SLIP model with a dual-mass system, separating the body weight into two masses on each hip. The last figure shows a slip-turning motion with the DSP-SLIP model.

The dual-mass system in the DSP-SLIP model is a novel approach designed to simulate the weight-shifting feature of bipedal locomotion. This separation allows for a more accurate simulation of human weight transfer during movement. The model enhances the robot's ability to manage the distribution of ground reaction forces during the double-support phase between the left and right hip.

4.3 Friction control method with dual-mass system simulating weight transfer

4.3.1 Weight transfer in bipedal locomotion

Weight transfer in bipedal locomotion is a critical mechanism that enables balance and stability during movement. As a person walks, runs, or turns, the center of gravity shifts dynamically from one foot to the other, with the hips playing a pivotal role as the central axis for weight redistribution. The hip joints allow for a wide range of motion, enabling the legs to move in various directions while maintaining balance. As weight transfers, the pelvis tilts and rotates, and the coordinated action of muscles around the hip provides necessary force and control. This intricate interplay allows for efficient weight transfer, enabling agility and stability. Inspired by this natural mechanism, the design of the dual-mass system in the DSP-SLIP model replicates this ability by separating the mass into the left hip and right hip, connected by the pelvis link, allowing dynamic adjustments to the mass distribution. Our hypothesis suggested that, by dynamically adjusting the distribution of mass on each leg, the robot can effectively control the frictional forces at the feet, reducing the risk of slipping and providing enhanced performance and adaptability in a wide range of motion scenarios.

4.3.2 Friction control in slip-turning motion

Friction control is a critical aspect of executing slip-turning motions effectively in bipedal robots. During slip-turning, precise management of friction between the robot's feet and the ground is necessary to maintain balance and ensure smooth direction changes. Excessive friction can impede movement, while insufficient friction can lead to uncontrolled slipping and loss of stability. Therefore, achieving the right balance of friction is essential for optimal performance.

In the context of a dual-mass system, friction control is particularly important as it directly influences the robot's ability to transfer weight between both sides of its body. By adjusting the distribution of forces at the feet, the robot can modulate the frictional forces to facilitate controlled slipping during turns. This involves dynamically altering the normal force through weight shifting, which in turn affects the frictional force. From the model, we can get the following equations,

when non-slip ($\Sigma F = 0$),

$$F_{hor} = f = \mu mg = -F_S \cos\theta_L \tag{2}$$

$$F_{ver} = GRF = -F_S \sin\theta_L - mg \tag{3}$$

when slip,

$$F_{hor} = m\ddot{x_S} = \mu mg - F_S \cos\theta_L \tag{4}$$

$$F_{ver} = m\ddot{z_S} = GRF - F_S \sin\theta_L - mg \tag{5}$$

where θ_L describes the angle between the leg and the ground with the body mass m and gravitational acceleration g. F_{hor} and F_{ver} are the horizontal and vertical forces, respectively, and f is the frictional force and μ is the friction coefficient. The displacements on the horizontal and vertical axes are denoted by x_S and z_S, respectively. From Eq.5 we can derive the horizontal displacement x_S as,

$$x_S = \iint_0^t \mu g - \frac{k}{m}(L_v - L_i)(\cos(\theta_L))dt^2 \tag{6}$$

and finally, we can achieve the rotational angle θ_R from,

$$\theta_R = \frac{x_S}{L_p} \tag{7}$$

where L_p is the fixed length of the pelvis link. The DSP-SLIP model employs a compliant structure to enhance this friction control. The compliant elements, designed to mimic the elasticity of human muscles and tendons, allow for smooth adjustments in response to changing forces and movements. This compliance not only helps absorb shocks and maintain stability but also aids in fine-tuning the frictional forces during slip-turning.

4.4 Experiments

4.4.1 Experimental Setup

Due to the robot's simple structure, the weight shifting between both feet is difficult, as all joints were placed on the same axis and flat-foot morphology. In this study, we would like to focus on the effect of mass on the slippage of the foot to find the proper way to manipulate the rotational angle through the friction control method, thus focusing on the slipping right foot. As the robot's left leg acted as a static pivoting axis of the slip-turning motion, the pole was provided instead of the leg

to prevent the displacement of the left hip, with the adjustable hip level to adapt to the motion of the right hip. The experimental setup is illustrated in Fig.3.

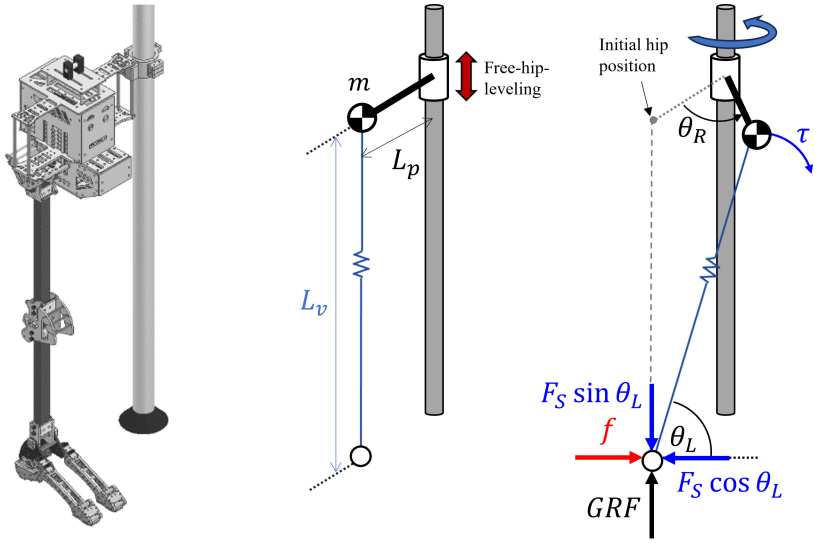

Figure 4.3: The experimental setup used in the experiment focused on the friction control of the right foot to simulate the weight transfer of the bipedal locomotion with a dual-mass system in the DSP-SLIP model.

4.4.2 Comparative conditions

The experiment used two different comparison settings to thoroughly investigate the dynamics of weight transfer and friction control in bipedal locomotion during the slip-turning motion.

In the first experimental condition, various weights were strategically attached to the robot to examine their impact on friction control during slip-turning motions (See Fig.4.4). This setup aimed to simulate the dynamic weight distribution that occurs naturally in human locomotion. By altering the mass attached to different parts of the robot, researchers could observe changes in the GRF and analyze how these changes affected the frictional forces at the feet and how they affected the slip-turning motion. The primary focus was on understanding how different weight distributions influence the robot's ability to maintain balance and execute precise movements without slipping. The data collected from this condition provided valuable insights into optimizing mass distribution for improved friction management and overall stability in bipedal robots.

In the second experimental condition, the focus was on changing the duration of the turning pattern (See Fig.4.5) to analyze the impact of varying force and the compliant structure during both the swing and stance phases of the robot's gait. As the robot executed turns, the applied force was incrementally increased to observe effects on stability and movement precision. During

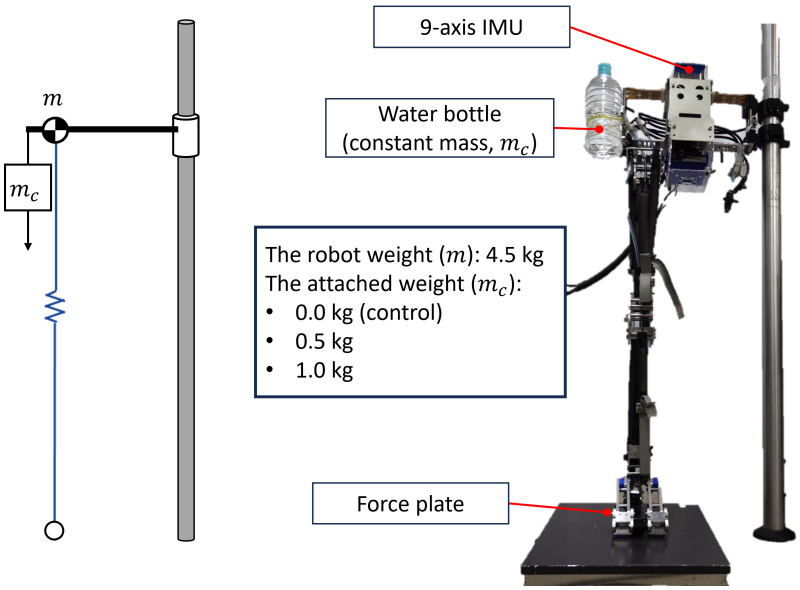

Figure 4.4: The total weight of the robot can be changed by substituting the constant mass m_c with different weights to investigate the changes in frictional force on the right foot.

the stance phase, the compliant structure absorbed and stored energy [150, 151], which was then released during the swing phase to propel the leg forward, mimicking human muscle elasticity. This mechanism facilitated smoother and more efficient transitions between movements. By adjusting the duration of the turning pattern and force, the experiment aimed to understand the role of the compliant structure in maintaining balance and agility during high-force maneuvers. The collected data provided insights into optimizing the robot's compliant elements for better energy efficiency and dynamic control in complex locomotion tasks.

Through these comparative conditions, the experiment provided comprehensive insights into the mechanics of bipedal locomotion, offering a deeper understanding of the interplay between weight transfer and friction control.

4.4.3 Results

The force plate data (TF-3040, Tec Gihan) was then processed in Python using a first-order low-pass Butterworth filter, a sampling rate of 1 kHz, and a cut-off frequency of 20 Hz.

Firstly, the result of GRF collected from the force plate is shown in Fig.4.6. According to Eq.3, the GRF would reduce as the body mass shifts forward, while in the results, the robot has been shown to regain GRF back for a short duration, probably due to the increasing stored-up energy in its structure F_S. This energy would then continue to increase until the slippage of the foot occurs, and the robot would lose the foot contact on its foot soon after. The increased swing duration resulted in a shorter time for the robot to maintain foot contact.

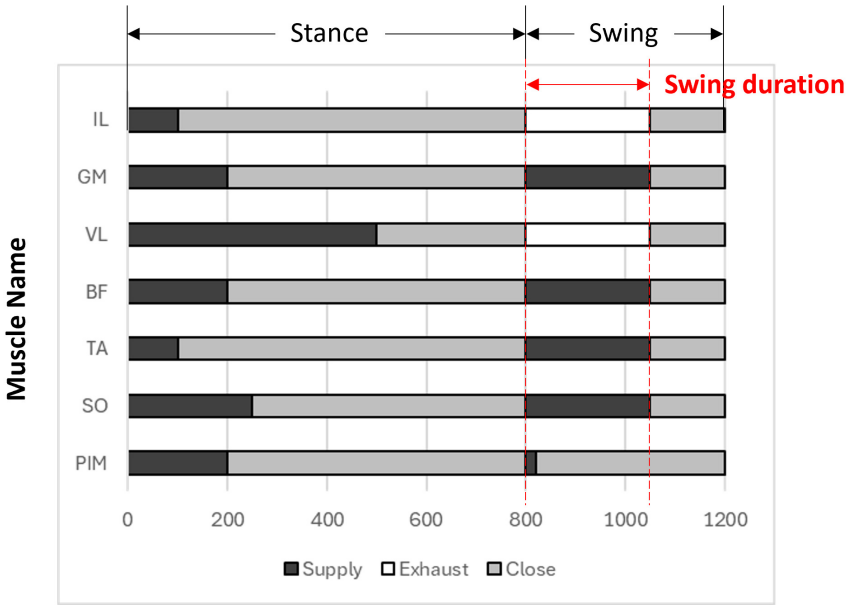

Figure 4.5: The muscle activation pattern used in the experiment controlled all of the seven PAMs of the robot. The swing duration can be changed in this pattern; the longer the activation time, the stronger the motion.

The frictional torque measured during the experiment is shown in Fig.4.7. The torque appeared to be stronger in shorter swings to resist the motion, whereas the torque increased with the heavier weight attached to the robot. The increased torque is probably generated by the robot's compliant structure, storing up the energy within its compliant leg.

As for the results of the rotational angle in Fig.4.8, the angle slightly increases when the force is applied to the foot, and in the early phase, the compression occurs in the leg, trying to resist the motion. In the shorter swing, 50-ms swing (see Fig.4.8a), the compressible structure attempted to resist the motion, resulting in minimal angle displacement. In Fig.4.8b, the robot slowly rotates its body around while the mass goes forward until the slip occurs, causing it to lose foot contact. Fig.4.8c and Fig.4.8d show that, as the swing increases, the force is stronger, and the robot slips faster with the stronger acceleration. In every case, the robot with 1 kg m_c has a slightly less steep curvature.

4.4.4 Discussions

The experiment aimed to enhance the understanding of weight transfer, friction control, and hip leveling in bipedal locomotion by employing two comparative conditions: varying attached weights and modifying turning patterns. The insights gained from these conditions are pivotal in refining the design and control strategies for bipedal robots, particularly those utilizing the DSP-SLIP model

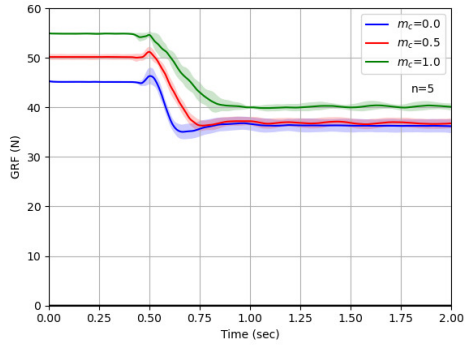

(a) Swing = 50 ms

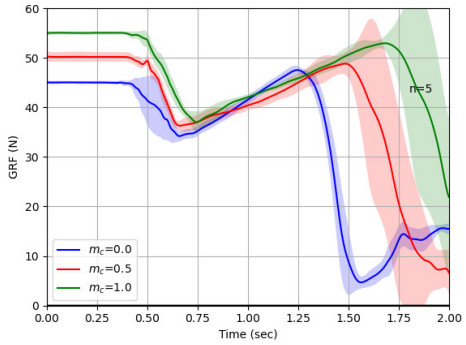

(b) Swing = 100 ms

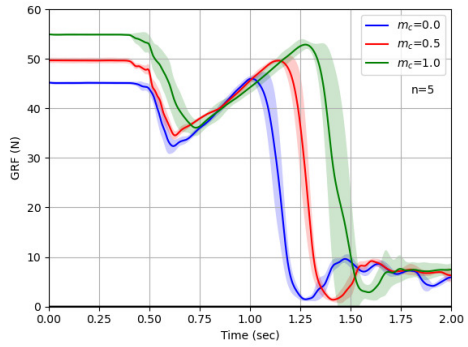

(c) Swing = 150 ms

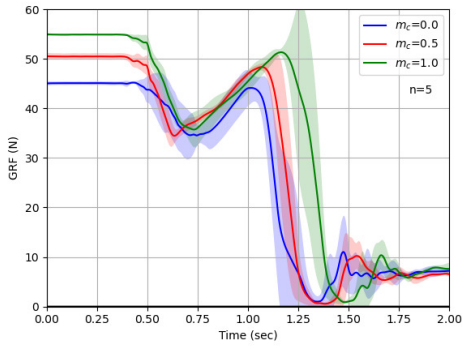

(d) Swing = 200 ms

Figure 4.6: The results of the GRF data show the robot's ability to maintain its body weight on its right leg during the slip-turning motion. The GRF would tremendously reduce after the slip occurs and the foot contact would be lost soon after. The results clearly show longer foot contact duration before slippage occurs in the robot with a heavier mass attached, indicating more stable motion.

with a compliant structure and dual-mass system.

Precision control is challenging to achieve with the musculoskeletal robot. As a result of its soft and compressible structure using the PAMs [71], the initial state of the robot is slightly different in every experiment. The stiffness of the joint changes according to the supplied air pressure; therefore, a slight change in these pressures, combined with stacking error from every joint, could cause a catastrophic error in the motion. Achieving the right level of compliance without compromising stability, especially under varying force conditions, remains a complex task.

The stability of the robot is one of the struggles, as the robot standing on one leg makes it less stable than other robots. Even if the robot were to apply the method to its bipedal form, stability is still one of the primary obstacles. As stability is difficult to obtain, the manipulation of the body weight and friction would be even more difficult. The challenge lay in precisely calibrating the weight distribution to mimic human-like adaptability, which requires sophisticated sensors and control algorithms to effectively manage the shifting center of gravity.

The structure of the robot also plays a significant role in this investigation. With the current design, the robot has a very simple structure to reduce the complexity of the controller. At the very least, the robot should have higher DoFs to help transfer the body weight dynamically to both of its feet. Ensuring that the robot's hip and leg adjustments are responsive and accurate enough to handle dynamic environments is crucial for achieving human-like locomotion.

4.5 Conclusion

This study investigates the friction control method in the foot-slip turning motion of the musculoskeletal robot using the DSP-SLIP model with a dual-mass system. The hypothesis suggests that the robot can control the friction by manipulating the weight on each foot, resulting in better control of the turning maneuver. In the experimental results, the robot shows the capability to resist slips with different attached weights and swing duration. The heavier weight shows better capability of maintaining foot contact without slippage and more substantial frictional torque, possibly due to the attempt to resist the jumpy behavior of the pneumatic actuators. In the early swing phase, the robot shows its compressible structure resisting motion, which significantly changes after the slip occurs, drastically affecting its rotational angle.

Our future work includes applying the method to the bipedal robot capable of shifting its body weight to any of its feet and trying to control the turning angle through friction manipulation of the foot. These insights could have practical implications in the design and control of bipedal robots, enabling them to navigate challenging environments, perform precise turning motions, and enhance their overall locomotion capabilities.

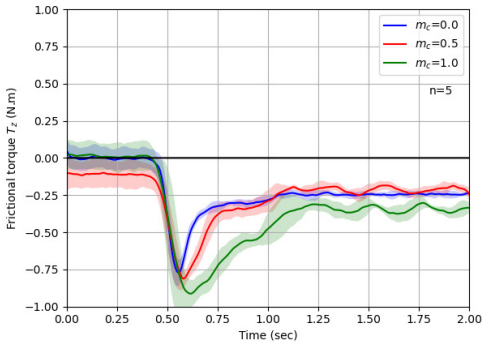

(a) Swing = 50 ms

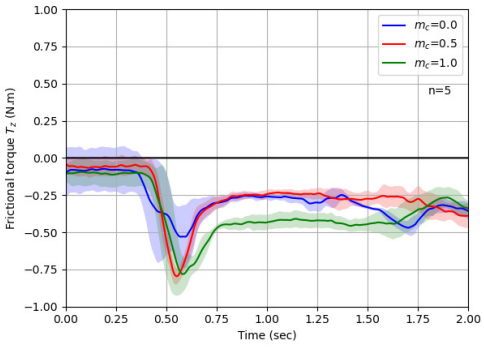

(b) Swing = 100 ms

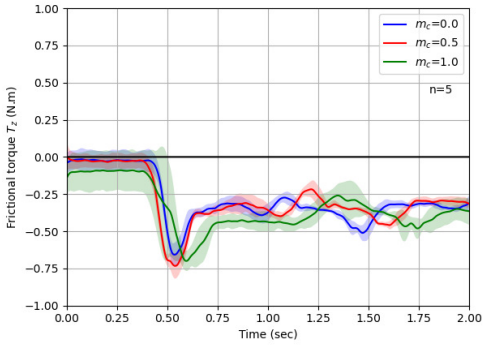

(c) Swing = 150 ms

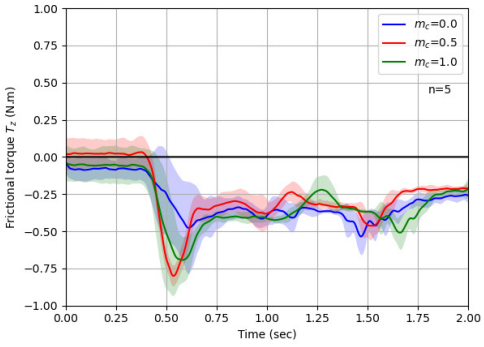

(d) Swing = 200 ms

Figure 4.7: The frictional torque data show more substantial torque in the heavier-weight robot. The apparent difference is best shown in (a) and (b), where the robot is in its compression state, attempting to resist the motion with its compliant structure.

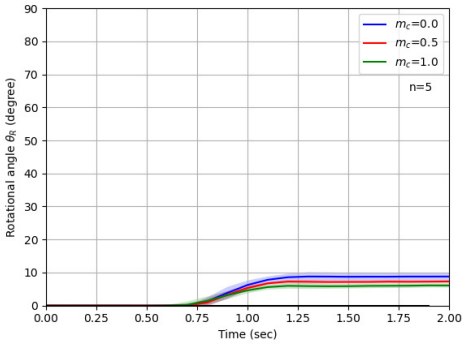

(a) Swing = 50 ms

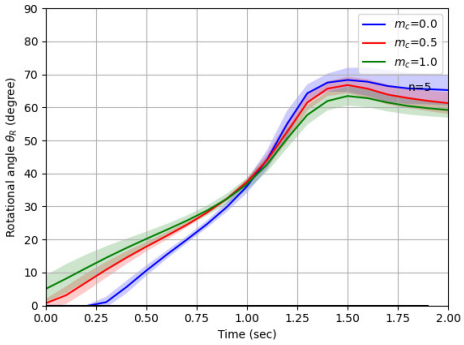

(b) Swing = 100 ms

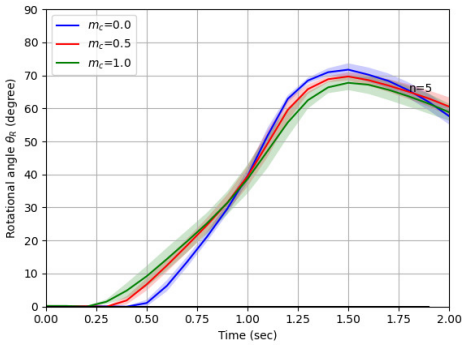

(c) Swing = 150 ms

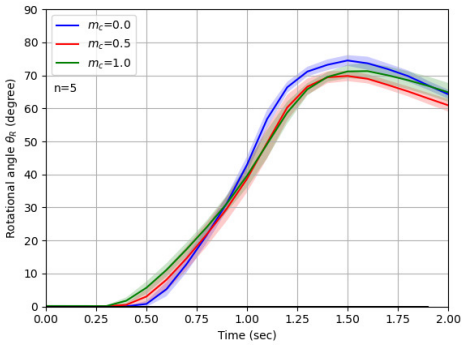

(d) Swing = 200 ms

Figure 4.8: The collected rotational angle data shows the angular velocity of the turning motion. The steeper curves indicate the faster motion and more acceleration as the robot mass gradually moves forward. Note that the motion is restricted to 70°as there was no antagonistic force to stop the motion; the robot would keep going forward without stopping.

Chapter 5

Conclusion

In conclusion, this thesis addresses the critical aspects of enhancing bipedal and humanoid robots, focusing on slip-turning maneuvers utilizing a musculoskeletal structure with toe joints and intrinsic muscles. The study demonstrates that integrating biomechanical features such as toe joints and compliant structures significantly improves the robots' motion flexibility, stability, and postural control. By mimicking the human musculoskeletal system, these robots achieve a higher degree of fluidity and adaptability in their movements, enabling them to perform complex tasks with greater precision.

The research emphasizes the importance of understanding the biomechanics of human feet, particularly the role of toe joints and plantar intrinsic muscles, in achieving efficient locomotion. The findings highlight that incorporating these features into robotic designs can lead to substantial improvements in stability and maneuverability, particularly during slip-turning motions. The compliant structure of musculoskeletal robots, with their ability to store and release energy, further enhances their functional capabilities, making them more adept at navigating diverse environments.

Experimental investigations conducted in this thesis validate the hypothesis that attaching toe joints to robots enhances motion flexibility and stability. The results show a reduction in frictional torque and an improvement in rotational angles, underscoring the effectiveness of toe joints and intrinsic muscle control in achieving precise and efficient slip-turns. Additionally, the study explores friction control methods through weight-shifting dynamics, providing insights into optimizing robotic movements to prevent slipping and maintain balance.

Overall, this thesis contributes to the field of robotics by advancing the integration of biomechanical principles into musculoskeletal robots, bringing them closer to replicating human-like movement and interaction capabilities. Future research should focus on further optimizing these features, exploring their applications in more complex locomotion tasks, and investigating potential medical applications such as gait training and rehabilitation.

In Chapter 2, we investigated the slip-turning capabilities of musculoskeletal robots equipped with

toe joints, aiming to enhance their mobility and stability. The study examined the mechanics and benefits of incorporating passive toe joints into the turning motions of these robots. This approach is intended to improve turning efficiency, expand the range of motion, and increase adaptability in complex tasks.

The experiments conducted demonstrated that toe joints significantly reduce frictional torque and enhance the robot's rotational angle, leading to improved mobility. Additionally, the study found that applying stiffness through plantar intrinsic muscles (PIM) aids in preventing over-dorsiflexion of the toes, which contributes to better postural stability. These findings support the hypotheses that slip-turning with toe joints and PIM activation can significantly enhance the agility and efficiency of musculoskeletal robots.

Despite the promising results, several challenges were identified. First, the lack of an upper body in the robot design led to a posterior inclination of the center of mass (COM), which made it difficult to maintain proper postural stability, especially during rapid motions. This limitation suggests the need for further research into balancing strategies and possibly incorporating upper body elements to better emulate human-like stability.

Secondly, the use of pneumatic artificial muscles (PAMs) introduced issues such as lower accuracy in joint control and unstable velocities due to the compressibility of air. These challenges hinder the robot's ability to perform tasks consistently and accurately. Future work should explore alternative actuation methods or advanced control systems to mitigate these issues.

Furthermore, the study highlighted that while PIMs contribute to foot stabilization, their role in overall balance control during dynamic postural challenges is limited. This indicates the need for additional mechanisms or control strategies to enhance overall stability, especially in scenarios involving significant body swaying or rapid movements.

The chapter underscores the potential of slip-turning mechanisms and biomechanical features in advancing the capabilities of musculoskeletal robots. Future research directions include optimizing the design and control of toe joints, exploring complex locomotion tasks, and investigating medical applications such as gait training and rehabilitation. Addressing the identified challenges will be crucial for developing more adaptable, efficient, and human-like robotic systems.

In summary, Chapter 3 delves into the innovative concept of intrinsic toe joint stabilization in foot-slip turning motion for musculoskeletal robots, presenting significant findings from recent research. This work addresses the inherent challenges in achieving stable turning motions in bipedal locomotion, which traditionally rely on complex control systems. By leveraging the advantages of musculoskeletal structures, such as passive motion enhancement and simplified mechanisms, the study highlights the potential for more efficient and stable robotic movements.

The introduction of the DSP-SLIP model marks a pivotal advancement, combining a slider-like mechanism with the double-support parallel spring-loaded inverted pendulum model. This approach mitigates stability issues during slip-turning by employing foot support polygons and plantar intrinsic

muscles (PIM) for enhanced toe stabilization. Through detailed analysis of the foot-slip turning mechanism, the chapter underscores the importance of compliant leg structures, which adapt to minor errors in foot positioning and enhance overall stability.

The development of a musculoskeletal robotic foot equipped with PIM demonstrates a significant leap in postural stability during slip-turning. Implemented with PAMs, the PIM enhances anterior-posterior stabilization, proving crucial in improving the stability margin of bipedal robots. Experimental results validate the efficacy of these compliant structures and passive intrinsic mechanisms, showing improved stability and performance in musculoskeletal robots like "PneuTurn-T."

However, several challenges remain. The reliance on a feedforward control system without precise feedback mechanisms complicates the execution of complex motions. The compressible nature of pneumatic actuators introduces instability, and the lack of precision in joint control due to adaptive compliant structures poses significant obstacles. The accumulation of errors in each joint can adversely affect the robot's overall stability and motion accuracy. The study's calculation methods also face limitations, particularly with significant errors in certain scenarios due to trigonometric function properties.

Future research aims to integrate slip-turning motion into walking robots, enhancing dynamic stability and locomotion capabilities. Incorporating additional sensors and feedback mechanisms will be crucial for improving the precision and adaptability of robotic movements. By addressing these challenges and building on the innovative strategies presented in this chapter, the field of musculoskeletal robotics can advance towards more efficient and stable bipedal locomotion.

Chapter 4 investigated a novel approach to friction control in the slip-turning motion of a musculoskeletal robot by simulating the weight-shifting of bipedal locomotion using the Double-Support Parallel Spring-Loaded Inverted Pendulum (DSP-SLIP) model integrated with a dual-mass system and compliant structure. The hypothesis posited that mimicking the weight transfer between legs would adjust frictional forces to prevent slipping and maintain balance during turns.

The experimental results confirmed the hypothesis, demonstrating that dynamic weight distribution is crucial for optimal frictional forces, stability, and slip prevention during complex maneuvers. Attaching different weights to the robot showed that heavier weights helped maintain foot contact longer and produced more substantial frictional torque, likely due to the robot's attempt to resist the motion with its compliant structure. Additionally, varying the swing duration revealed the importance of the compliant structure's energy storage capability, highlighting the balance needed between the swing and stance phases for efficient locomotion.

However, this research also highlighted several challenges. The musculoskeletal robot's soft and compressible structure, coupled with the complexity of achieving precise control, made consistent and stable movements difficult. Furthermore, the robot's stability was compromised due to its simplistic design and the limited degrees of freedom, which restricted its ability to dynamically shift weight between both feet.

In conclusion, while this study advances the development of more adaptable and efficient bipedal robotic systems, it underscores the need for further refinement in robot design and control strategies. Future work should focus on enhancing the robot's structural complexity to improve dynamic weight transfer and exploring more sophisticated control algorithms to achieve human-like locomotion capabilities. These insights have significant implications for the fields of robotics, automation, and assistive technologies, potentially enabling robots to navigate challenging environments with greater agility and stability.

This thesis presents significant advancements in the field of bipedal and humanoid robotics, with a particular focus on enhancing slip-turning maneuvers through the integration of musculoskeletal structures, toe joints, and intrinsic muscles. The research demonstrates that incorporating biomechanical features inspired by the human musculoskeletal system can markedly improve a robot's motion flexibility, stability, and postural control, allowing for more fluid and precise movements.

Key findings emphasize the importance of understanding the biomechanics of human feet, specifically the role of toe joints and plantar intrinsic muscles in achieving efficient locomotion. By integrating these features, robotic designs can achieve substantial improvements in stability and maneuverability, particularly during slip-turning motions. The compliant structures within the musculoskeletal robots contribute to their ability to store and release energy, enhancing their overall functionality in diverse environments.

The introduction of the DSP-SLIP model, combining a slider-like mechanism with a double-support parallel spring-loaded inverted pendulum model, marks a pivotal advancement. This approach mitigates stability issues during slip-turning by employing foot support polygons and plantar intrinsic muscles for enhanced toe stabilization. However, the reliance on feedforward control systems without precise feedback mechanisms and the instability introduced by pneumatic actuators pose significant obstacles.

Experimental results validate the hypothesis that attaching toe joints to robots enhances their motion flexibility and stability. Suggesting that the adaptability of the robotics foot is a passive feature that utilizes its structure to allow a little joint error without compromising its stability, which could be beneficial to complex control systems of pneumatic-driven robots, requiring less precision. The research also explores friction control methods through weight-shifting dynamics, highlighting the potential for optimizing robotic movements to prevent slipping and maintain balance. Despite promising results, challenges such as the lack of an upper body for proper postural stability and the issues associated with PAMs need to be addressed in future work.

Future works

Future research should focus on integrating slip-turning motion into walking robots, enhancing dynamic stability and locomotion capabilities. Incorporating additional sensors and feedback mechanisms will be crucial for improving the precision and adaptability of robotic movements. Addressing the identified challenges will be essential for developing more adaptable, efficient, and human-like robotic systems. These advancements hold significant implications for the fields of robotics, automation, and assistive technologies, potentially enabling robots to navigate challenging environments with greater agility and stability.

Moreover, this study opens new possibilities for applying its findings in yaw moment control [159, 163] in bipedal robots to enhance or compensate them in motion [158, 162, 164, 165, 166, 167]. By leveraging the integration of toe joints and intrinsic muscles, robots can achieve more precise control over yaw moments, enhancing their ability to turn and maneuver efficiently. Other yaw moments compensation, such as rotational moment from arm swing [168, 169, 170], pelvis [171], foot [172, 173, 174], or gait [175, 176], are also valid choices. Moment control on the foot level, as seen in some research [160, 161], can benefit from the study's insights into weight-shifting dynamics and friction management, leading to more stable and adaptable locomotion. Additionally, the enhanced rotational moment control will enable robots to perform complex rotational tasks with greater accuracy, further advancing their operational capabilities in various environments.

Finally, as the neural network control model has been popular in the robotics field in recent years, applying reinforcement learning to the robot can be used to help them optimize the parameter to reach our desired result, reducing our workload in the fine-tuning process, whilst the method usually take a huge amount of training time and resource to complete a simple task [177].

Extensions of this research

The content of this research can be applied to many fields. They can be separated into three major fields: bio-inspired structure, slip-turning motion, and optimal control. First, in the biomechanic aspect, the bio-inspired structure can be further studied to improve the flexibility of the robot, human-like features, and adaptability of the robot.

Second, the proposed method of slip-turning strategy can be integrated as a turning motion in bipedal locomotion, improving their overall agility during movements to realize smooth locomotion. The motion can also be extended to the study of the slippage in other parts of the robot's contact point such as hands and tactile slippage. The tactile slippage of robotic hands is vastly studied, either to control the gripping force [178] or to reduce the friction with lubricant [179].

Finally, the research suggested an optimal control method based on the slippage that can be used to control the foot slippage for safety purposes with higher precision. There are many research that focuses on the slippage of the foot other than slip-turning. Mostly, the goal of those research is to

detect the slippage and use feedback control to prevent the slip, while some have pointed out that the slippage might be useful to the motion as it improves average speed and energy efficiency [180]. Some researchers try to use the slippage to make the robot slide while maintaining its balance [181].

Acknowledgements

This research was conducted under the supervision of Professor Koh Hosoda, the head of the Adaptive Robotics Laboratory from the Department of System Innovation, Graduate School of Engineering Science, Osaka University. The author would like to express my sincere gratitude to him for the thoughtful discussions, insightful commentary, and inspirational encouragement he gave me during the five years I worked on this work. Most importantly, he has given me the freedom to research the specific topic I am interested in. I am indebted to Professor Tadakuma Kenjiro, whose I have been working under for a recent year, as he provided me with helpful instructions on experimental design and was a supportive advisor. I would like to show my deep gratitude to Professor Hiroshi Ishiguro and Professor Kensuke Harada from the same department for their advice and guidance during the review process of this thesis. I would like to express my gratitude to Professor Takumi Kawasetsu for their commentaries and support. The various procedures and documentation could not been done without the support of Ms. Kawamura Tomoko, the secretary of our laboratory, who has been helpful to me and every student in the laboratory. I want to give my special thanks to my admirable senior, Dr. Tsung-Yuan Chen, all of my fellow laboratory members, and my friends for a lot of help, commentaries, and discussions I had with them. Finally, this work could not have been done without the financial support from the "Special Training Program for Robotics Engineers" given by the Ministry of Education, Culture, Sports, Science, and Technology of the Japanese Government.

Bibliography

[1] K. Hirai, M. Hirose, Y. Haikawa, and T. Takenaka. The development of honda humanoid robot. In *Proceedings of the 1998 IEEE International Conference on Robotics and Automation*, volume 2, pages 1321–1326, 1998.

[2] M. Hirose and K. Ogawa. Honda humanoid robots development. *Philosophical Transactions of the Royal Society A: Mathematical, Physical and Engineering Sciences*, 365(1850):11–19, 2007.

[3] G. Nelson, A. Saunders, and R. Playter. *The PETMAN and Atlas Robots at Boston Dynamics*. Springer Netherlands, 2019.

[4] J. W. Luo, Y. L. Fu, and S. G. Wang. 3d stable biped walking control and implementation on real robot. *Advanced Robotics*, 31(12):634–649, 2017.

[5] C. G. Atkeson, J. G. Hale, F. Pollick, M. Riley, S. Kotosaka, S. Schaul, T. Shibata, G. Tevatia, A. Ude, S. Vijayakumar, E. Kawato, and M. Kawato. Using humanoid robots to study human behavior. *IEEE Intelligent Systems and their Applications*, 15(4):46–56, jul 2000.

[6] K. Kaneko, F. Kanehiro, S. Kajita, H. Hirukawa, T. Kawasaki, M. Hirata, K. Akachi, and T. Isozumi. Humanoid robot hrp-2. In *Proceedings of the 2004 IEEE International Conference on Robotics and Automation*, volume 2, pages 1083–1090, 2004.

[7] M. Vukobratović and B. Borovac. Zero-moment point thirty five years of its life. *International Journal of Humanoid Robotics*, 1(1):157–173, 2004.

[8] N. Napoleon, S. Nakaura, and M. Sampei. Balance control analysis of humanoid robot based on zmp feedback control. In *Proceedings of the 2002 IEEE/RSJ International Conference on Intelligent Robots and Systems*, volume 3, pages 2437–2442, Sep. 2002.

[9] T. Gabriel and M. W. Han. Control of a humanoid robot based on the zmp method. *IFAC Proceedings Volumes*, 41(2):3065 – 3069, 2008. 17th IFAC World Congress.

[10] S. Kajita, F. Kanehiro, K. Kaneko, K. Fujiwara, K. Harada, K. Yokoi, and H. Hirukawa. Biped walking pattern generation by using preview control of zero-moment point. In *Proceedings of the 2003 IEEE International Conference on Robotics and Automation*, volume 2, pages 1620–1626, Sep. 2003.

[11] S. Lee and A. Goswami. Ground reaction force control at each foot: A momentum-based humanoid balance controller for non-level and non-stationary ground. In *Proceedings of the 2010 IEEE/RSJ International Conference on Intelligent Robots and Systems*, pages 3157–3162, Oct 2010.

[12] T. J. Klein, M. A. Lewis, J. Jeka, and T. Kiemel. Postural control in a bipedal robot using sensory reweighting. In *Proceedings of the 2011 IEEE International Conference on Robotics and Automation*, pages 2053–2058, 2011.

[13] T. Sugihara and Y. Nakamura. Whole-body cooperative balancing of humanoid robot using cog jacobian. In *Proceedings of the 2002 IEEE/RSJ International Conference on Intelligent Robots and Systems*, volume 3, pages 2575–2580, 2002.

[14] C. Ott, M. A. Roa, and G. Hirzinger. Posture and balance control for biped robots based on contact force optimization. In *Proceedings of the 2011 IEEE-RAS 11th International Conference on Humanoid Robots (Humanoids)*, pages 26–33, 10 2011.

[15] K. Erbatur and U. Seven. An inverted pendulum based approach to biped trajectory generation with swing leg dynamics. In *Proceedings of the 2007 IEEE-RAS 7th International Conference on Humanoid Robots (Humanoids)*, pages 216–221, 2007.

[16] H. Zhu and U. Thomas. Mechanical design of a biped robot forrest and an extended capture-point-based walking pattern generator. *Robotics*, 12(3):82, 2023.

[17] L. Chang, S. Piao, X. Leng, Z. He, and Z. Zhu. Inverted pendulum model for turn-planning for biped robot. *Physical Communication*, 42:101168, 2020.

[18] H. Geyer and U. Saranli. Gait based on the spring-loaded inverted pendulum. *Humanoid Robotics: A Reference*, 2018.

[19] M. Millard, E. Kubica, and J. McPhee. Forward dynamic human gait simulation using a slip target model. *Procedia IUTAM*, 2:142–157, 2011.

[20] N. T. Doan, T. Hayashi, and M. Yamakita. High speed running of flat foot biped robot with inerter using slip model. In *Proceedings of the 2015 IEEE International Conference on Advanced Intelligent Mechatronics (AIM)*, pages 110–115, 2015.

[21] G. Garofalo, C. Ott, and A. Albu-Schaffer. Walking control of fully actuated robots based on the bipedal slip model. In *Proceedings of the 2012 IEEE International Conference on Robotics and Automation*, pages 1456–1463, 2012.

[22] A. Hereid, M. J. Powell, and A. D. Ames. Embedding of slip dynamics on underactuated bipedal robots through multi-objective quadratic program based control. In *Proceedings of the 53rd IEEE Conference on Decision and Control*, pages 2950–2957, 2014.

[23] M. Hutter, C. D. Remy, M. A. Hopflinger, and R. Siegwart. Slip running with an articulated robotic leg. In *Proceedings of the 2010 IEEE/RSJ International Conference on Intelligent Robots and Systems*, pages 4934–4939, 2010.

[24] G. Piovan and K. Byl. Reachability-based control for the active slip model. *The International Journal of Robotics Research*, 34(3):270–287, 2015.

[25] R. Blickhan. The spring-mass model for running and hopping. *Journal of biomechanics*, 22:1217–1227, 1989.

[26] T. Hirabayashi, B. Ugurlu, A. Kawamura, and C. Zhu. Yaw moment compensation of biped fast walking using 3d inverted pendulum. In *Proceedings of the 10th IEEE International Workshop on Advanced Motion Control*, pages 296–300, 2008.

[27] M. M. ANKARALI, O. ARSLAN, and U. SARANLI. An analytical solution to the stance dynamics of passive spring-loaded inverted pendulum with damping. *Mobile Robotics*, pages 693–700, August 2009.

[28] M. M. Pelit, J. Chang, R. Takano, and M. Yamakita. Bipedal walking based on improved spring loaded inverted pendulum model with swing leg (slip-sl). In *Proceedings of the 2020 IEEE/ASME International Conference on Advanced Intelligent Mechatronics (AIM)*, pages 72–77, 2020.

[29] M. N. Vu, J. Lee, and Y. Oh. Control strategy for stabilization of the biped trunk-slip walking model. In *Proceedings of the 2017 14th International Conference on Ubiquitous Robots and Ambient Intelligence (URAI)*, pages 1–6, 2017.

[30] B. Han, H. Yi, Z. Xu, X. Yang, and X. Luo. 3d-slip model based dynamic stability strategy for legged robots with impact disturbance rejection. *Scientific Reports*, 12(1):5892, 2022.

[31] Y. Liu, P. M. Wensing, D. E. Orin, and Y. F. Zheng. Dynamic walking in a humanoid robot based on a 3d actuated dual-slip model. In *Proceedings of the 2015 IEEE International Conference on Robotics and Automation*, pages 5710–5717, 2015.

[32] Y. Liu, P. M. Wensing, D. E. Orin, and Y. F. Zheng. Trajectory generation for dynamic walking in a humanoid over uneven terrain using a 3d-actuated dual-slip model. In *Proceedings of the 2015 IEEE/RSJ International Conference on Intelligent Robots and Systems*, pages 374–380, 2015.

[33] Y. Liu, P. M. Wensing, J. P. Schmiedeler, and D. E. Orin. Terrain-blind humanoid walking based on a 3-d actuated dual-slip model. *IEEE Robotics and Automation Letters*, 1(2):1073–1080, 2016.

[34] S. Kajita, M. Morisawa, K. Miura, S. Nakaoka, K. Harada, K. Kaneko, F. Kanehiro, and K. Yokoi. Biped walking stabilization based on linear inverted pendulum tracking. In *Proceedings of the 2010 IEEE/RSJ International Conference on Intelligent Robots and Systems*, pages 4489–4496, 2010.

[35] A. Elhasairi and A. Pechev. Humanoid robot balance control using the spherical inverted pendulum mode. *Frontiers in Robotics and AI*, 2:21, 2015.

[36] W. T. Chew, A. Astolfi, and X. Ming. Robust control of bipedal humanoid (tpinokio). *Procedia Engineering*, 41:643–649, 2012.

[37] H. Hamzacebi and O. Morgul. Enlarging the region of stability using the torque-enhanced active slip model. In *Proceedings of the 2015 International Conference on Advanced Robotics (ICAR)*, pages 345–350, 2015.

[38] X. Meng, Z. Yu, G. Huang, X. Chen, W. Qi, Q. Huang, and B. Su. Walking control of biped robots on uneven terrains based on slip model. In *Proceedings of the 2019 IEEE International Conference on Advanced Robotics and Its Social Impacts (ARSO)*, pages 174–179, 2019.

[39] S. Feng, E. Whitman, X. Xinjilefu, and C. G. Atkeson. Optimization based full body control for the atlas robot. In *Proceedings of the 2014 IEEE-RAS 14th International Conference on Humanoid Robots (Humanoids)*, pages 120–127, Nov 2014.

[40] Y. Gong, R. Hartley, X. Da, A. Hereid, O. Harib, J. K. Huang, and J. Grizzle. Feedback Control of a Cassie Bipedal Robot: Walking, Standing, and Riding a Segway. *arXiv e-prints*, page arXiv:1809.07279, Sep 2018.

[41] A. Ramezani, J. Hurst, K. A. Hamed, and J. W. Grizzle. Performance analysis and feedback control of atrias, a three-dimensional bipedal robot. *Journal of Dynamic Systems, Measurement, and Contro*, 136, 12 2013.

[42] D. A. Neumann. *Kinesiology of the Musculoskeletal System: Foundations for Rehabilitation 1st Edition*. Mosby, 2002.

[43] A. M. R. Agur and A. F. Dalley. *Grant's Atlas of Anatomy 13 edition*. Wolters Kluwer, 2013.

[44] M. Schuenke, E. Schulte, and U. Schumacher. *General Anatomy and Musculoskeletal System (THIEME Atlas of Anatomy)*. Thieme, 2020.

[45] M. Nordin and V. H. Frankel. *Basic Biomechanics of the Musculoskeletal System*. Lippincott Williams & Wilkins, 2001.

[46] R. Pfeifer and J Bongard. *How the Body Shapes the Way We Think*. The MIT Press, 2006.

[47] A. Tongen and R. E. Wunderlich. Biomechanics of running and walking. *Mathematics and Sports*, pages 315–326, 2010.

[48] Y. L. Han and X. S. Wang. The biomechanical study of lower limb during human walking. *Science China Technological Sciences*, 54(4):983–991, Apr 2011.

[49] C. A. Oatis. *Kinesiology: The mechanics and pathomechanics of human movement: Second edition*. Lippincott Williams & Wilkins, 07 2013.

[50] W. B. Kibler, J. Press, and A. Sciascia. The role of core stability in athletic function. *Sports Medicine*, 36(3):189–198, Mar 2006.

[51] D. A. Winter. Human balance and posture control during standing and walking. *Gait & Posture*, 3(4):193–214, 1995.

[52] A. J. Ijspeert. Biorobotics: Using robots to emulate and investigate agile locomotion. *Science (New York, N.Y.)*, 346:196–203, 10 2014.

[53] K. Hosoda, T. Takuma, A. Nakamoto, and S. Hayashi. Biped robot design powered by antagonistic pneumatic actuators for multi-modal locomotion. *Robotics and Autonomous Systems*, 56:46–53, 2008.

[54] K. Hosoda and K. Narioka. Synergistic 3d limit cycle walking of an anthropomorphic biped robot. In *Proceedings of the 2007 IEEE/RSJ International Conference on Intelligent Robots and Systems*, pages 470–475, 2007.

[55] K. Narioka and K. Hosoda. Designing synergistic walking of a whole-body humanoid driven by pneumatic artificial muscles: An empirical study. *Advanced Robotics*, 22(10):1107–1123, 2008.

[56] K. Narioka and K. Hosoda. Motor development of an pneumatic musculoskeletal infant robot. In *Proceedings of the 2011 IEEE International Conference on Robotics and Automation*, 2011.

[57] K. Ogawa, K. Narioka, and K. Hosoda. Development of whole-body humanoid "pneumat-bs" with pneumatic musculoskeletal system. In *Proceedings of the 2011 IEEE/RSJ International Conference on Intelligent Robots and Systems*, pages 4838–4843, 2011.

[58] Y. Asano, K. Okada, and M. Inaba. Musculoskeletal design, control, and application of human mimetic humanoid kenshiro. *Bioinspiration & Biomimetics*, 14(3):036011, Apr 2019.

[59] Y. Nakanishi, S. Ohta, T. Shirai, Y. Asano, T. Kozuki, Y. Kakehashi, H. Mizoguchi, T. Kurotobi, Y. Motegi, K. Sasabuchi, J. Urata, , K. Okada, I. Mizuuchi, and M. Inaba. Design approach of biologically-inspired musculoskeletal humanoids. *International Journal of Advanced Robotic Systems*, 10:216, 2013.

[60] T. Kozuki, Y. Motegi, T. Shirai, Y. Asano, J. Urata, Y. Nakanishi, K. Okada, and M. Inaba. Design of upper limb by adhesion of muscles and bones — detail human mimetic musculoskeletal humanoid kenshiro. In *Proceedings of the 2013 IEEE/RSJ International Conference on Intelligent Robots and Systems*, pages 935–940, 2013.

[61] Y. Asano, H. Mizoguchi, T. Kozuki, Y. Motegi, M. Osada, J. Urata, Y. Nakanishi, K. Okada, and M. Inaba. Lower thigh design of detailed musculoskeletal humanoid "kenshiro". In *Proceedings of the 2012 IEEE/RSJ International Conference on Intelligent Robots and Systems*, pages 4367–4372, 2012.

[62] S. Kurumaya, K. Suzumori, H. Nabae, and S. Wakimoto. Musculoskeletal lower-limb robot driven by multifilament muscles. *ROBOMECH Journal*, 3(1):18, Sep 2016.

[63] H. Shin, S. Ikemoto, and K. Hosoda. Constructive understanding and reproduction of functions of gluteus medius by using a musculoskeletal walking robot. *Advanced Robotics*, 32(4):202–214, 2018.

[64] K. Narioka, T. Homma, and K. Hosoda. Humanlike ankle-foot complex for a biped robot. In *Proceedings of the 2012 IEEE-RAS 12th International Conference on Humanoid Robots (Humanoids)*, pages 15–20, 2012.

[65] C. P. Chou and B. Hannaford. Measurement and modeling of mckibben pneumatic artificial muscles. *IEEE Transactions on Robotics and Automation*, 12(1):90–102, Feb 1996.

[66] G. Klute, J. Czerniecki, and B. Hannaford. Artificial muscles: Actuators for biorobotic systems. *International Journal of Robotic Research*, 21:295–309, 2002.

[67] B. Tondu. Modelling of the mckibben artificial muscle: A review. *Journal of Intelligent Material Systems and Structures*, 23(3):225–253, 2012.

[68] C. J. Chiang and Y. C. Chen. Neural network fuzzy sliding mode control of pneumatic muscle actuators. *Engineering Applications of Artificial Intelligence*, 65:68–86, 2017.

[69] J. Huang, Y. Cao, and Y. W. Wang. Adaptive proxy-based sliding mode control for a class of second-order nonlinear systems and its application to pneumatic muscle actuators. *ISA Transactions*, 124:395–402, 2022.

[70] W. Zhao and A. Song. Active motion control of a knee exoskeleton driven by antagonistic pneumatic muscle actuators. *Actuators*, 9(4):134, 2020.

[71] A. Al-Ibadi, S. Nefti-Meziani, and S. Davis. Efficient structure-based models for the mckibben contraction pneumatic muscle actuator: The full description of the behaviour of the contraction pma. *Actuators*, 6(4):32, 2017.

[72] B. Ulrich, A. N. Santos, B. M. Jolles, D. H. Benninger, and J. Favre. Gait events during turning can be detected using kinematic features originally proposed for the analysis of straight-line walking. *Journal of Biomechanics*, 91:69–78, 2019.

[73] D. Conradsson, C. Paquette, and E. Franzén. Medio-lateral stability during walking turns in older adults. *PLOS ONE*, 13(6):e0198455, 2018.

[74] T. Dos'Santos, C. Thomas, P. Comfort, and P. A. Jones. The effect of angle and velocity on change of direction biomechanics: An angle-velocity trade-off. *Sports Medicine*, 48(10):2235–2253, 2018.

[75] K. Hase and R. B. Stein. Turning strategies during human walking. *Journal of Neurophysiology*, 81(6):2914–2922, 1999.

[76] T. Yang, W. Zhang, X. Chen, Z. Yu, L. Meng, and Q. Huang. Turning gait planning method for humanoid robots. *Applied Sciences*, 8(8):1257, 2018.

[77] G. Menga and M. Ghirardi. Modeling, simulation and control of the walking of biped robotic devices—part iii: Turning while walking. *Inventions*, 1(1):8, 2016.

[78] M. Farrell and H. Herr. Angular momentum primitives for human turning: Control implications for biped robots. In *Proceedings of 2008 IEEE-RAS 8th International Conference on Humanoid Robots (Humanoids)*, pages 163–167, 2008.

[79] C. Zhu and A. Kawamura. What is the real frictional constraint in biped walking? discussion on frictional slip with rotation. In *Proceedings of the 2006 IEEE/RSJ International Conference on Intelligent Robots and Systems*, pages 5762–5768, oct 2006.

[80] F. Zhao and J. Gao. Anti-slip gait planning for a humanoid robot in fast walking. *Applied Sciences*, 9(13), 2019.

[81] K. Hashimoto, Y. Yoshimura, H. Kondo, H. O. Lim, and A. Takanishi. Realization of quick turn of biped humanoid robot by using slipping motion with both feet. In *Proceedings of the 2011 IEEE International Conference on Robotics and Automation*, pages 2041–2046, 2011.

[82] K. Miura, S. Nakaoka, M. Morisawa, F. Kanehiro, K. Harada, and S. Kajita. Analysis on a friction based "twirl" for biped robots. In *Proceedings of the 2010 IEEE International Conference on Robotics and Automation*, pages 4249–4255, 06 2010.

[83] K. Miura, F. Kanehiro, K. Kaneko, S. Kajita, and K. Yokoi. Quick slip-turn of hrp-4c on its toes. In *Proceedings of the 2012 IEEE International Conference on Robotics and Automation*, pages 3527–3528, 2012.

[84] K. Miura, F. Kanehiro, K. Kaneko, S. Kajita, and K. Yokoi. Slip-turn for biped robots. *IEEE Transactions on Robotics*, 29(4):875–887, 2013.

[85] J. S. Yeon and J. H. Park. A fast turning method for biped robots with foot slip during single-support phase. *IEEE/ASME Transactions on Mechatronics*, 19(6):1847–1858, 2014.

[86] K. Nishiwaki, S. Kagami, Y. Kuniyoshi, M. Inaba, and H. Inoue. Toe joints that enhance bipedal and fullbody motion of humanoid robots. In *Proceedings of the 2002 IEEE International Conference on Robotics and Automation*, volume 3, pages 3105–3110, 2002.

[87] Y. Ogura, K. Shimomura, A. Kondo, A. Morishima, T. Okubo, S. Momoki, Hun ok Lim, and A. Takanishi. Human-like walking with knee stretched, heel-contact and toe-off motion by a humanoid robot. In *Proceedings of the 2006 IEEE/RSJ International Conference on Intelligent Robots and Systems*, pages 3976–3981, 2006.

[88] D. Tlalolini, C. Chevallereau, and Y. Aoustin. Human-like walking: Optimal motion of a bipedal robot with toe-rotation motion. *IEEE/ASME Transactions on Mechatronics*, 16(2):310–320, 2011.

[89] K. Miura, M. Morisawa, F. Kanehiro, S. Kajita, K. Kaneko, and K. Yokoi. Human-like walking with toe supporting for humanoids. In *Proceedings of the 2011 IEEE/RSJ International Conference on Intelligent Robots and Systems*, pages 4400–4407, 2011.

[90] Y. Liu, X. Zang, S. Heng, Z. Lin, and J. Zhao. Human-like walking with heel off and toe support for biped robot. *Applied Sciences*, 7(5), 2017.

[91] K. Hashimoto. Mechanics of humanoid robot. *Advanced Robotics*, 34(21–22):1390–1397, 2020.

[92] F. B. Ouezdou, S. Alfayad, and B. Almasri. Comparison of several kinds of feet for humanoid robot. In *Proceedings of the 2005 IEEE-RAS 5th International Conference on Humanoid Robots (Humanoids)*, pages 123–128, 2005.

[93] S. Agarwal and M. Popovic. Study of toe joints to enhance locomotion of humanoid robots. In *Proceedings of the 2018 IEEE-RAS 18th International Conference on Humanoid Robots (Humanoids)*, pages 4909–4914, 2018.

[94] E. P. Jr1 Salathé, G. A. Arangio, and E. P. Salathé. The foot as a shock absorber. *Journal of Biomechanics*, 27(7):655–659, 1990.

[95] A. Lees, M. Lake, and L. Klenerman. Shock absorption during forefoot running and its relationship to medial longitudinal arch height. *Foot & ankle international*, 26:1081–1088, Dec 2005.

[96] Y. Ito, T. Nakaoka, J. Urata, Y. Nakanishi, K. Okada, and M. Inaba. Design and development of a tendon-driven and axial-driven hybrid humanoid leg with high-power motor driving system. In *Proceedings of the 2012 IEEE-RAS 12th International Conference on Humanoid Robots (Humanoids)*, pages 475–480, Nov 2012.

[97] R. Sellaouti, O. Stasse, S. Kajita, K. Yokoi, and A. Kheddar. Faster and smoother walking of humanoid hrp-2 with passive toe joints. In *Proceedings of the 2006 IEEE/RSJ International Conference on Intelligent Robots and Systems*, pages 4909–4914, 2006.

[98] S. Kajita, K. Kaneko, M. Morisawa, S. Nakaoka, and H. Hirukawa. Zmp-based biped running enhanced by toe springs. In *Proceedings of the 2007 IEEE International Conference on Robotics and Automation*, pages 3963–3969, 2007.

[99] R. Zaier and A. Al-Yahmedi. Design of biomechanical legs with a passive toe joint for enhanced human-like walking. *The Journal of Engineering Research [TJER]*, 14(2):166, 2017.

[100] S. K. Au, J. Weber, and H. Herr. Biomechanical design of a powered ankle-foot prosthesis. In *Proceedings of the 2007 IEEE 10th International Conference on Rehabilitation Robotics*, pages 298–303, June 2007.

[101] V. T. Nguyen and H. Hasegawa. Effect of toe length on biped walking behavior. *International Journal of Mechanical Engineering and Robotics Research*, 7(6):599–603, 2018.

[102] C. W. Chan and A. Rudins. Foot biomechanics during walking and running. *Mayo Clinic Proceedings*, 69(5):448 – 461, 1994.

[103] O. S. Moreno-Barriga, C. Romero-Morales, R. Becerro-de Bengoa-Vallejo, M. E. Losa-Iglesias, J. Gómez-Salgado, J. Caballero-López, L. C. Vidal-Valverde, and D. López-López. Effects of foot structure type on core stability in university athletes. *Life*, 13(7):1487, 2023.

[104] L. A. Bolgla and T. R. Malone. Plantar fasciitis and the windlass mechanism: a biomechanical link to clinical practice. *Journal of athletic training*, 39:77–82, Jan 2004.

[105] N. L. Griffin, C. E. Miller, D. Schmitt, and K. D'Août. Understanding the evolution of the windlass mechanism of the human foot from comparative anatomy: Insights, obstacles, and future directions. *American journal of physical anthropology*, 156:1–10, Jan 2015.

[106] P. Caravaggi, T. Pataky, J. Y. Goulermas, R. Savage, and R. Crompton. A dynamic model of the windlass mechanism of the foot: evidence for early stance phase preloading of the plantar aponeurosis. *Journal of Experimental Biology*, 212(15):2491–2499, 2009.

[107] L. Welte, L. A. Kelly, G. A. Lichtwark, and M. J. Rainbow. Influence of the windlass mechanism on arch-spring mechanics during dynamic foot arch deformation. *Journal of The Royal Society Interface*, 15(145):20180270, 2018.

[108] L. Welte, L. A. Kelly, S. E. Kessler, D. E. Lieberman, S. E. D'Andrea, G. A. Lichtwark, and M. J. Rainbow. The extensibility of the plantar fascia influences the windlass mechanism during human running. In *Proceedings of the Royal Society B: Biological Sciences*, page 20202095, 2021.

[109] G. A. Arangio, C. Chen, and E. P. Salathé. Effect of varying arch height with and without the plantar fascia on the mechanical properties of the foot. *Foot & ankle international*, 19:705–709, Oct 1998.

[110] J. H. Hicks. The mechanics of the foot. ii. the plantar aponeurosis and the arch. *Journal of anatomy*, 88:25–30, Jan 1954.

[111] S. M. Stearne, K. A. McDonald, J. A. Alderson, I. North, C. E. Oxnard, and J. Rubenson. The foot's arch and the energetics of human locomotion. *Scientific Reports*, 6(1):19403, 2016.

[112] R. F. Ker, M. B. Bennett, S. R. Bibby, R. C. Kester, and R. McN. Alexander. The spring in the arch of the human foot. *Nature*, 325(6100):147–149, January 1987.

[113] M. Venkadesan, A. Yawar, C. M. Eng, M. A. Dias, D. K. Singh, S. M. Tommasini, A. H. Haims, M. M. Bandi, and S. Mandre. Stiffness of the human foot and evolution of the transverse arch. *Nature*, 579(7797):97–100, 2020.

[114] E. Anzai, K. Nakajima, Y. Iwakami, M. Sato, S. Ino, T. Ifukube, K. Yamashita, and Y. Ohta. Effects of foot arch structure on postural stability. *Clinical Research on Foot & Ankle*, 2:132, 2014.

[115] K. A. Kirby. Longitudinal arch load-sharing system of the foot. *Revista Española De Podología*, 28(1):e18–e26, 2017.

[116] K. Hashimoto, Y. Takezaki, K. Hattori, H. Kondo, T. Takashima, H. O. Lim, and A. Takanishi. A study of function of foot's medial longitudinal arch using biped humanoid robot. In *Proceedings of the 2010 IEEE/RSJ International Conference of Intelligent Robots and Systems*, 2010.

[117] X. Liu, Y. Duan, A. Hitzmann, Y. Xu, T. Chen, S. Ikemoto, and K. Hosoda. Using the foot windlass mechanism for jumping higher: A study on bipedal robot jumping. *Robotics and Autonomous Systems*, 110:85 – 91, 2018.

[118] S. Kwon and J. Park. Kinesiology-based robot foot design for human-like walking. *International Journal of Advanced Robotics Systems*, 9, 2012.

[119] J. T. Seo and B. J. Yi. Modeling and analysis of a biomimetic foot mechanism. In *Proceedings of the 2009 IEEE/RSJ International Conference on Intelligent Robots and Systems*, pages 1472–1477, 2009.

[120] S. Davis and D. G. Caldwell. The design of an anthropomorphic dexterous humanoid foot. In *Proceedings of the 2010 IEEE/RSJ International Conference on Intelligent Robots and Systems*, pages 2200–2205, 2010.

[121] C. Piazza, C. Della Santina, G. M. Gasparri, M. G. Catalano, G. Grioli, M. Garabini, and A. Bicchi. Toward an adaptive foot for natural walking. In *Proceedings of the 2016 IEEE-RAS 16th International Conference on Humanoid Robots (Humanoids)*, pages 1204–1210, 2016.

[122] L. Colasanto, N. Van Der Noot, and A. J. Ijspeert. Bio-inspired walking for humanoid robots using feet with human-like compliance and neuromuscular control. In *Proceedings of the 2015 IEEE-RAS 15th International Conference on Humanoid Robots (Humanoids)*, pages 1039–1044, 2015.

[123] K. Yamamoto, T. Sugihara, and Y. Nakamura. Toe joint mechanism using parallel four-bar linkage enabling humanlike multiple support at toe pad and toe tip. In *Proceedings of the 2007 IEEE-RAS 7th International Conference on Humanoid Robots(Humanoids)*, pages 410–415, 2007.

[124] K. Yamamoto. *Human-Like Toe Joint Mechanism. Humanoid Robotics: A Reference*, pages 435–456. Springer, 01 2018.

[125] M. Russo, B. D. M. Chaparro-Rico, L. Pavone, G. Pasqua, and D. Cafolla. A bioinspired humanoid foot mechanism. *Applied Sciences*, 11(4), 2021.

[126] F. Sichting, N. B. Holowka, O. B. Hansen, and D. E. Lieberman. Effect of the upward curvature of toe springs on walking biomechanics in humans. *Scientific Reports*, 10:14643, 2020.

[127] N. B. Holowka and D. E. Lieberman. Rethinking the evolution of the human foot: insights from experimental research. *Journal of Experimental Biology*, 221(17), 2018.

[128] J. Hughes, P. Clark, and L. Klenerman. The importance of the toes in walking. the journal of bone and joint surgery. *British Volume*, 72-B(2):245–251, 1990.

[129] E. C. Honert, G. Bastas, and K. E. Zelik. Effect of toe joint stiffness and toe shape on walking biomechanics. *Bioinspiration & Biomimetics*, 13(6):066007, 2018.

[130] E. C. Honert, G. Bastas, and K. E. Zelik. Effects of toe length, foot arch length and toe joint axis on walking biomechanics. *Human Movement Science*, 70:102594, 2020.

[131] P. O. McKeon, J. Hertel, D. Bramble, and I. Davis. The foot core system: a new paradigm for understanding intrinsic foot muscle function. *British Journal of Sports Medicine*, 49(5):290–290, 2015.

[132] D. J. Farris, L. Kelly, A. G. Cresswell, and G. A. Lichtwark. The functional importance of human foot muscles for bipedal locomotion. In *Proceedings of the National Academy of Sciences*, pages 1645–1650, 2019.

[133] E. Ferrari, G. Cooper, N. Reeves, and E. Hodson-Tole. Intrinsic foot muscles act to stabilise the foot when greater fluctuations in centre of pressure movement result from increased postural balance challenge. *Gait & Posture*, 79:229–233, 2020.

[134] P. X. Ku, N. A. Abu Osman, A. Yusof, and W. a. B. Wan Abas. The effect on human balance of standing with toe-extension. *PLOS ONE*, 7(7):e41539, 2012.

[135] N. Maeda, A. Hirota, M. Komiya, M. Morikawa, R. Mizuta, H. Fujishita, Y. Nishikawa, T. Kobayashi, and Y. Urabe. Intrinsic foot muscle hardness is related to dynamic postural stability after landing in healthy young men. *Gait & Posture*, 86:192–198, 2021.

[136] X. Zhang, K. H. Schütte, and B. Vanwanseele. Foot muscle morphology is related to center of pressure sway and control mechanisms during single-leg standing. *Gait & Posture*, 57:52–56, 2017.

[137] D. J. Farris, J. Birch, and L. Kelly. Foot stiffening during the push-off phase of human walking is linked to active muscle contraction, and not the windlass mechanism. *Journal of the Royal Society Interface*, 17(168):20200208, 2020.

[138] N. A. Sharkey and A. J. Hamel. A dynamic cadaver model of the stance phase of gait: performance characteristics and kinetic validation. *Clinical Biomechanics*, 13(6):420 – 433, 1998.

[139] T. G. McPoil and H. G. Knecht. Biomechanics of the foot in walking: A function approach. *Journal of Orthopaedic & Sports Physical Therapy*, 7(2):69–72, 1985.

[140] S. Angin, K. J. Mickle, and C. J Nester. Contributions of foot muscles and plantar fascia morphology to foot posture. *Gait & Posture*, 61:238–242, 2018.

[141] Y. Yuasa, T. Kurihara, and T. Isaka. Relationship between toe muscular strength and the ability to change direction in athletes. *Journal of Human Kinetics*, 64(1):47–55, 2018.

[142] K. J. Mickle, B. J. Munro, S. R. Lord, H. B. Menz, and J. R. Steele. Isb clinical biomechanics award 2009. *Clinical Biomechanics*, 24(10):787–791, 2009.

[143] T. Fujimaki, M. Wako, K. Koyama, N. Furuya, R. Shinohara, S. Otawa, A. Kobayashi, S. Horiuchi, M. Kushima, Z. Yamagata, and H. Haro. Prevalence of floating toe and its relationship with static postural stability in children: The yamanashi adjunct study of the japan environment and children's study (jecs-y). *PLOS ONE*, 16(3):e0246010, 2021.

[144] L. Willemse, E. J. M. Wouters, H. M. Bronts, M. F. Pisters, and B. Vanwanseele. The effect of interventions anticipated to improve plantar intrinsic foot muscle strength on fall-related dynamic function in adults: a systematic review. *Journal of Foot and Ankle Research*, 15(1):3, 2022.

[145] K. Kimura, N. Imaoka, S. Noda, Y. Kakiuchi, K. Okada, and M. Inaba. Locomotion approach of bipedal robot utilizing passive wheel without swing leg based on stability margin maximization and fall prevention functions. *ROBOMECH Journal*, 7(1):35, 2020.

[146] D. Torricelli, J Gonzalez, M Weckx, R. Jiménez-Fabián, B. Vanderborght, M. Sartori, S. Dosen, D. Farina, D. Lefeber, and J. L. Pons. Human-like compliant locomotion: state of the art of robotic implementations. *Bioinspiration & Biomimetics*, 11(5):051002, August 2016.

[147] H. Geyer, A. Seyfarth, and R. Blickhan. Compliant leg behaviour explains basic dynamics of walking and running. In *Proceedings of the Royal Society B: Biological Sciences*, pages 2861 – 2867, 2006.

[148] J. Luo, Y. Fu, S. Wang, and M. Qiao. How do the compliant legs affect walking stability. In *Proceedings of the 2017 IEEE International Conference on Robotics and Biomimetics (ROBIO)*, pages 599–604, 2017.

[149] T. J. Roberts. The integrated function of muscles and tendons during locomotion. *Comparative Biochemistry and Physiology Part A: Molecular & Integrative Physiology*, 133(4):1087–1099, 2002.

[150] D. Labonte and N. C. Holt. Elastic energy storage and the efficiency of movement. *Current Biology*, 32(12):R661–R666, 2022.

[151] R. M. ALEXANDER. Elastic energy stores in running vertebrates. *American Zoologist*, 24(1):85–94, 1984.

[152] W. Wang and R. H. Crompton. The role of load-carrying in the evolution of modern body proportions. *Journal of Anatomy*, 204(5):417–430, 2004.

[153] K. Goto, Y. Tazaki, and T. Suzuki. Bipedal locomotion control based on simultaneous trajectory and foot step planning. *Journal of Robotics and Mechatronics*, 28(4):533–542, 2016.

[154] J. Tang, Y. Zhu, W. Gan, H. Mou, J. Leng, Q. Li, Z. Yu, and J. Zhang. Design, control, and validation of a symmetrical hip and straight-legged vertically-compliant bipedal robot. *Biomimetics*, 8(4):340, 2023.

[155] J. D. Ventura, G. K. Klute, and R. R. Neptune. Individual muscle contributions to circular turning mechanics. *Journal of Biomechanics*, 48(6):1067–1074, 2015.

[156] Y. Choi, Y. Kim, M. Kim, and B. Yoon. Muscle synergies for turning during human walking. *Journal of Motor Behavior*, 51(1):1–9, 2017.

[157] K. Nipatphonsakun, T. Kawasetsu, and K. Hosoda. The experimental investigation of foot slip-turning motion of the musculoskeletal robot on toe joints. *Frontiers in Robotics and AI*, 10:1187297, 2023.

[158] S. Zhang, Q. Huang, H. Wang, W. Xu, G. Ma, Y. Liu, and Z. Yu. The mechanism of yaw torque compensation in the human and motion design for humanoid robots. *International Journal of Advanced Robotic Systems*, 10(1):57, 2013.

[159] T. Negishi and N. Ogihara. Functional significance of vertical free moment for generation of human bipedal walking. *Scientific Reports*, 13(1):6894, 2023.

[160] T. Y. Chen, T. Kawakami, N. Ogihara, and K. Hosoda. Free moment induced by oblique transverse tarsal joint: investigation by constructive approach. *Royal Society Open Science*, 8(4):201947, 2021.

[161] T. Y. Chen, S. Shigaki, and K. Hosoda. Bevel-geared mechanical foot: a bioinspired robotic foot compensating yaw moment of bipedal walking. *Advanced Robotics*, 36(13):631–640, 2021.

[162] B. Ugurlu, J. A. Saglia, N. G. Tsagarakis, and D. G. Caldwell. Yaw moment compensation for bipedal robots via intrinsic angular momentum constraint. *International Journal of Humanoid Robotics*, 09(04):1250033, 2012.

[163] J. R. Rebula, L. V. Ojeda, P. G. Adamczyk, and A. D. Kuo. The stabilizing properties of foot yaw in human walking. *Journal of Biomechanics*, 53:1 – 8, 2017.

[164] R. Cisneros, K. Yokoi, and E. Yoshida. Yaw moment compensation by using full body motion. In *Proceedings of the 2014 IEEE International Conference on Mechatronics and Automation*, pages 119–125, Aug 2014.

[165] R. Cisneros, E. Yoshida, and K. Yokoi. Partial yaw moment compensation through whole-body motion. In *Proceedings of the 2014 IEEE-RAS 14th International Conference on Humanoid Robots (Humanoids)*, pages 329–335, Nov 2014.

[166] J. Ueda, K. Shirase, Y. Matsumoto, S. Oda, and T. Ogasawa. Momentum compensation for fast dynamic walking of humanoids based on pelvic rotation of contact sport athletes. In *Proceedings of the 2004 IEEE/RAS 4th International Conference on Humanoid Robots,*, volume 2, pages 592–607, 2004.

[167] C. Chevallereau, D. Djoudi, and J. Grizzle. Stable bipedal walking with foot rotation through direct regulation of the zero moment point. *IEEE Transactions on Robotics*, 24(2):390–401, 2008.

[168] Y. Li, W. Wang, R. H. Crompton, and M. M. Gunther. Free vertical moments and transverse forces in human walking and their role in relation to arm-swing. *Journal of Experimental Biology*, 204(1):47–58, 2001.

[169] Y. Fujimoto and A. Kawamura. Robust control of biped walking robot with yaw moment compensation by arm motion. *Asian Control Conference (ASCC)*, pages 327–330, Jul 1997.

[170] L. Yang and C. Deng. Yaw moment compensation for humanoid robot via arms swinging. *The Open Automation and Control Systems Journal*, 6:1371–1377, 12 2014.

[171] J. Ueda, K. Shirae, S. Oda, and T. Ogasawara. Moment compensation for fast dynamic walking of humanoids based on human athletes pelvis rotation. *Journal of the Robotics Society of Japan*, 23(4):457–465, 2005.

[172] S. Almosnino, T. Kajaks, and P. A. Costigan. The free moment in walking and its change with foot rotation angle. *Sports Medicine, Arthroscopy, Rehabilitation, Therapy & Technology*, 1:19, 2009.

[173] A. Goswami. Postural stability of biped robots and the foot-rotation indicator (fri) point. *The International Journal of Robotics Research*, 18:522–233, 1999.

[174] P. Daniel and G. Stan. A method for the analysis of the free moment's variability: A case study. *Proc. Rom. Acad., Series B*, pages 241 – 249, 2013.

[175] J. Begue, T. Caderby, N. Peyrot, and G. Dalleau. Influence of gait speed on free vertical moment during walking. *Journal of Biomechanics*, 75:186 – 190, 2018.

[176] H. Herr and M. Popovic. Angular momentum in human walking. *Journal of Experimental Biology*, 211(4):467–481, 2008.

[177] D. Buchler, S. Guist, R. Calandra, V. Berenz, B. Scholkopf, and J. Peters. Learning to play table tennis from scratch using muscular robots. *IEEE Transactions on Robotics*, 38(6):3850–3860, Dec. 2022.

[178] M. Farag, N. Z. Azlan, M. H. Alzibai, and A. N. A. Ghafar. Slippage detection for grasping force control of robotic hand using force sensing resistors. In *Proceedings of the 2019 5th International Conference on Computer and Technology Applications*, pages 98–102, 2019.

[179] K. Mizushima, Y. Suzuki, T. Tsuji, and T. Watanabe. Deformable fingertip with a friction reduction system based on lubricating effect for smooth operation under both dry and wet conditions. *Advanced Robotics*, 33(10):508–519, Apr. 2019.

[180] Y. Or and M. Moravia. Effects on an actuated spring-mass model of dynamic legged locomotion. *International Journal of Advanced Robotic Systems*, 13(2):69, Mar. 2016.

[181] Y. Lu, J. Gao, X. Shi, D. Tian, and Y. Liu. Sliding balance control of a point-foot biped robot based on a dual-objective convergent equation. *Applied Sciences*, 11(9):4016, Apr. 2021.

Publication List

Journal Papers

K. Nipatphonsakun, T. Kawasetsu, and K. Hosoda, "The experimental investigation of foot slip-turning motion of the musculoskeletal robot on toe joints", Frontiers in Robotics and AI, 10:1187297, 2023.

K. Nipatphonsakun, T. Kawasetsu, and K. Hosoda, "Intrinsic Toe Joint Stabilization in Foot-Slip Turning Motion of Musculoskeletal Robot with DSP-SLIP Model", Advanced Robotics, pages 1-13, 2024.

K. Nipatphonsakun, and K. Hosoda, "Friction Control in Foot-Slip Turning of the Musculoskeletal Robot Using DSP-SLIP Model with Dual-Mass System", IEEE Robotics and Automation Letters (RA-L), 2024. (Submitted)

International Conference Papers

K. Nipatphonsakun, T. Kawasetsu, and K. Hosoda, "Bio-inspired Musculoskeletal Robotics Foot with Toe Joint and Plantar Intrinsic Muscle in Tiptoe Motion", In Proceedings of the 11th International Symposium on Adaptive Motion of Animals and Machines (AMAM2023), pages 120-121, 2023.

Awards

"Kanako Miura Award" Awardee, IEEE-RAS, Humanoids 2022, Okinawa, Japan, 2022